

5-31-1991

Modification of wear testing methodology

Muhammed Farooq
New Jersey Institute of Technology

Follow this and additional works at: <https://digitalcommons.njit.edu/theses>



Part of the [Mechanical Engineering Commons](#)

Recommended Citation

Farooq, Muhammed, "Modification of wear testing methodology" (1991). *Theses*. 2476.
<https://digitalcommons.njit.edu/theses/2476>

This Thesis is brought to you for free and open access by the Electronic Theses and Dissertations at Digital Commons @ NJIT. It has been accepted for inclusion in Theses by an authorized administrator of Digital Commons @ NJIT. For more information, please contact digitalcommons@njit.edu.

Copyright Warning & Restrictions

The copyright law of the United States (Title 17, United States Code) governs the making of photocopies or other reproductions of copyrighted material.

Under certain conditions specified in the law, libraries and archives are authorized to furnish a photocopy or other reproduction. One of these specified conditions is that the photocopy or reproduction is not to be “used for any purpose other than private study, scholarship, or research.” If a user makes a request for, or later uses, a photocopy or reproduction for purposes in excess of “fair use” that user may be liable for copyright infringement,

This institution reserves the right to refuse to accept a copying order if, in its judgment, fulfillment of the order would involve violation of copyright law.

Please Note: The author retains the copyright while the New Jersey Institute of Technology reserves the right to distribute this thesis or dissertation

Printing note: If you do not wish to print this page, then select “Pages from: first page # to: last page #” on the print dialog screen

The Van Houten library has removed some of the personal information and all signatures from the approval page and biographical sketches of theses and dissertations in order to protect the identity of NJIT graduates and faculty.

ABSTRACT

Modification of The Wear Testing Methodology

by

Muhammad Farooq
Master of Science in M.E., 1991

In this work the existing computer controlled methodology has been modified. A loading and unloading mechanism has been designed, manufactured and assembled. A specimen fixture has been designed and installed. Alloy steel specimens with different surface treatment were tested on the modified wear testing machine. Operational surface roughness was measured in all stages of running-in, steady state and catastrophic wear. The difference between technological and operational surface roughness was observed. The results show that the surface treatment by Plasma Ion-Nitriding with Magnetic treatment increases wear resistance. It was found that the coated material which had been magnetically treated with a large number of cycles had the least wear rate.

MODIFICATION OF WEAR TESTING METHODOLOGY

by
Muhammad Farooq

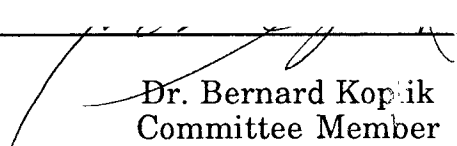
A Thesis
Submitted to the Faculty of the Graduate Division of the
New Jersey Institute of Technology
in Partial Fulfillment of the Requirements for the Degree of
Master of Science
Department of Mechanical and Industrial Engineering
May 1991

APPROVAL

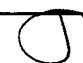
Modification of The Wear Testing Methodology

by
Muhammad Farooq

Dr. Roman Dubrovsky
Thesis Adviser
Associate Professor of Mechanical Engineering
New Jersey Institute of Technology


Dr. Bernard Koplik
Committee Member
Professor of Mechanical Engineering
Chairperson of Mechanical Engineering Department
New Jersey Institute of Technology

5/1/91


Dr. Nouri Levy
Committee Member
Associate Professor of Mechanical Engineering
New Jersey Institute of Technology

BIOGRAPHICAL SKETCH

Author: Muhammad Farooq

Degree: Master of Science in Mechanical Engineering

Date: May, 1991

Date of Birth:

Place of Birth:

Undergraduate and Graduate Education:

- Master of Science in Mechanical Engineering,
New Jersey Institute of Technology, Newark, NJ, 1991
- Bachelor of Science in Mechanical Engineering,
N. E. D. University of Engineering and Technology,
Karachi, Pakistan

Major: Mechanical Engineering

Position held: Teaching Assistant, 1989-90,
Mechanical Engineering Department,
New Jersey Institute of Technology, Newark, NJ

This thesis is dedicated to parents:
Mr. and Mrs. Muhammad Abbas Ansari

ACKNOWLEDGEMENT

The author wishes to express his sincere appreciation to his advisor, Dr. Roman Dubrovsky, for his guidance, friendship and moral support throughout this thesis.

The author wishes to thank Mr. Don Rosander and Mr. Karl Ulatowski of the Mechanical Engineering Department, NJIT, for their friendly and helpful assistance in modifying the wear testing machine.

The author is also pleased to express his sincere gratitude to his friend Mr. I-Tsung Shih, who has been of assistance in every step of this work. Also thank you to Mr. Wenge Yang and Mr. Nien-Sheng Lin in preparing specimens and performing wear tests.

A thank you to author's brother Mr. Muhammad Iqbal, for his advice and help. And finally, the author wishes to thank his parents, without whose support it would have been impossible to achieve this task, and he would like to dedicate this thesis to them, hoping that they will understand how much they gave to it. Thank you both.

Contents

	page
1 INTRODUCTION	1
2 BACKGROUND	3
2.1 Wear	3
2.1.1 Wear Mechanism	4
2.1.2 Wear Measurement	24
2.2 Wear Testing Devices	25
2.2.1 Rotating Disc Assemblies	30
2.2.2 External and Internal Drum Equipment	30
2.2.3 Flat-Belt Apparatus	34
2.2.4 Reciprocating Sliding Machines	36
2.3 Goals and Objective	38
3 IMPROVEMENT OF WEAR TESTING MACHINE AND ITS METHODOLOGY	39
3.1 Introduction	39
3.2 General Description of Wear Testing Machine	41
3.3 Modification of the Testing Machine	43
3.3.1 Loading and Unloading Mechanism	43
3.3.2 Design of Cam	46
3.3.2.1 Manufacturing of Cam	47

3.3.3	Design of Shoe Holder	50
3.3.4	Design of Shafts for Reducer	50
3.3.4.1	Design of High Speed Shaft	53
3.3.4.2	Design of Low Speed Shaft	57
4	RESULTS AND DISCUSSION	58
4.1	Calibration	58
4.2	Testing Materials	64
4.3	Testing Parameter	67
4.4	Testing Procedure	68
4.5	Wear and Friction Analysis	69
4.6	Surface Roughness Analysis	80
5	CONCLUSION	93

APPENDIX

REFERENCES

LIST OF FIGURES

Figures	Page
2.1 Low - Stress Abrasion	7
2.2 High - Stress Abrasion	7
2.3 Gauging Abrasion	8
2.4 Polishing Wear	8
2.5 Solid-Particle Impingement	9
2.6 Fluid-Impingement Erosion	9
2.7 Cavitation	10
2.8 Erosive Wear	10
2.9 Fretting Wear	11
2.10 Adhesive Wear	11
2.11 Seizure	12
2.12 Galling	12
2.13 Oxidative Wear	13
2.14 Pitting	13
2.15 Spalling	14
2.16 Impact Fatigue	14
2.17 Brinelling	14
2.18 Adhesive Wear	17
2.19 Range of Operation of Surface Forces	18
2.20 Transition from Mild to Severe Wear by Load Increase	20
2.21 Schematic Outline for Simulative Tribo-testing	27

2.22 Examples of Geometric Arrangement of Wear Testing Machine	28
2.23 A Simple Rotating Disc Assembly for Friction Measurement	31
2.24 Internal Drum Apparatus	33
2.25 External Drum Apparatus	33
2.26 General Layout of Flat-belt Apparatus	35
2.27 Reciprocating Wear and Abrasion Machine	37
2.28 Attachment of Shaping Machine	37
3.1 General View of Wear Testing Machine	42
3.2 Loading-unloading Mechanism	45
3.3 Cam	48
3.4 Shoe (specimen)	51
3.5 Shoe Holder	52
3.6 Modified Reducer	54
3.8 High Speed Shaft	55
3.9 Low Speed Shaft	56
4.1 Calibration Chart (Computer Reading vs. Input Load)	60
4.2 Calibration Chart (Computer Reading vs. Motor Moment)	61
4.3 Calibration Chart (Computer Reading vs. Friction Force)	62
4.4 Calibration Chart (Computer Reading vs. Friction Force)	63
4.5 Microstructure View Showing Ion-Nitrided Layer on Bulk	66
4.6 Microhardness of Ion-Nitriding Material	66
4.7 Friction Coefficient vs. Sliding Distance (Type A)	70
4.8 Friction Coefficient vs. Sliding Distance (Type A1)	71
4.9 Friction Coefficient vs. Sliding Distance (Type A2)	72
4.10 Friction Coefficient vs. Sliding Distance (Type A3)	73
4.11 Wear Rate vs. Sliding Distance (Type A)	74
4.12 Wear Rate vs. Sliding Distance (Type A1)	75

4.13 Wear Rate vs. Sliding Distance (Type A2)	76
4.14 Wear Rate vs. Sliding Distance (Type A3)	77
4.15 Comparison of Weight Loss in 15 Minutes	78
4.16 Friction Coefficient and Wear Rate vs. Sliding Distance (Type A1)	81
4.17 Friction Coefficient and Wear Rate vs. Sliding Distance (Type A2)	82
4.18 Friction Coefficient and Wear Rate vs. Sliding Distance (Type A3)	83
4.19 Comparison of Wear Rate of Type A1, A2 and A3 Materials	79
4.20 Comparison of Weight Loss vs. Time for Type A1, A2 and A3 Materials	84
4.21 Roughness Parameter Ra vs. Sliding Distance (Type A)	86
4.22 Roughness Parameter Ra vs. Sliding Distance (Type A1)	87
4.23 Roughness Parameter Ra vs. Sliding Distance (Type A3)	88
4.24 Roughness Parameter Ra vs. Sliding Distance (Type A4)	89
4.25 Ra and Friction Coefficient vs. Sliding Distance (Type A1)	90
4.26 Ra and Friction Coefficient vs. Sliding Distance (Type A2)	91
4.27 Ra and Friction Coefficient vs. Sliding Distance (Type A3)	92

LIST OF TABLES

Tables	Page
2.1 Classification of Wear Mechanisms	5
3.1 CNC Code for Cam	49
4.1 Chemical Composition of Specimens	64
4.2 Ion-Nitriding Parameters	65
4.3 Magnetic Treatment	65
4.4 Chemical Composition of Roller	67
4.5 Testing Parameters	67

Chapter 1

INTRODUCTION

Wear is one of the three most commonly encountered industrial problems leading to the replacement of components and assemblies in engineering, the others being fatigue and corrosion. Wear reduces the operating efficiency by increasing the power losses, oil consumption, and the rate of component replacement. Every year industries must spent millions of dollars in replacing the wear components of machine.

Sufficient is known about wear mechanisms and their solution to encourage greater application of this knowledge. There are, however, a number of problems which cause considerable difficulty in translating the results of research in industrial practice.

Friction and wear are not intrinsic material properties but are the characteristics of the engineering system. Any change in load, speed or environmental conditions may cause catastrophic changes in the wear rate of one or both of the surfaces in contact.

Wear resistance can be improved by developing surface layer on the bulk material. Plasma Ion Nitriding is one of the methods to apply Ion Nitriding layer. This kinds of layer can be different depending on bulk material on which the layer is generated, the operating temperature and

pressure of the gas, its composition and the process time.

Selection of test rigs and procedure is only difficult where simulation of an application is necessary. Under these circumstances it is necessary to consider the important variables. Many types of test rigs are available to make such evaluations.

A new wear testing methodology has been developed which describes the phenomenon of adhesive wear, which is most common in industries. With the development of this methodology it is hoped that wear mechanism can be understood and the knowledge for the selection of materials having a right kind of coating layer for specific application can be gained.

Chapter 2

BACKGROUND

2.1 Wear

Wear can be defined in a variety of ways. One way to define wear is "the deterioration of surface due to use [4]. This, of course, is too broad for a technical definition. The American Society of Lubrication Engineers (ASLE) and others have accepted the definition as "removal of material by mechanical action", while The Organization for Economic Cooperation and Development (OECD) Research Group on wear of Engineering materials defines wear as "progressive loss of substance from the operating surface of a body occurring as a result of relative motion at the surface" [2].

Wear may be either destructive or normal; but even when normal it may be more severe than desirable because of the frequency of parts replacements. No machine member is immune from wear; wear manifests itself whenever there are load and motion. Scuffing of pistons in internal combustion engines, pitting in power transmission gears, fretting in press-fitted assemblies, and cavitation corrosion in cylinder liners are all manifestations of wear [4].

More and more attention is being devoted to the question of what exactly constitute wear, how it should be measured, what interacting factors determine its magnitude, and how it can be minimized and controlled [5].

In this chapter an attempt is made to describe different wear mechanism and the variables that affect the wear mechanism. The information gained in this manner can then be applied to the design of suitable experiments from which quantitative data can be obtained.

2.1.1 Wear Mechanisms

There are several ways to classify wear mechanism. Here the mechanism of wear is classified into five categories as follows

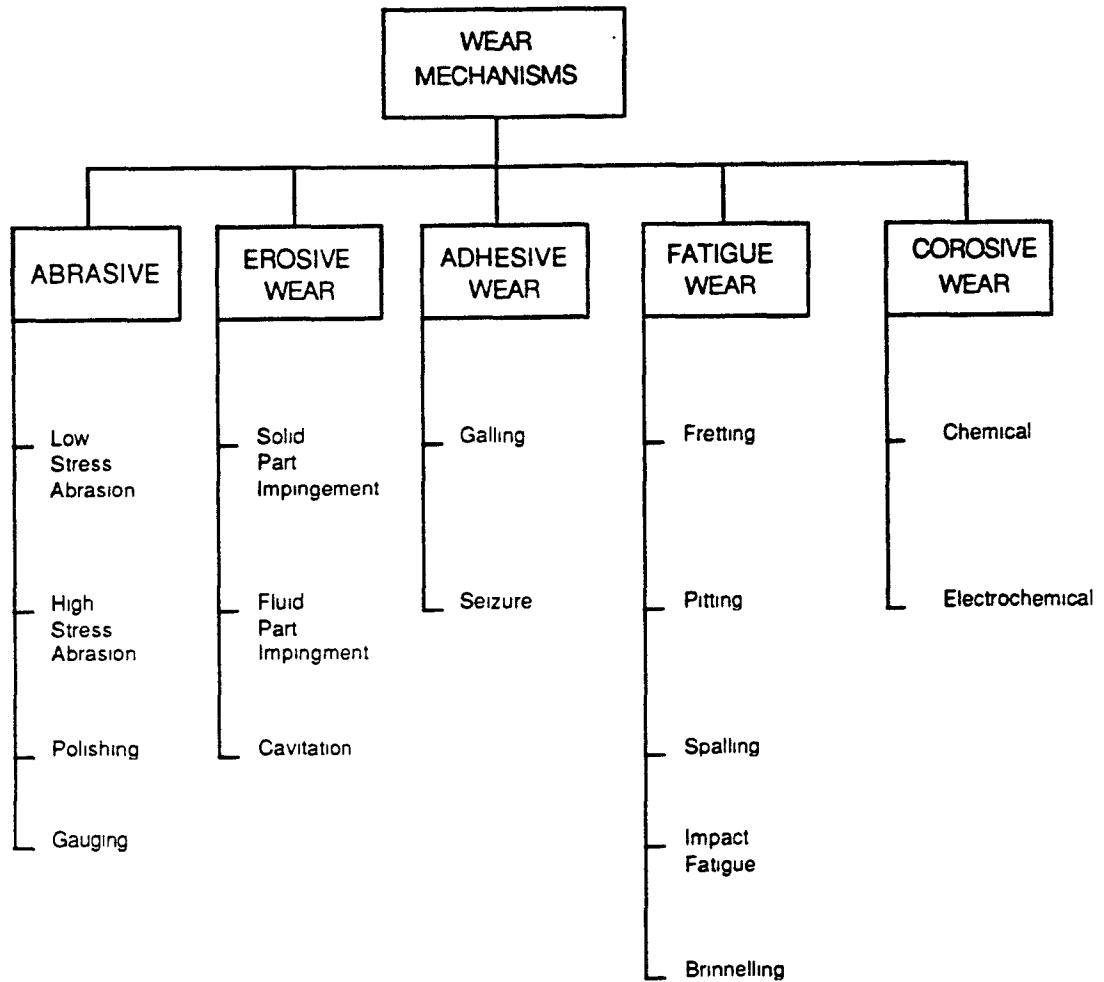
- (i) Abrasive Wear
- (ii) Erosive Wear
- (iii) Adhesive Wear
- (iv) Fatigue Wear
- (v) Corrosive Wear

(i) Abrasive Wear

Wear produced by cutting or ploughing is "abrasive wear", which can be defined as wear due to the penetration and ploughing-out of material from a surface by another body. The degree of penetration is given by:

$$\frac{\text{Load on particle}}{\text{Hardness of the surface}} = \frac{W}{H_v}$$

Table 2.1 Classification of Wear Mechanisms



$$\text{Volume wear} = \frac{W}{H_v} A L$$

where

A = area of cross section of groove

L = Length of the groove

(i) a. Low Stress Abrasion (Or Scratching)

One kind of abrasive wear is low stress abrasion or two body abrasion. This condition operated under low stress condition, with particles being transferred across the surface with little breakdown in particle size of the abrasive. The example of this type of wear is particles sliding and rolling over a conveyor surface.

(i) b. High-Stress Abrasion (Or Grinding)

This results in high stresses because the particles are being deliberately reduced in sizes or trapped between two bearing surfaces. The grains are easily fractured. The broken abrasive grains are sharp and can scratch the hardest type of steel. Deterioration then occurs from scratching, local plastic flow, and microcracking.

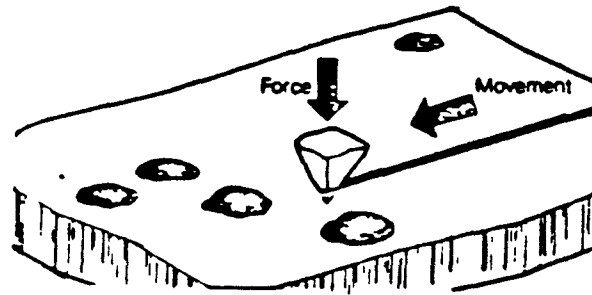


Fig. 2.1 Low - Stress Abrasion

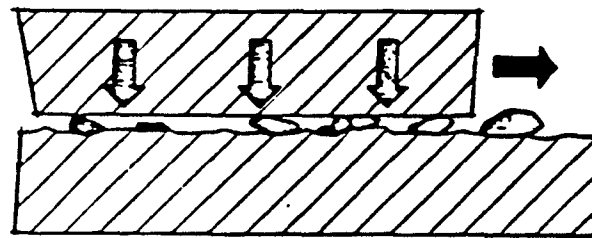


Fig. 2.2 High - Stress Abrasion

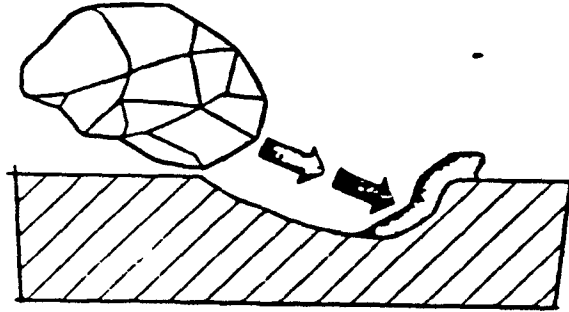


Fig. 2.3 Gauging Abrasion

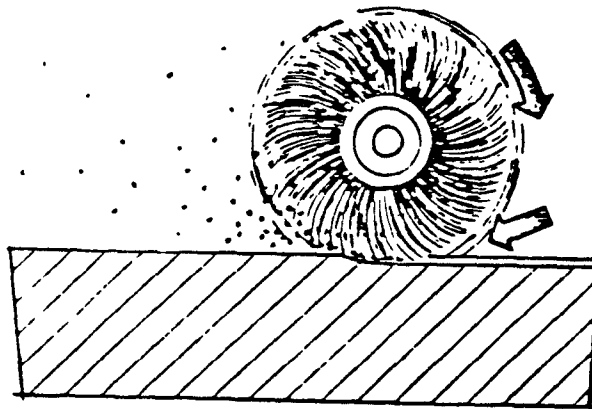


Fig. 2.4 Polishing Wear

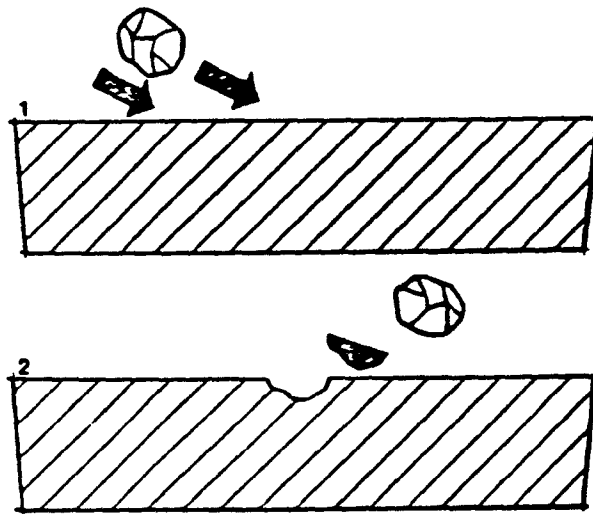


Fig. 2.5 Solid-Particle Impingement

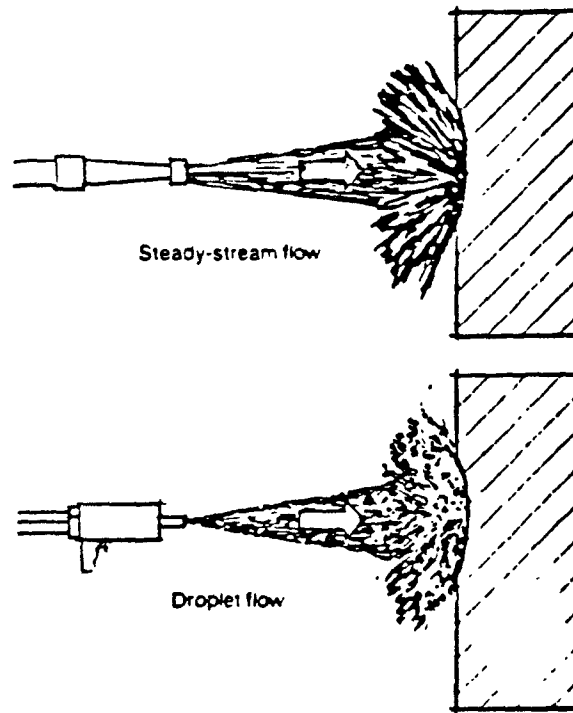


Fig. 2.6 Fluid-Impingement Erosion

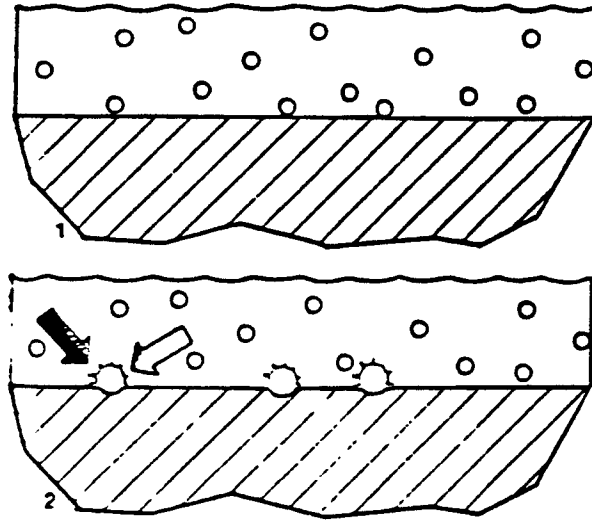


Fig. 2.7 Cavitation

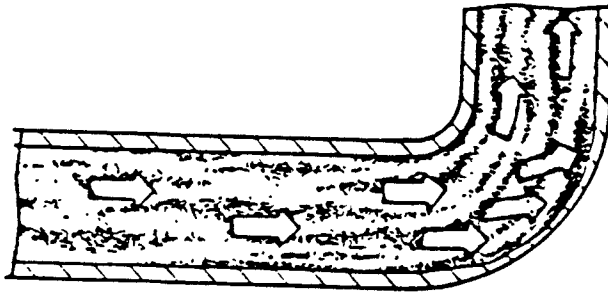


Fig. 2.8 Erosive Wear

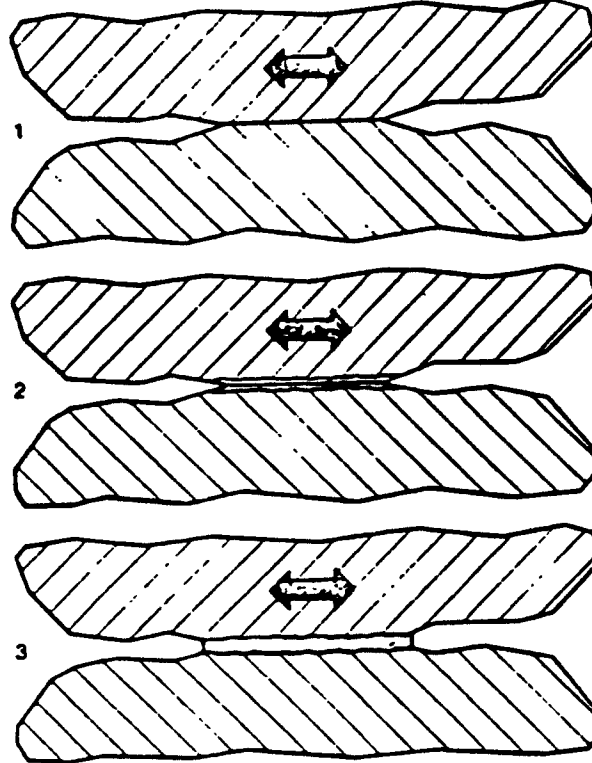


Fig. 2.9 Fretting Wear

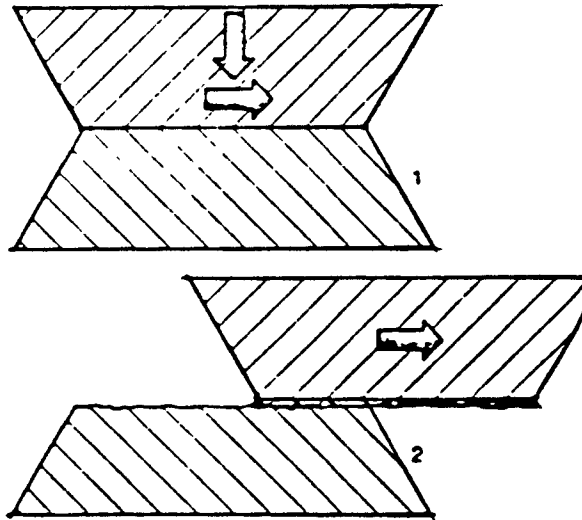


Fig. 2.10 Adhesive Wear

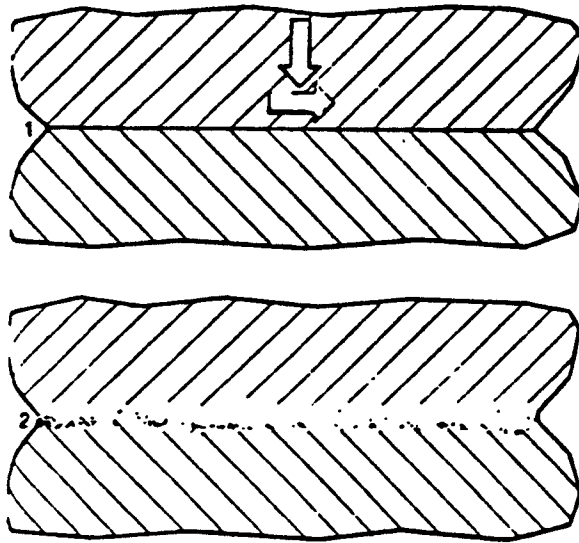


Fig. 2.11 Seizure

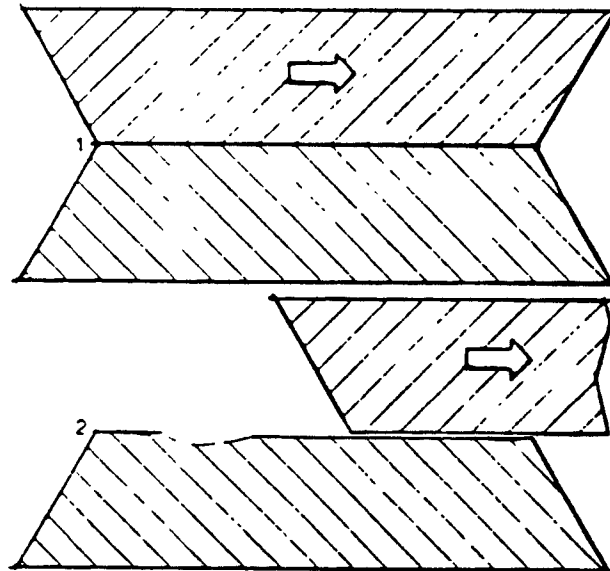


Fig. 2.12 Galling

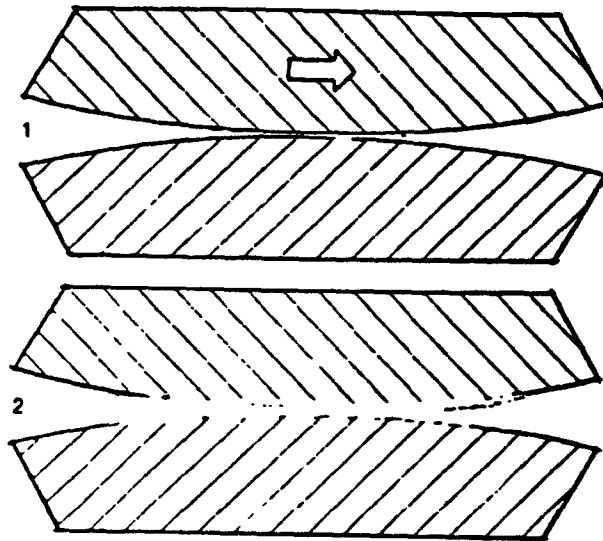


Fig. 2.13 Oxidative Wear

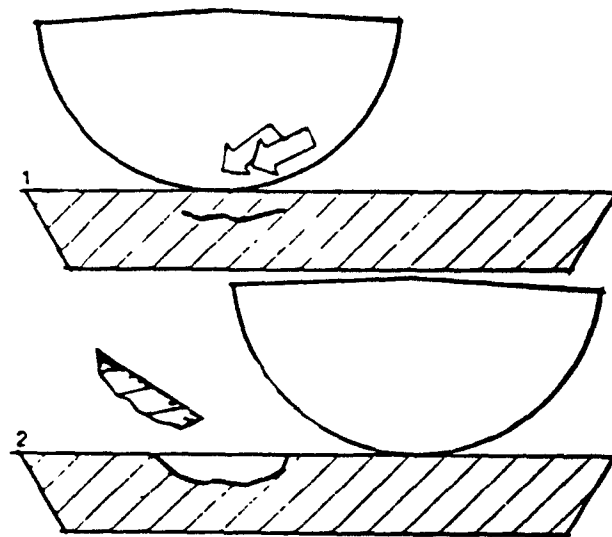


Fig. 2.14 Pitting

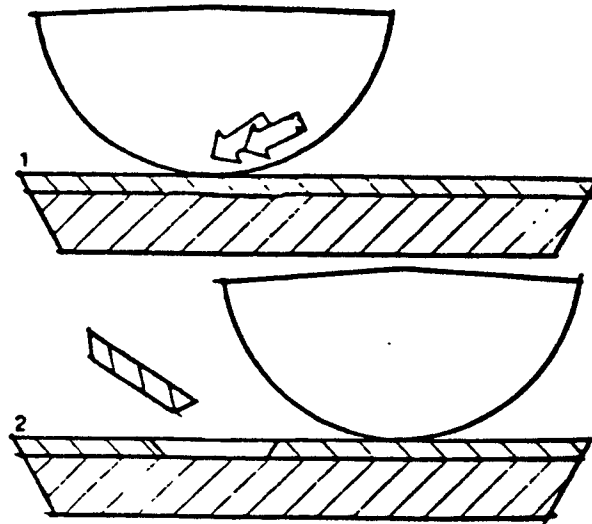


Fig. 2.15 Spalling

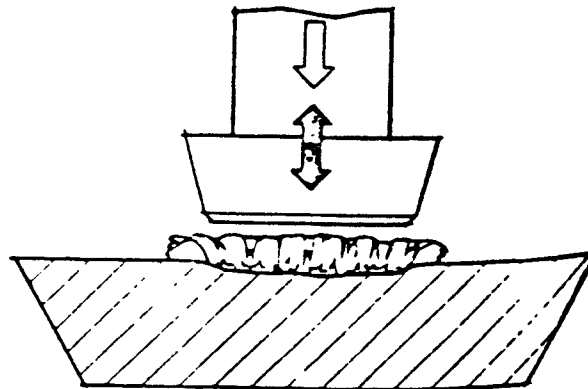


Fig. 2.16 Impact Fatigue

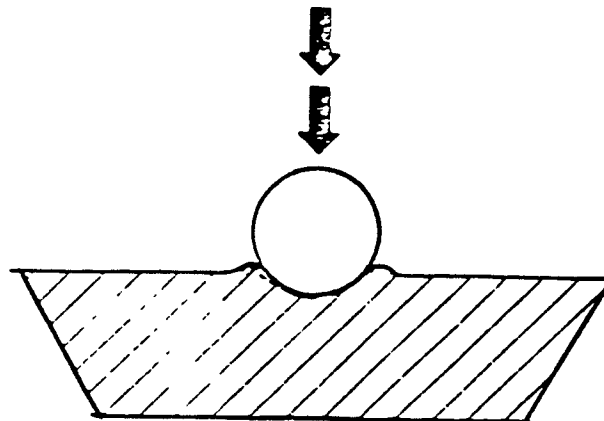


Fig. 2.17 Brinelling

(i) c. Polishing Wear

Polishing wear is characterized by the use of very small abrasive grains, (order of 5 microns or less) on an elastic backing.

(i) d. Gauging

Scratching, scoring and gauging shows the degree of severity. Gauging is characterized by high stress (usually caused by impact) and results in considerable micro-deformation of the surface.

(ii) Erosive Wear

Erosive wear is a form of abrasion which is generally treated rather differently because the contact stresses arises from the kinetic energy of particle flowing in air or liquid stream as it encounters a surface. Measure of kinetic energy is the angle of impact and the size of abrasive.

It could be solid particle impingement or fluid impingement erosion or cavitation which is the formation of bubbles within fluid which has a movement with some solid surface. Cavitation bubbles are formed when static pressure reduced to vapor pressure of liquid, boiling occurs and cavitation bubbles are formed.

(iii) Adhesive Wear

Adhesive wear is the most common form of wear. This is a special form of wear where material is transferred from one surface to the other rather than being removed completely from the interacting system. It occurs when surfaces slide against each other, and the pressure between the contacting asperities is high enough to cause local plastic deformation and adhesion. The sliding motion causes tangential force to fracture the adhered surface and form fragments which are pulled off from one surface to adhere to the other. Later, these fragments may come off the surface on which they are formed and be transferred back to the original surface, or form wear particles. Fig. 2.18 illustrate the mechanism.

The tendency of contacting surfaces to adhere arises from the attractive forces which exist between the surface atoms of the two materials. When clean surfaces are brought into contact a strong chemical bond is formed between them. Ferrante and Smith [13] have reported calculations of adhesive energy and conclude that the range of strong chemical bonding is 0.2nm.

At greater separations than this bodies in close proximity are attracted to each other by Van der waal's forces. Depending on atomic structure of the interacting bodies two groups of forces exist known respectively as the 'retarded' and the 'non-retarded' forces. When the distance between the interacting bodies is below 10^{-8}m the retarded forces operate and the attraction forces are determined by the square of the distance between the surfaces. When the spacing is in the range 10^{-8}m to 10^{-7}m a transition takes place. The

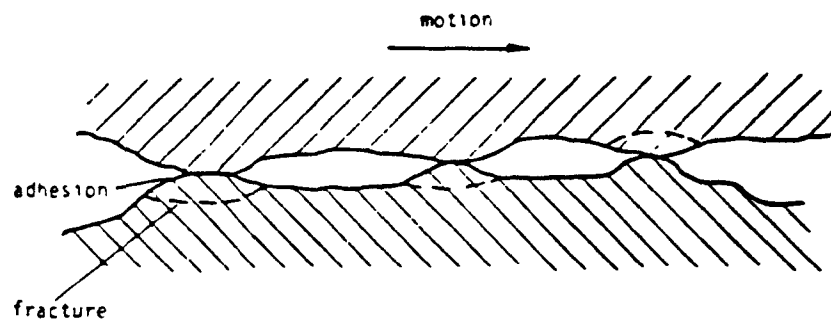


Fig. 2.18 Adhesive Wear

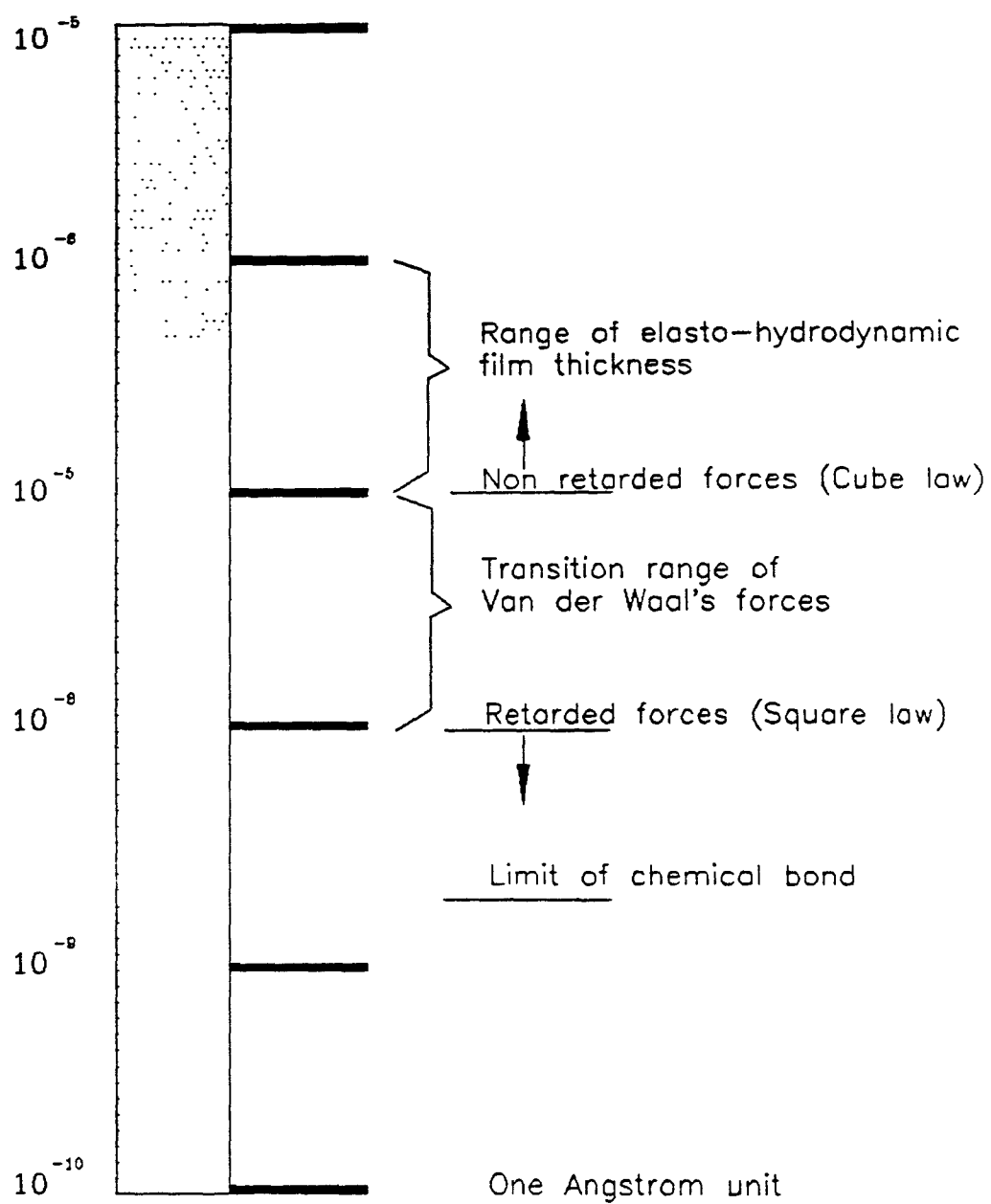


Fig. 2.19 Range of operation of surface forces

'non-retarded' forces act at separations above 10^{-7}m when the Van der waal's forces fall off according to a cube law. See Fig. 2.19.

Adhesion is favored by clean surfaces, non-oxidizing conditions, and by chemical and structural similarities between the sliding couple. Wear decreases if the asperity is harder, because the contact area is lower; increases if the asperity is chemically clean, because bonding and welding is more likely; and increases if the wear couple is mutually soluble.

Rabinowicz has expressed the dependence of adhesion of pure metals on their ability to form solid solution [1].

Wear under adhesive conditions, unlike abrasive wear, is subject to sharp transitions in behavior as load varies. At light loads, a fraction of the metallic junctions welded and sheared according to the welding-shearing-ploughing theory becomes detached to form wear particles. If the load is increased to a value such that the average pressure exceeds about one third of the hardness of the softer metal, a large increase in the volume of wear particles occurs. This is due to the fact that at high loads the true contact area approaches the apparent contact area in size, and a loose wear particles once formed is unable to escape without producing further particles in a self-accelerating process. The accumulation of loose debris therefore leads to a rapid acceleration of the wear process, and the wear particles thus formed are relative fine [5].

Fig. 2.20 shows the abrupt transition from mild to severe wear for a brass pin rubbing on a hard, steel disk [5].

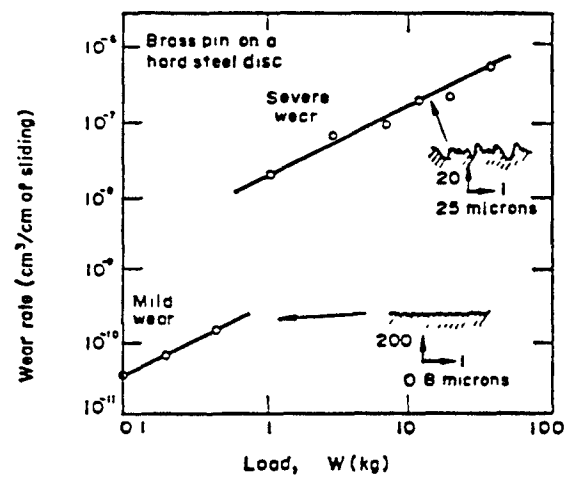


Fig. 2.20 Transition from mild to severe wear by load increase

(iii) a. Seizure

Seizure is a special form of adhesive wear in which a large mass is transferred between contact surfaces. It can also be described as one surface picking up material from the adjacent surface during load and sliding contact.

When metal surfaces are placed together, the area over which they touch is usually very small. As a result, the localized pressure at the points of real contact is finally and sufficiently high to produce plastic flow of the metal. Under these high pressure the diffusion of atoms may occur and form atomic bonds at contact area. This is sometimes called "cold-welding" between the surfaces. These bonds are sheared during sliding and if they are stronger than one of the parent metals, heavy damage may result. As long as sliding goes on the atomic bonds are continuously formed and sheared, and heat is generated by friction. Without stopping relative rotation, instantaneous heating and fast cooling of the small contact area at high pressure condition causes elastic-plastic deformation at asperity tips, cold work hardening, recrystallization, and mutual diffusion at contact surfaces.

(iv) Fatigue Wear

Fatigue results when repeated sliding, rolling, or impacting motions subject a surface to repeated cycles of stress. The stress cycles initiate cracks in or near the surface which, with time, spread, link up and form discrete particles, free to move between the contacting surfaces.

(iv) a. Fretting

Fretting is a form of surface change which occurs when surfaces which are loaded against each other undergo small amplitude oscillatory slop. Because of the oscillatory small amplitude motion (130 microns) the surfaces are never brought out of contact and therefore there is little opportunity for the loose particles to escape and cause increased wear of surface by abrasion. Seizure may result because of the blockage of the free space and prevention of the further lubrication.

(iv) b. Pitting

Pitting is defined as surface fatigue failure of the material as a results of repeated surface or subsurface stresses that exceed the endurance limit of the material. It is characterized by the removal of metal and the formation of cavities. These cavities can be small and can remain small. They may be small initially and then combine or increase in size.

(iv) c. Spalling

Spalling is generally considered a special form of destructive pitting. Large pits formed by the joining of smaller adjacent pits due to failure of the adjoining material is type of spalling. Other forms are characterized by more of a flaking of the surface larger with the fractured surface running substantially parallel to the original surface. Flaking is usually associated with

a severe stress gradient near the surface.

(v) Corrosive Wear

Corrosive wear has been defined as a wear process in which chemical and electrochemical reaction with the environment predominates.

Because the wear rate of a corroded surface, and the corrosion of worn surface will often be higher than that of an unworn surface, the total rate of loss of material in corrosive wear can be high and the resulting problems can be very serious.

There might be other possible classification of wear process. Kislik [8] uses a classification based upon sliding process: (a) mechanical destruction of interlocking asperities, (b) asperity fatigue, (c) failure due to working, (d) flaking of oxide films, (e) molecular interaction, and (f) mechanical destruction due to high temperature [2].

Kragelskii [9] suggests that the proper classification should be based upon the way the junctions are broken; that is, elastic displacement, plastic displacement, cutting, destruction of surface films, and destruction of bulk material. Archard [10] suggests a classification which distinguish between elastic and plastic deformation of the contact area and between surface and bulk material effects.

Wear has also been classified into categories based upon the results

achieved. Archard and Hirst [11] use "mild" and "sever" which distinguishes whether a material combination can or cannot be used.

Peterson [12] suggest that the classification should be based upon how the particle is removed and whether the event takes place at the asperity level, in bulk, or via a surface film.

Whatever classification system might be adopted, it is felt that one is essential for the orderly collection of scientific information, the adoption of standard test devices and procedures, and the solution of service wear problems.

2.1.2 Wear Measurement

Wear debris can be measured either as a weight loss or as a change in volume or dimension of one or both sliding members. The following six wear criteria have been proposed and used [5]:

1. *Linear wear rate*

$$K_L = \frac{\text{thickness of layer removed}}{\text{sliding distance}} = \frac{h}{L}$$

2. *Volumetric wear rate*

$$K_v = \frac{\text{volume of layer removed}}{\text{sliding distance} \times \text{apparent area}} = \frac{\Delta v}{LA_a}$$

3. Energetic wear rate

$$K_E = \frac{\text{volume of layer removed}}{\text{work of friction}} = \frac{\Delta v}{FL}$$

4. Gravimetric wear rate

$$K_W = \frac{\text{weight of layer removed}}{\text{sliding distance} \times \text{apparent area}} = \frac{\Delta W}{LA_a}$$

5. Abradability

$$\gamma = \frac{\text{volume abraded}}{\text{work of friction}} = \frac{\Delta v}{FL} = \frac{\Delta v}{fWL} = \frac{(\Delta v/WL)}{f} = \frac{A'}{f}$$

6. Coefficient of abrasion resistance

$$\beta = \frac{\text{work of friction}}{\text{volume abraded}} = \frac{1}{\gamma} = \frac{1}{K_E} = \frac{f}{A'}$$

where

L is the sliding distance, F the friction force, f the coefficient of sliding friction, and A' the abrasion factor.

2.2 Wear Testing Devices

The selection of a wear test depends not only on the mode of wear

being investigated but also on the objective of the test. For wear testing the first choice to make is the selection of a suitable wear testing machine. It has become essential that the best wear test is one that closely approximates the actual conditions encountered in service. Simulative testing is one of the most difficult areas in tribology. This difficulty is a consequences of the complexity of tribological processes and the large number of influencing parameter. Fig. 2.21 shows a schematic outline for simulative tribo-testing.

However, most wear tests are done using simplified geometry arrangements of specimens such as shown in the figure 2.22 in a collection of friction and wear devices edited by the American Society of Lubrication Engineers (ASLE), the various test devices can be classified according to their geometry into the following groups:

- (1) Multiple Sphere
- (2) Crossed Cylinders
- (3) Pin on Flat (reciprocating or linear motion)
 - (a) Moving Pin
 - (b) Moving Flat
 - (c) Multiple Contact

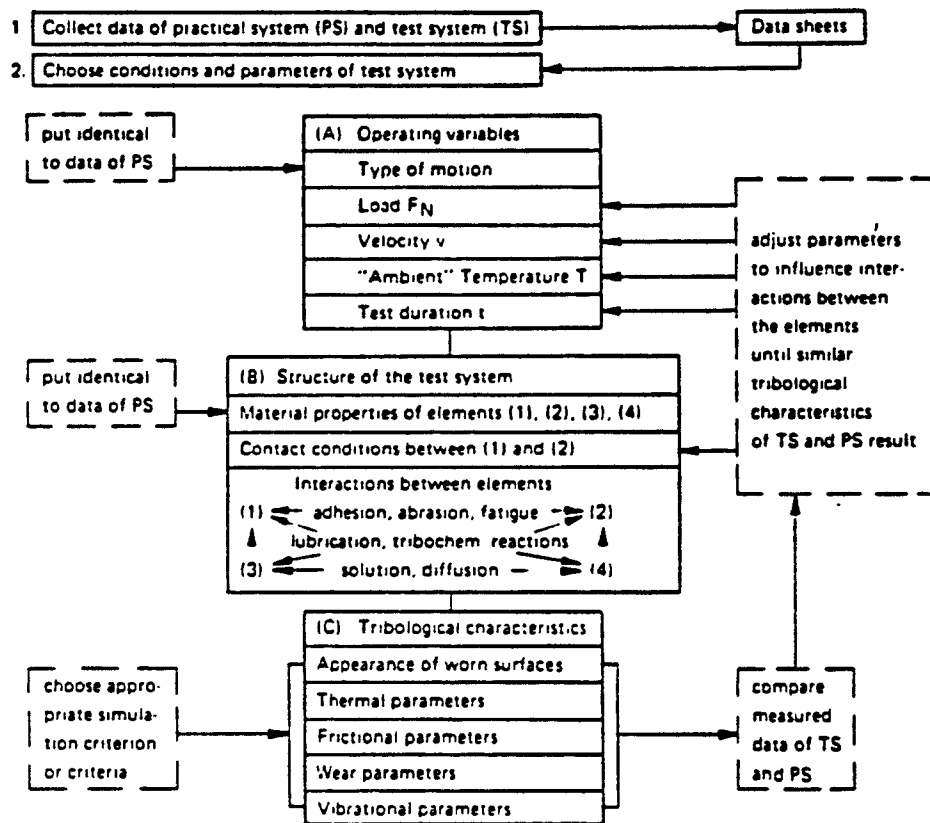


Fig. 2.21 Schematic outline for simulative tribo-testing

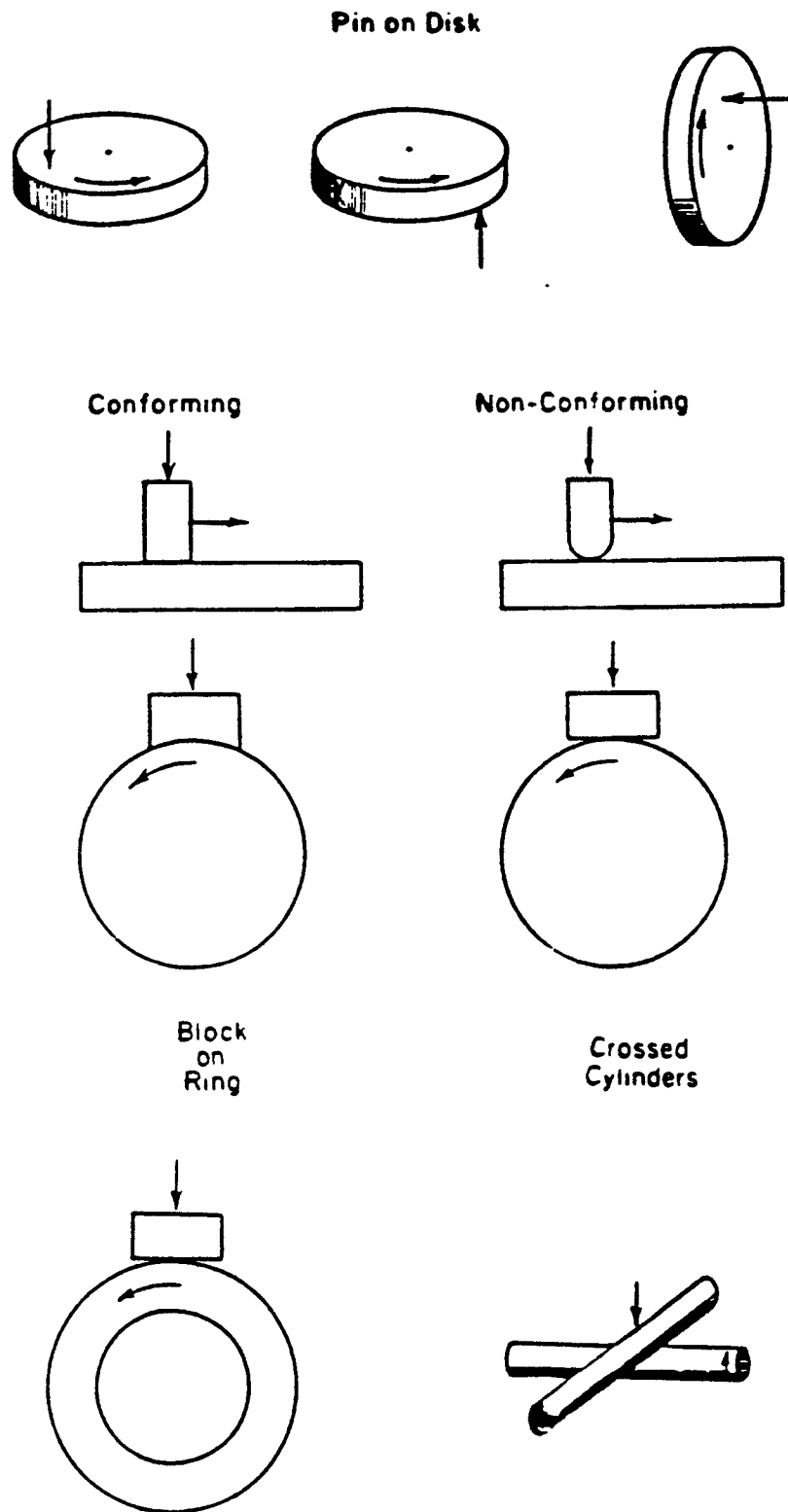


Fig. 2.22 Examples of geometric arrangement of wear testing machine

- (4) Flat on Flat (reciprocating or linear motion)
- (5) Rotating Pins on Disk (face load)
- (6) Pin on Rotating Disk (face load)
- (7) Cylinder on Cylinder (face load)
- (8) Cylinder on Pin on Rotating Cylinder (edge load)
- (9) Rectangular Flat on Rotating Cylinder (edge load)
- (10) Disk on Disk (edge load)
- (11) Multiple Specimen
- (12) Miscellaneous

The other considerations are numerous. The mode of sliding can be unidirectional as in simple rotating systems, or it can be oscillating.

In the following section some of the wear testing machines and their geometrical arrangements are mentioned.

2.2.1 Rotating Disc Assemblies

It consists of a horizontal rotating disc with a superimposed circular sample usually of metallic or elastomeric composition. The mating surface is usually a cone, sphere, or cylindrical pin fabricated from a hard material (typically a metal), and it is mounted as shown on a balanced lever arm and loaded against the rotating surface. Friction force is commonly measured by strain gauges mounted on the vertical sides of the lever arm in such a manner as to record the horizontal bending stresses induced in the latter. The normal load may be applied as a dead weight as shown or by a hydraulic cylinder device.

The most serious difficulties arise from vibrations of the lever arm which applies the normal load to the sample and grooving of the rotating disc after a relatively small number of revolutions. One drawback of the rotating disc method is the curved path of points on the surface of the disc as they come into contact with the mating frictional slider. To avoid the consequent distortion of the contact area itself, the area of the latter must be quite small. There is further disadvantage that it is virtually impossible to control lubricant film thickness on a rotating disc because of centrifugal acceleration effects.

2.2.2 External and Internal Drum Equipment

The use of either external or internal drum equipment for measuring frictional force represents a more precise and somewhat more

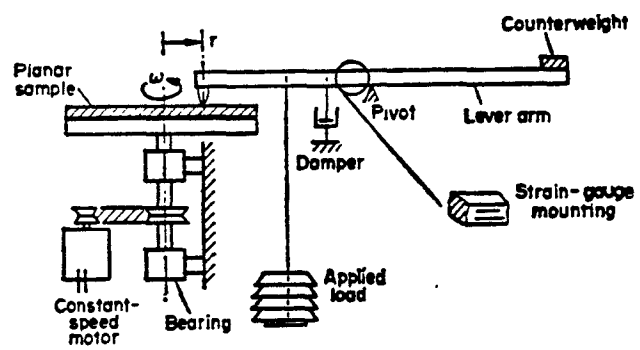


Fig. 2.23 A simple rotating disc assembly for friction measurement

complex experimental approach. External drums are more accessible for dismantling or assembling the slider head, but at higher speeds it is impossible to sustain a lubricant film on the external drum surface because of centrifugal effects. By contrast internal drums provide a stable lubricant film, and the degree of uniformity of film thickness increases with rotational speed.

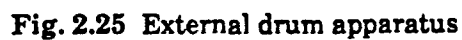
Fig. 2.24 shows a schematic arrangement of an internal drum apparatus and associated equipment. The load is applied in this case by means of weights and the drum is driven by an electric motor

The frictional force at the surface produces very small deflections in a steel support block, and these in turn are measured by four temperature-compensated strain gauges. The output signal is then amplified and recorded.

An external drum apparatus is reported by R. Blickensderfer and G. Laird II in 1988 in which they represent the type of abrasive wear test in which the end of a pin test specimen is rubbed against a surface covered with abrasive cloth or abrasive paper.

A general view of the equipment is shown in Fig. 2.25. The major components of the equipment are identified in the figure. A carriage rotates the test specimen at 17 rpm while it slowly traverses the length of the rotating drum covered with abrasive cloth. The carriage also has provision for loading the specimen with dead weights.

One distinct disadvantage of internal and external drum equipment is



the curvature of the drum itself. Although not a serious problem in applications, corrections must be made from drum curvature in instances where contact takes place over an appreciable length of drum circumference.

The flat-belt apparatus is used in cases where we wish to eliminate entirely the effects of drum curvature.

2.2.3 Flat-Belt Apparatus

Fig. 2.26 shows the general layout of a flat-belt apparatus, consisting essentially of a flexible belt passing over two large cylinders. The belt itself may be of fabric, rubber, steel strip, or some reinforced composite material, and a surface texture may be incorporated into it either during manufacture or by glueing sandpaper or abrasive sheeting on to one side after assembly of the apparatus.

The normal load on the test sample is supplied by a hydraulic cylinder. A friction load cell mounted alongside one of the guides is calibrated to record frictional force.

The great advantage of the system is the absence of curvature in the contact patch. However, difficulties may arise if the vertical distance between the line-of-action of the friction load cell and the plane of friction is not kept to a minimum value because such distance produces a couple which effectively modifies the applied load. One limitation is the bursting strength

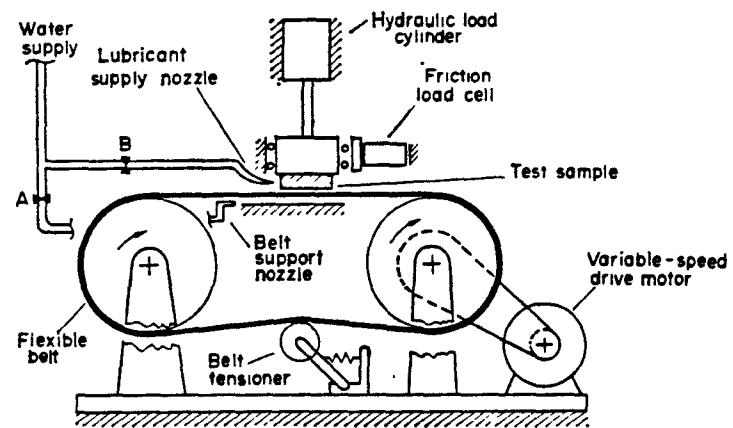


Fig. 2.26 General layout of flat-belt apparatus

of the belt itself. A more practical limitation is rapid wear of the sample particularly if the belt has a rough or emery-type texture and if an interfacial lubricant is not used between sample and belt.

2.2.4 Reciprocating Sliding Machines

The machine shown in Fig. 2.27 has a reciprocating method of measuring wear and abrasion. The apparatus consists of a traveling platform which is driven at constant speed by a motor and variable-speed transmission. The base track on which the platform slides is mounted on a pedestal and contains a flat horizontal plate resting on frictionless rollers. The platform contains a vertical air cylinder for load. Various asperity shapes (hemispheres, cones etc.) of different sizes may be mounted at the end of the plunger. The friction force between the slider and the rubber track is at the longitudinal motion of the plate.

Another simple reciprocating machine for measuring wear is reported by G. Sridharan. The device is an attachment to a shaping machine. The unit shown in Fig. 2.28 is held by tool post attached to the arm of the shaping machine. The mechanism provides a constant, downward vertical force.

The wear rate is computed using the volume of the material worn out. In this kind of device no provision is given for measuring frictional force so it cannot be applicable where frictional force is required to be measured.

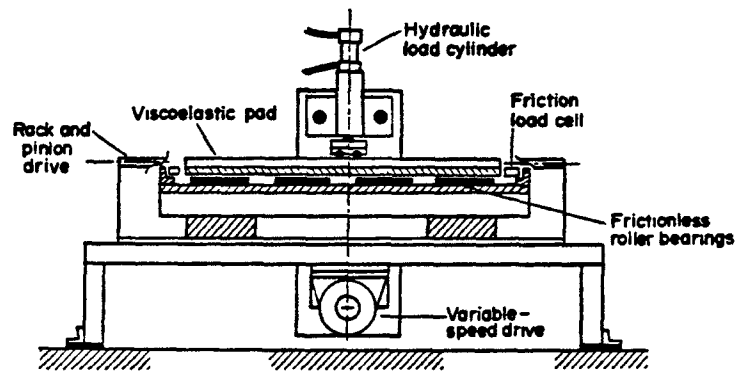


Fig. 2.27 Reciprocating wear and abrasion machine

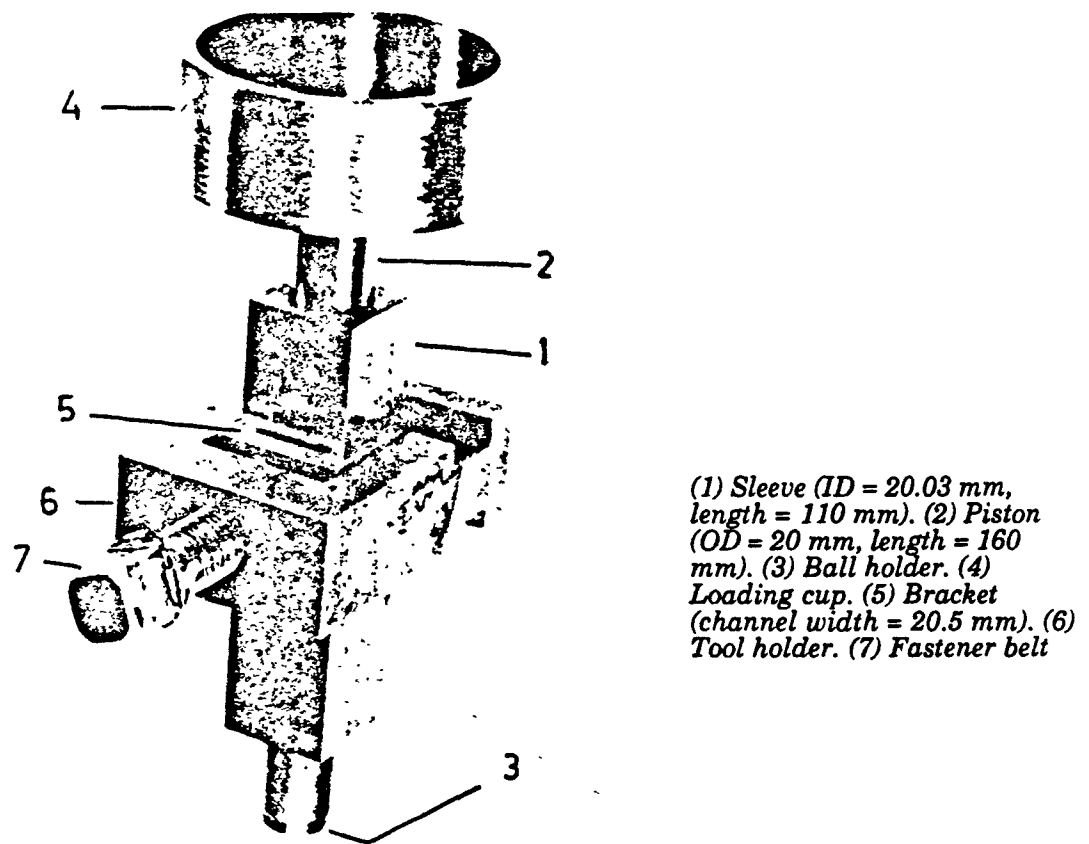


Fig. 2.28 Attachment of shaping machine

2.3 Goals and Objective

The goal of this work is to improve existing computer controlled wear testing methodology by designing, manufacturing and assembling loading-unloading mechanism. The new shoe and shoe holder are to be designed and installed on existing machine. This work also includes the modification of reducer by replacing existing high speed shaft to make gear reducer suspended, and low speed shaft so that the roller can be attached to one end of this shaft.

Another goal is using modified wear testing machine to test differently treated specimens to defined their wear resistance, friction coefficient and change in surface roughness.

Chapter 3

IMPROVEMENT OF WEAR TESTING MACHINE AND ITS METHODOLOGY

3.1 Introduction

The wear testing methodology is based on the reaction produced in the stator of a suspended motor, when the load is applied to its shaft. If the shaft is made to rotate a roller, any resistance for shaft rotation will cause the body of the motor to rotate in a direction opposite to that of the shaft. By deducing this reaction, the losses caused by friction in the area of load and slide contact between engaged roller and shoe can be found after eliminating the total loss in the system.

So the power generated at roller,

$$P_f = P_m \eta \quad (3.1)$$

where P_m is power generated by motor and η is efficiency of whole system.

But
$$P_f = \frac{T_f N_r}{63000} \quad (3.2)$$

$$P_m = \frac{M_m N}{63000} \quad (3.3)$$

where T_f is the torque generated by friction, N_r and N is the rotational speed of the roller and motor respectively, and M_m is moment at the motor.

$$T_f = F_f r \quad (3.4)$$

Where F_f is the frictional force and r is the radius of the roller.

The friction force is equal to the friction coefficient, f , times the normal applied load W .

$$F_f = f W \quad (3.5)$$

Substituting (3.2) and (3.3) in (3.1)

$$\frac{T_f N_r}{63000} = \frac{M_m N}{63000} \eta \quad (3.6)$$

Substituting (3.4) and (3.5) in (3.6)

$$F_f r N_r = M_m N \eta \quad (3.7)$$

$$\text{or} \quad F_f = \frac{N}{N_r} \frac{\eta}{r} \frac{1}{W} M_m \quad (3.8)$$

since input load W , η , r , N , N_r are constant

$$F_f = K' M_m \quad (3.9)$$

$$f = KM_m \quad (3.10)$$

where

$$K' = \frac{N}{N_r} \frac{\eta}{r} \quad (3.11)$$

and

$$K = \frac{N}{N_r} \frac{\eta}{r} \frac{1}{W} \quad (3.12)$$

3.2. General Description of Wear Testing Machine

A general view of wear testing machine is shown in Fig. 3.1. A one horse power, 1750 rpm, three phase induction motor is suspended between two pillow block bearings. One end of the motor is connected to a mechanical counter which is capable of recording number of revolution. Other end of the motor is coupled to parallel shaft gear reducer with a total reduction capacity of 6.3 : 1. The other end of the reducer is coupled to the shaft to which the roller is fixed. The shoe is fixed directly below the roller, to the shoe holder of the loading mechanism.

The shoe holder is attached to a linear bearing which is connected to loading and unloading mechanism. The loading and unloading mechanism consists of levers, cam and follower, and a D.C. motor for driving cam.

⊠ : BEARING

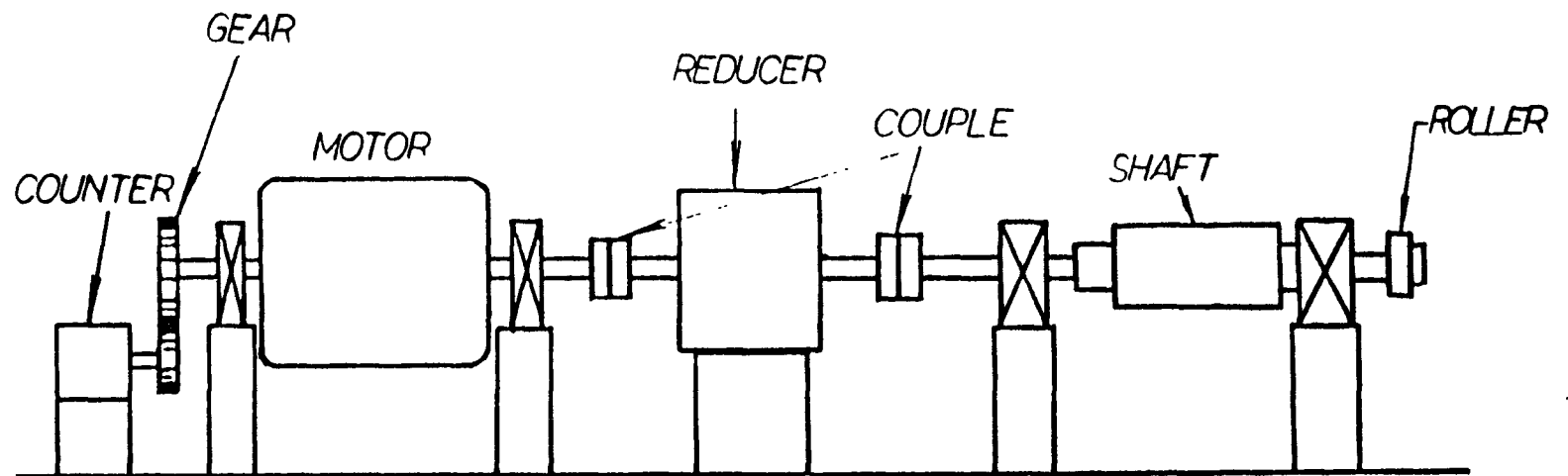


Fig. 3.1 General view of wear testing machine

The whole unit consisting of motor, reducer, shaft with roller, loading and unloading mechanism and counter, is mounted on a rigid steel table to prevent any vibration caused during the test runs. The output unit which consists of a steel bar with strain gages that show the moment produced in the motor shaft is attached to the motor. The change of this moment is recorded by a computer through a strain gage meter. A Programmable Logical Controller has been programmed to run the entire test automatically.

3.3 Modification of the Testing Machine

3.3.1 Loading and Unloading Mechanism

The main assembly of loading and unloading mechanism can be divided into three subassemblies.

1. Sliding System.
2. Lever Mechanism.
3. Driving System.

The sliding system consists of a shoe holder and a sliding bearing. A new shoe holder is designed that provides a new geometrical arrangement for testing, that is, flat on roller. The design feature of this shoe holder is described in section 3.3.3.

The LWA 30C linear bearing is used for smooth vibrationless vertical movement. The precision of this bearing is 0.06 mm and friction coefficient is 0.004-0.006.

The lever mechanism consists of three levers. The input load is applied at the end of lever 1 which has a ratio of 1:12. Levers 2 and 3 are identical and have ratios of 2:3 and 1:4 respectively. The overall magnification factor of this lever mechanism is 1 : 72. These three levers are connected to each other by means of links. The free end of the output lever 3 is connected to the linear bearing.

The main parts of the driving system are D.C. motor, cam, follower, a frame that holds follower, and guides which provide motion in only one plane.

The assembly of this system is shown in Fig. 3.2. The follower consists of a roller which is attached to one end of a rod. The height of the rod, which is clamped to a frame, can be adjusted according to the height of the specimen. An attachment is given at the bottom part of the frame for connecting the lever as well as for hanging the loads. Guide slots are provided on each side of the frame so that guide pins keep the motion of the frame in vertical direction only.

A cam is attached to a D.C. motor. The motion of the cam can be controlled by manually as well as by PLC for loading and unloading position.

45

3.3.2 Design of Cam

Since the loading and unloading of the specimen was required at exactly the same time when computer starts and ends taking reading from the strain gage a high speed cam with good accelerating properties was required. A high order polynomial curve is chosen for this purpose. The seven degree polynomial curve for cam profile is given as follow.

$$y = h [35 (\frac{\theta}{\beta_1})^4 - 84 (\frac{\theta}{\beta_1})^5 + 70 (\frac{\theta}{\beta_1})^6 - 20 (\frac{\theta}{\beta_1})^7] \quad (3.13)$$

$$v = \frac{h}{T_1} [140 (\frac{\theta}{\beta_1})^3 - 420 (\frac{\theta}{\beta_1})^4 + 420 (\frac{\theta}{\beta_1})^5 - 140 (\frac{\theta}{\beta_1})^6] \quad (3.14)$$

$$a = \frac{h}{T_1^2} [420 (\frac{\theta}{\beta_1})^2 - 1680 (\frac{\theta}{\beta_1})^3 + 2100 (\frac{\theta}{\beta_1})^4 - 840 (\frac{\theta}{\beta_1})^5] \quad (3.15)$$

where β_1 is rising angle.

The equations shown below are for returning cam curve design :

$$y = h [1 - 35 (\frac{\theta}{\beta_2})^4 + 84 (\frac{\theta}{\beta_2})^5 - 70 (\frac{\theta}{\beta_2})^6 + 20 (\frac{\theta}{\beta_2})^7] \quad (3.16)$$

$$v = \frac{h}{T_2} [- 140 (\frac{\theta}{\beta_2})^3 + 420 (\frac{\theta}{\beta_2})^4 - 420 (\frac{\theta}{\beta_2})^5 + 140 (\frac{\theta}{\beta_2})^6] \quad (3.17)$$

$$a = \frac{h}{T_2^2} [- 420 (\frac{\theta}{\beta_2})^2 + 1680 (\frac{\theta}{\beta_2})^3 - 2100 (\frac{\theta}{\beta_2})^4 + 840 (\frac{\theta}{\beta_2})^5] \quad (3.18)$$

where β_2 is returning angle.

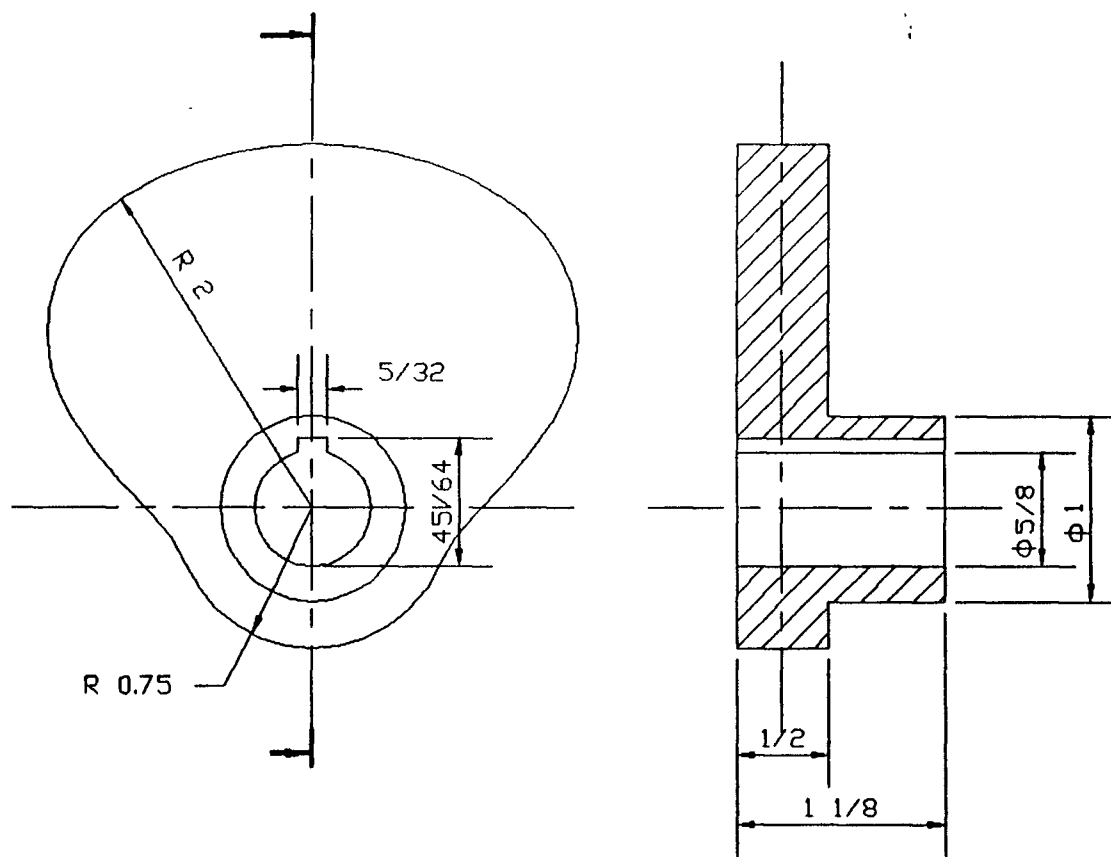
With the help of a C program, 360 coordinates of this profile are generated. A listing of these coordinates is given in the appendix.

3.3.2.1 Manufacturing of Cam

To cut cam on CNC milling machine with 360 different x-y coordinates is somewhat time consuming and less efficient. Moreover, a CNC program with this approach requires a lot of memory. To avoid this situation the whole profile is divided into 9 regular arcs. The starting point, end point and radii of these arcs are obtained with VersaCAD software on computer so that this profile exactly overlaps the 360 coordinates. Fig. 3.3 shows the profile of this cam.

To make cam manufacturing more effective and extremely precise, the whole geometry is transferred to SmartCAM software. In this mode tool radius, tool compensation, feed rate and spindle speed are set and a CNC code is generated from this software. Table 3.1 shows this CNC code.

Later the cam is cut on NASA CNC milling machine.



NEW JERSEY INSTITUTE OF TECHNOLOGY
MECHANICAL ENGINEERING DEPARTMENT

SCALE: 1 : 1	APPROVED BY:	DRAWN BY: M.FAROOQ
DATE: 11/2/89	DR. DUBROVSKY	REVISED BY:

CAM

QTY

1

ALL DIMENSIONS ARE IN INCHES

DRAWING NO:
WTM 2-013-90-04

Fig. 3.3 Cam

Table 3.1 CNC Code for Cam

Line Number	Command				
N0	G92	X0	Y0	Z0	
N10	M3				
N20	G90	G0	G17	F50	S1200
N30	G41	X2	Y0.25		T1.1
N40				Z-0.7	
N50	G01			Z-0.8	
N60	G02	X1.3120	Y0.7014		R0.75
N70	G03	X1.1222	Y0.9694		R0.8
N80	G02	X0.6931	Y1.4858		R2.6
N90		X0.9730	Y2.6608		R0.8438
N100		X3.0270	Y2.6608		R2.0
N110		X3.3069	Y1.4858		R0.8438
N120		X2.8778	Y0.9694		R2.6
N130	G03	X2.6880	Y0.7012		R0.8
N140	G02	X2.0000	Y0.2500		R0.75
N150	G40				
N160	G00			Z0	
N170		X0	Y0		
N180	M02				

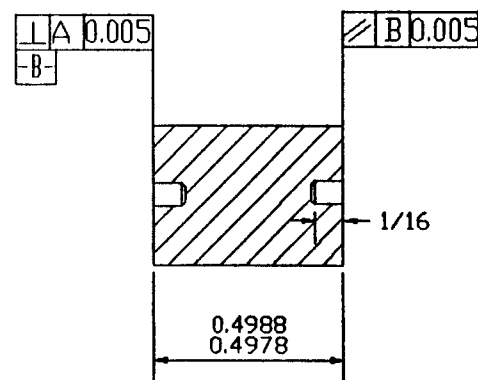
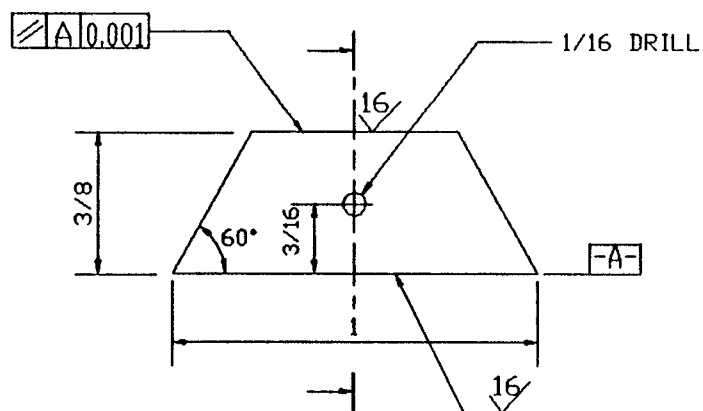
3.3.3 Design of Shoe Holder

The old shoe holder is replaced by a new shoe holder. This shoe holder holds the newly designed specimen for tests. The necessity of the new design of specimen arises from the fact that more number of specimen can be manufactured from the given piece of material as compared to the old design. The specimen is shown in Fig. 3.4

During wear testing, after some preset interval of time, the specimen has to be taken out from the fixture for analysis purposes. Since very high friction force is acting in the area of contact, the specimen as well as the shoe holder become very hot. So the main feature of the design should be that specimen can be removed and put back into the holder with least effort and without consuming much time. The new design provides these both options. Now the tester can loose and take out the specimen with the help of a clip in no time. Moreover it provides the firm grip for specimen when the test is running. The assembly of this design is shown in Fig. 3.5.

3.3.4 Design of Shafts for Reducer

A new parallel shaft reducer is to be installed on wear testing machine. This reducer which has a roller attached to its output shaft will be used for new geometrical arrangement for wear testing specimen i.e. roller to roller. This is shown in Fig. 3.7.



NEW JERSEY INSTITUTE OF TECHNOLOGY
MECHANICAL ENGINEERING DEPARTMENT

SCALE: 2 : 1

APPROVED BY:

DRAWN BY: FAROOQ

DATE: 6/5/90

R DUBROVSKY

REVISED BY:

SHOE

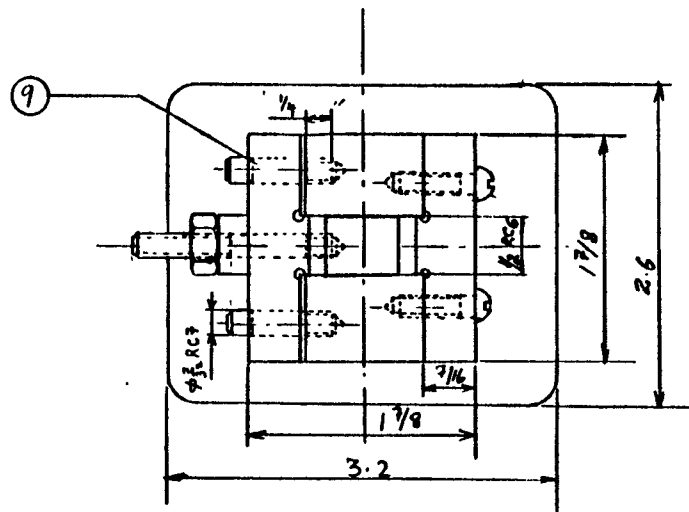
QTY

ALL DIMENSIONS ARE IN INCHES

DRAWING NO:

WTM 00-09N-01N-01

Fig. 3.4 Shoe (specimen)



9	WTM-00-09N-09N-09	GUIDE PIN	2	
8	WTM-00-09N-09N-09	BODY	1	
7	WTM-00-09N-09N-09	PIN	1	
6		HEX NUT 0.19-32 UNF	1	
5		C-WASHER 0.2 - $\frac{3}{8}$ - $\frac{1}{4}$	1	
4	WTM-00-09N-09N-09	LEFT SIDE CLAMP	1	
3		RD HD M/C SCR EW 0.19-32 UNF	2	
2	WTM-00-09N-09N-09	RIGHT SIDE CLAMP	1	
1	WTM-00-09N-09N-09	SHOE	1	
P/N	DRAWING NO	PART NAME	NO REC	MATERIAL

NEW JERSEY INSTITUTE OF TECHNOLOGY			
MECH. ENG. DEPARTMENT			
SCALE 1:1	APPROVED BY <u>RI</u>		DRAWN BY FAROOQ
DATE 6/4/90			REWSED BY
SHOE HOLDER		QTY	1
ALL DIMENSIONS ARE IN INCHES		DRAWING NO WTM 00-01N - 01N	

Fig. 3.5 Shoe holder

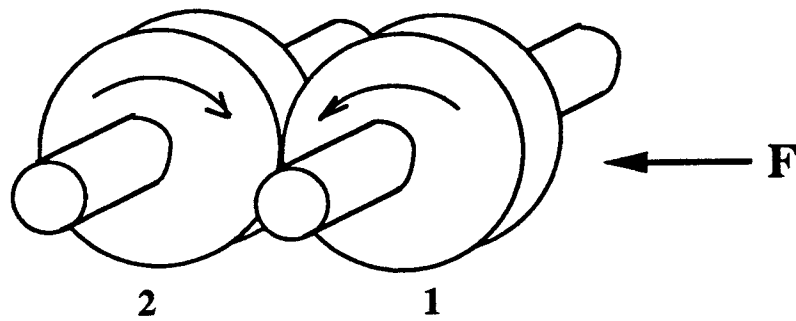


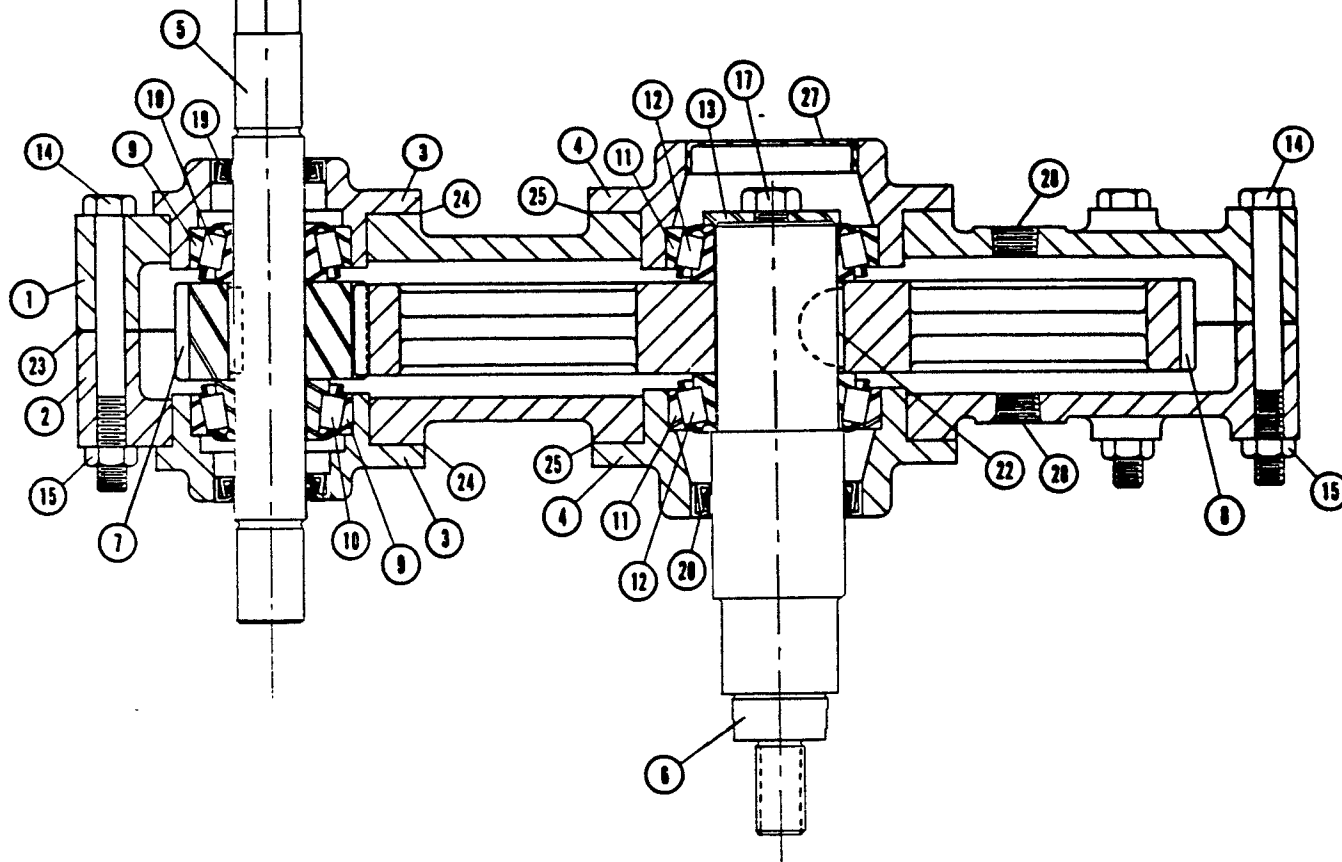
Fig. 3.6 Roller to roller contact

For this purpose Hub City parallel shaft drive Model 240 which has a reduction capacity of 6:1 is chosen. According to the wear testing methodology used in this wear research, the reducer with roller 1 should not be rigidly held. It should be suspended from high speed shaft on pillow blocks so that a linear load can be applied to the other end and causing roller 1 to exert a force on roller 2. The main advantage of this suspension is that at any moment of operation the applied load can be kept under control. The modified reducer is shown in Fig. 3.6.

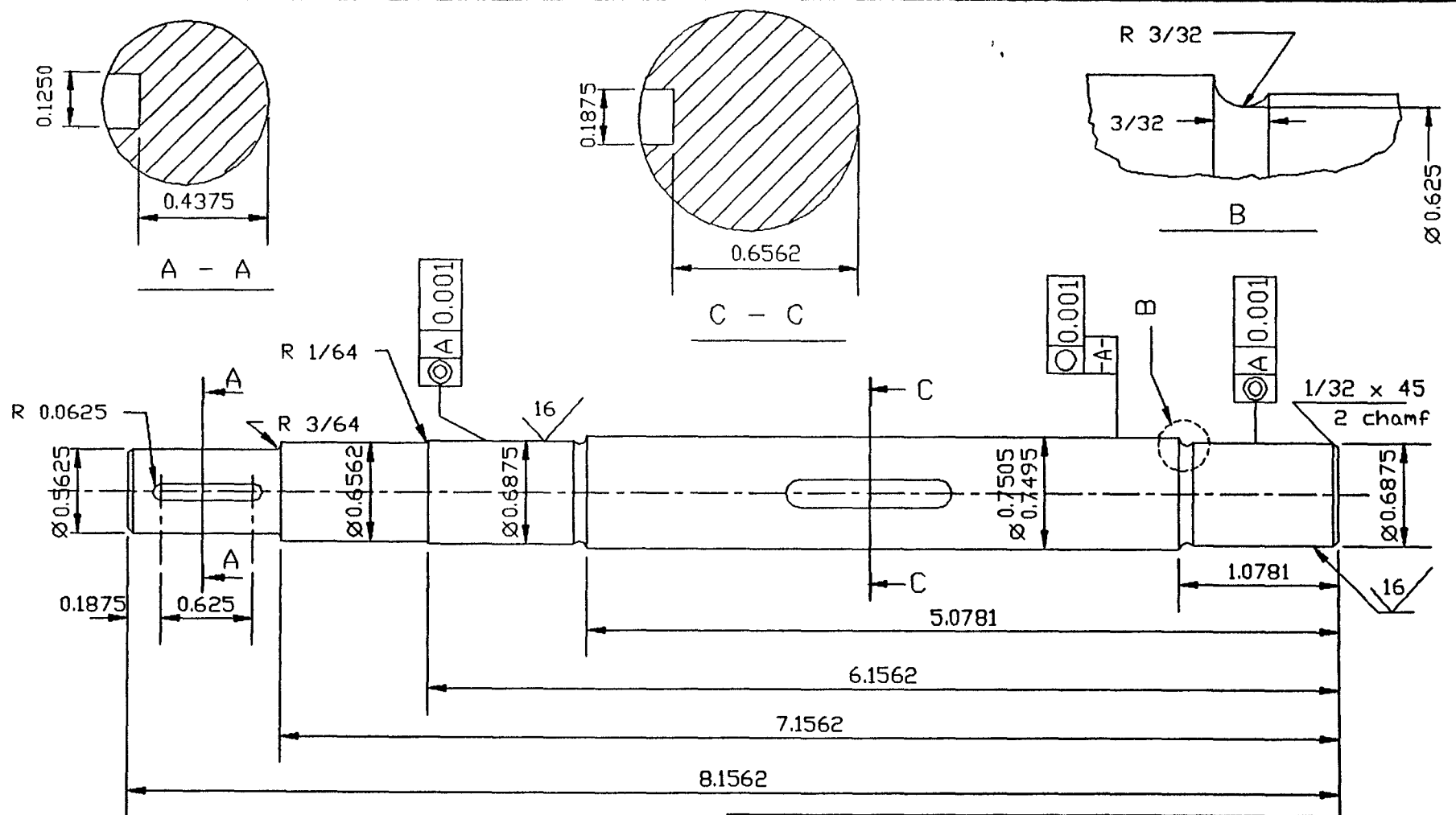
3.3.4.1 Design of High Speed Shaft

The existing high speed shaft in the selected reducer had an extension on only one side of the reducer while the other end of the shaft was covered by a seal. A new shaft was required that has extension on both side so that it can be held by two pillow block and the whole reducer can be suspended. One

Fig. 3.6 Modified reducer



REF. NO.	PART NUMBER	DESCRIPTION	QTY. REQ.	REF. NO.	PART NUMBER	DESCRIPTION	QTY. REQ.
1	02-23-01500-240	Housing, Half with Tag Holes	1	8	02-23-00237-240	Gear, Spur, Low Speed Shaft .	1
2	02-23-02854-240	Housing, Half without Tag Holes	1		02-23-00240-240	5:1 Ratio, 90 Teeth	
3	02-23-01502-240	Cap, Open, High Speed Shaft .	2		02-23-00244-240	6:1 Ratio, 93 Teeth	
4	02-23-01501-240	Cap, Open, Low Speed Shaft .	2		02-23-00242-240	7:1 Ratio, 95 Teeth	
5	02-23-01525-240	Shaft, High Speed, All Ratios . . .	1			8:1 Ratio, 96 Teeth	
6	02-23-00239-240	Shaft, Low Speed, All Ratios . . .	1	9	8-32-20-58-022	Cup, Bearing (Timken LM11910)	2
CAUTION — Hub City recommends that the complete gear set be replaced to obtain maximum life from the repaired unit. Replacement of only one member will result in an unsatisfactory life.				10	8-32-20-68-022	Cone, Bearing (Timken LM11949)	2
7		Gear, Spur, High Speed Shaft	1	11	8-32-20-58-014	Cup, Bearing (Timken LM67010)	2
	02-23-00236-240	5:1 Ratio, 18 Teeth		12	8-32-20-68-014	Cone, Bearing (Timken LM67048)	2
	02-23-00241-240	6:1 Ratio, 15 Teeth		13	8-47-16-01-071	Washer	1
	02-23-00245-240	7:1 Ratio, 13 Teeth		14	8-47-14-04-004	Screw, Hex Cap (5/16 NC x 3) GR5	8
	02-23-02757-230	8:1 Ratio, 12 Teeth		15	8-47-16-04-002	Nut (5/16 NC)	8
18	02-23-02089-240	KIT, REPAIR (INCLUDES ITEMS 19-28) THESE ITEMS ARE AVAILABLE IN REPAIR KIT ONLY					
19	8-74-21-25-020	Seal, High Speed Shaft (C/R 7443) . . .	1	16	8-47-14-04-027	Screw, Hex Cap (5/16 NC x 3/4) GR5 (not shown)	16
20	8-74-21-25-017	Seal, Low Speed Shaft (C/R 13535) . . .	1	17	8-47-14-04-023	Screw, Hex Cap (5/8 NC x 1) GR5	1
21		Key, P & W	1	23	02-23-00834-240	Gasket	2
	8-47-17-05-020	5:1, 6:1, 7:1 Ratios (5/16 sq. x 1 1/4)		24	02-23-01519-240	Gasket	12
	8-47-17-05-142	8:1 Ratio (5/16 x 1 1/2 x 1 1/4)		25	02-23-00879-011	Gasket	12
22	8-47-17-06-002	Key, Woodruff No 807 (1/4 x 7/4)	1	26	8-54-21-11-003	Plug, Expansion, Cup (1 1/4 Diameter) . . .	1
				27	8-54-32-11-002	Plug, Expansion, Cup (1 1/2 Diameter) . . .	1
				28	8-63-12-61-004	Plug, Pipe, Socket (1/2 NPT)	4

**NOTE:**

1. Position of keyslot at C-C is according to the old shaft. (Key 3/16 SQ x 15/16)
2. Position of keyslot at A-A is according to the coupler.
3. Tolerances have to be provided at bearing surfaces.

NEW JERSEY INSTITUTE OF TECHNOLOGY
MECHANICAL ENGINEERING DEPARTMENT

SCALE: 1 : 1

APPROVED BY:

DRAWN BY: M.FAROOQ

DATE: 3/28/91

DR. R.DUBROVSKY

REVISED BY:

REDUCER SHAFT

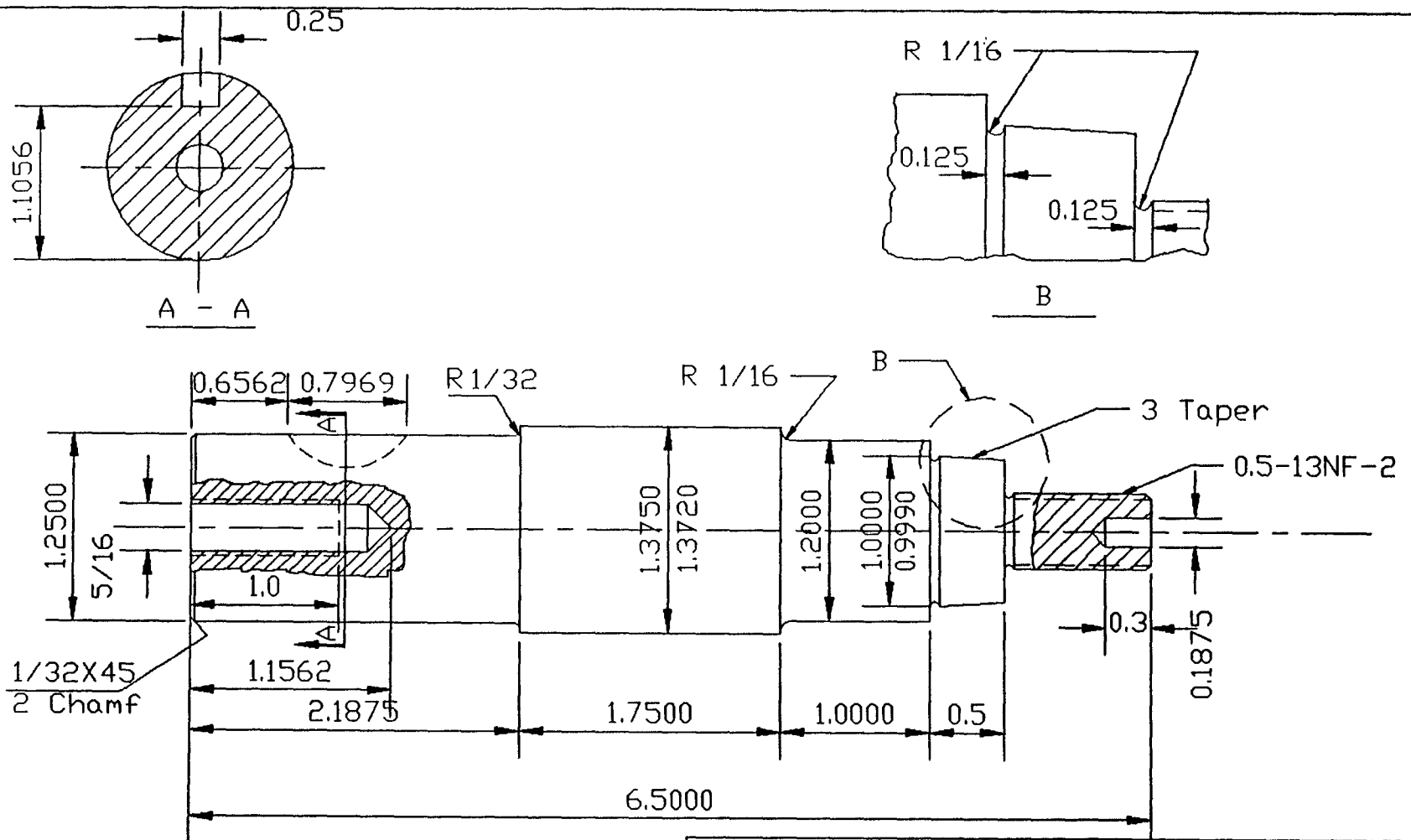
QTY

1

ALL DIMENSIONS ARE IN INCHES

DRAWING NO:

Fig. 3.8 High speed shaft



- NOTE:**
1. TAPER IS EXACTLY ACCORDING TO THE MANDREL WHICH IS USED TO MAKE ROLLERS.
 2. POSITION AND SIZE OF KEYWAY IS ACCORDING TO THE OLD SHAFT.

NEW JERSEY INSTITUTE OF TECHNOLOGY
MECHANICAL ENGINEERING DEPARTMENT

SCALE: 1 : 1

APPROVED BY:

DRAWN BY: M.FAROOQ

DATE: 4/9/91

Dr. R.DUBROVSKY

REVISED BY:

LOW SPEED SHAFT

QTY

1

ALL DIMENSIONS ARE IN INCHES

DRAWING NO:

Fig. 3.9 Low speed shaft

end of this shaft has to be coupled with variable speed motor. The detailed design of this shaft is shown in Fig. 3.8.

3.3.4.2 Design of Low Speed Shaft

A new output shaft of the reducer is also designed to replace the old one. At one end of this shaft a roller is to be attached. For this purpose a taper and threads are given at that end for tightening roller. The detailed design of this shaft is shown in Fig. 3.9.

Chapter 4

RESULTS AND DISCUSSION

The modified wear testing machine mentioned in the last chapter is used to test different type of specimens. Materials without any coating and treatment, and Ion-Nitrided materials with different magnetic treatment are tested. The method for testing and their results are given in the following sections.

4.1 Calibration

A new strain gauge is mounted on the new deformation bar which is attached to the motor. This strain gauge has a gage factor of 2.1. According to the methodology used in this wear testing machine, the deformation in the bar which is caused by the reaction of the stator give us friction force. The amount of this deformation is recorded in the PC through strain gauge recorder. Strain gauge can give only relative reading, therefore it is very important to obtain a correct calibration chart. Later readings from stain gage has to be compared with this chart.

To obtain a calibration chart machine is allowed to run for some time without any load at contacting surfaces. Once the motor is running smoothly the known loads are applied steadily in steps on the lever which is attached to the other side of the motor. The loads are applied at a distance of 13.25 inches

from the center of the shaft. The moment at the motor can be calculated by the following equation

$$M_m = 13.25 P_i$$

where P_i is the input load. The corresponding strain gauge readings are obtained from the computer. By computing the difference of the readings (i.e. reading at load - reading at no load), relationship between reading against input load and reading against moment are obtained. These calibration charts are shown in Fig. 4.1 and 4.2.

These calibration charts can be converted into friction force and friction coefficient which are very important from testing point of view. Using equation (3.9) and (3.10) these two parameters can be calculated as follows

$$F_f = K' M_m$$

$$f = K M_m$$

where

$$K' = \frac{N}{N_r} \frac{\eta}{r}$$

and

$$K = \frac{N}{N_r} \frac{\eta}{r} \frac{1}{W}$$

In our testing system, we have

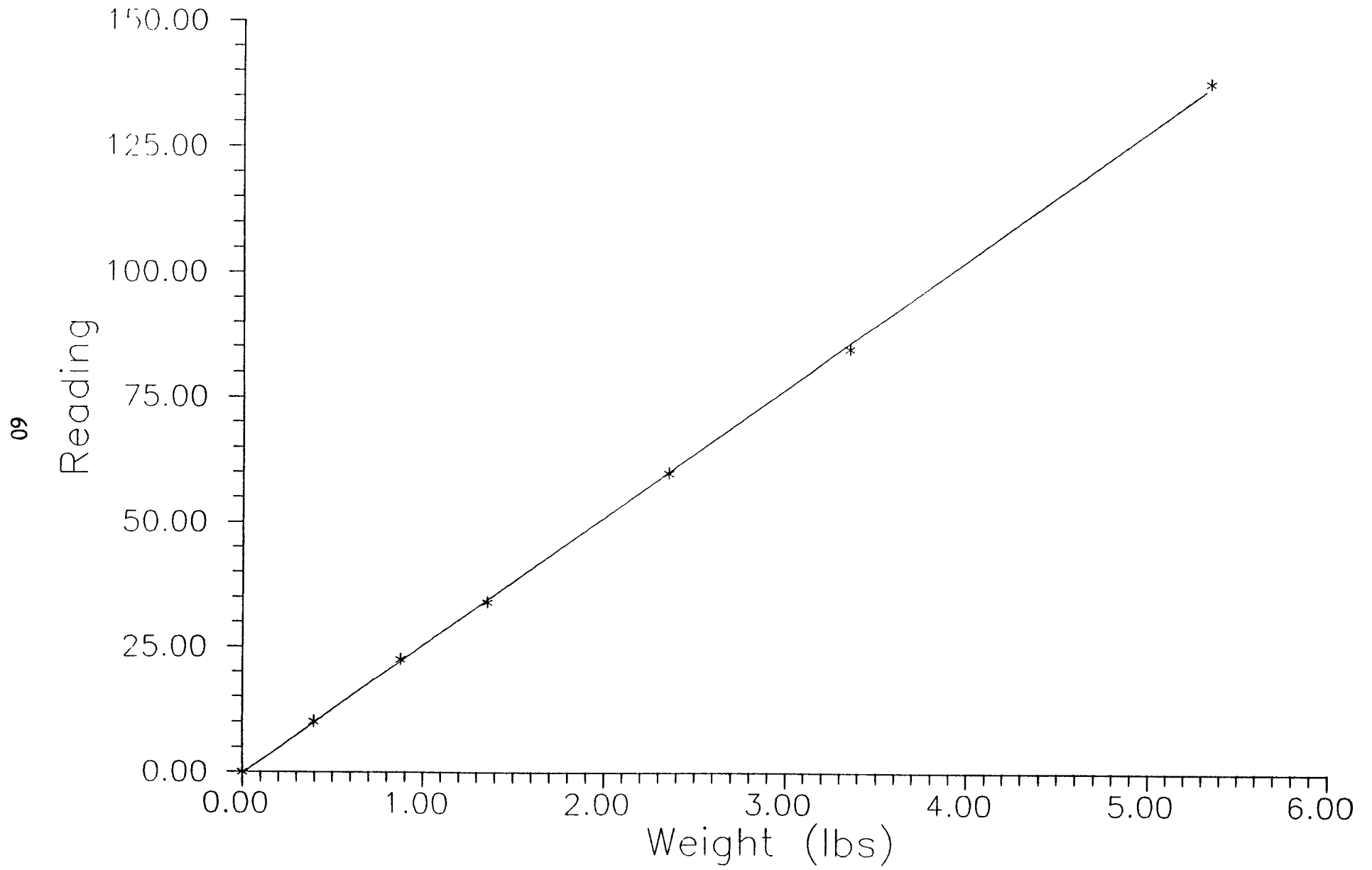


Fig. 4.1 Calibration Chart (Computer Reading vs. Input Load)

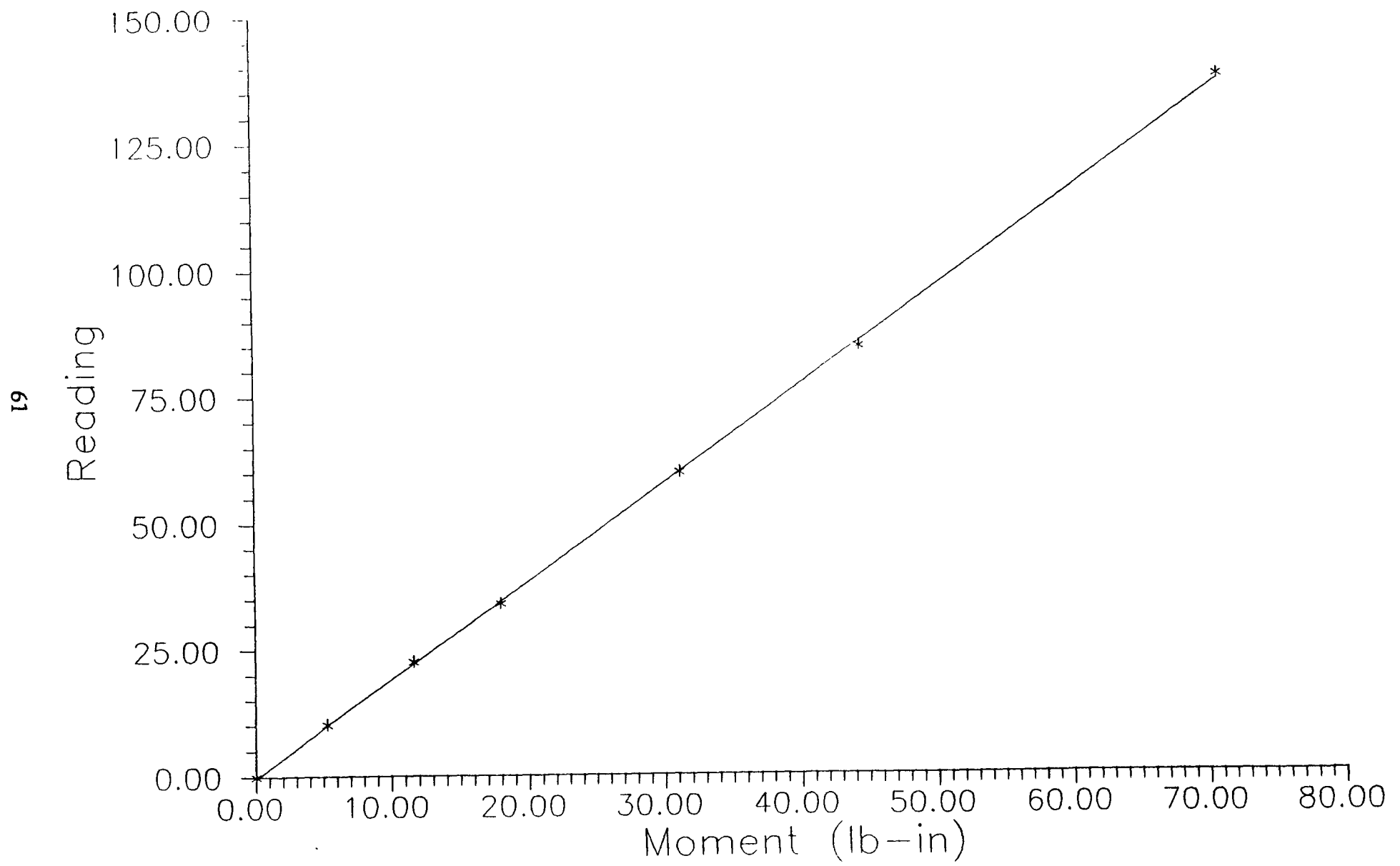


Fig. 4.2 Calibration Chart (Computer Reading vs. Motor Moment)

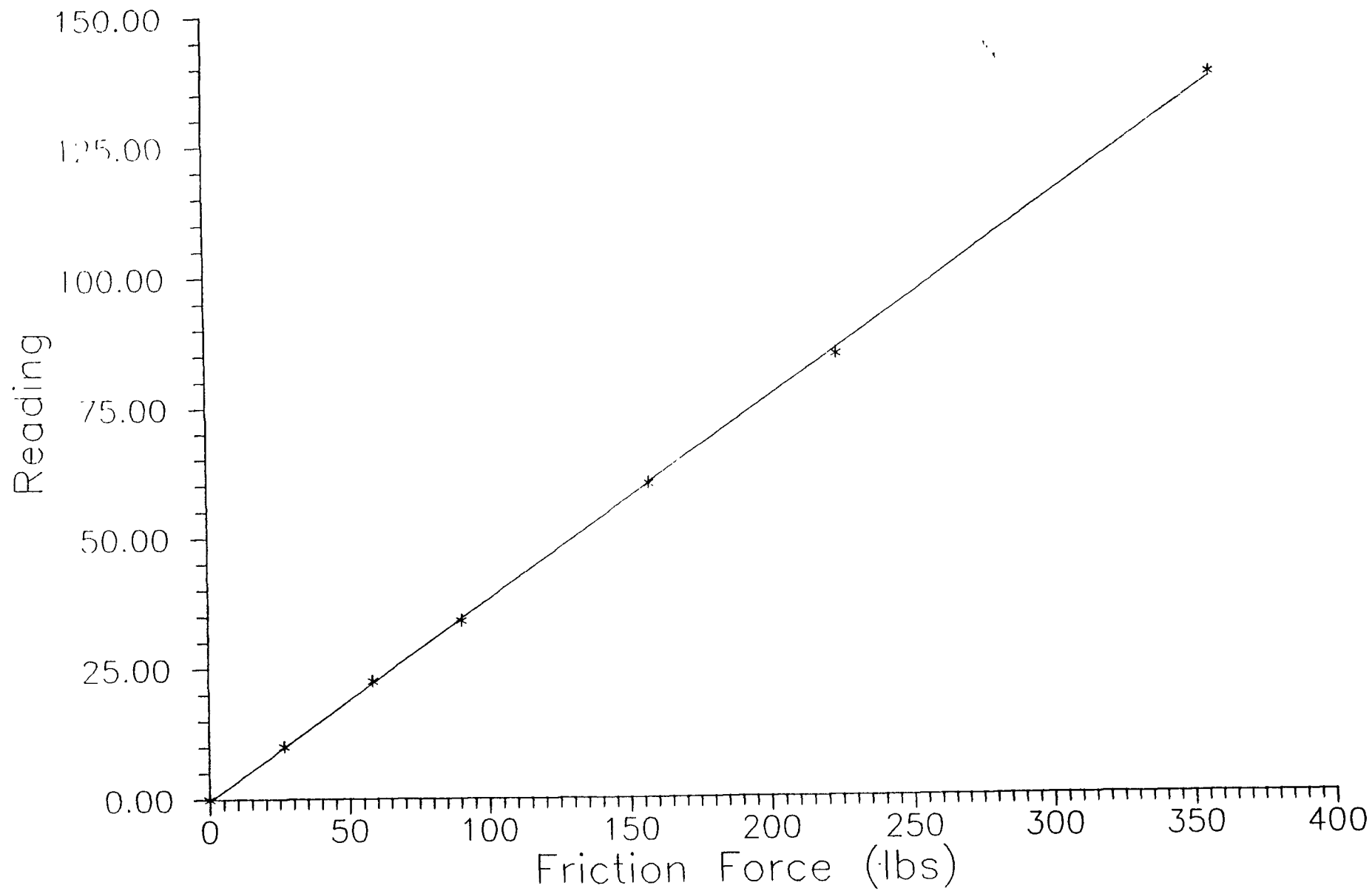


Fig. 4.3 Calibration Chart (Computer Reading vs. Friction Force)

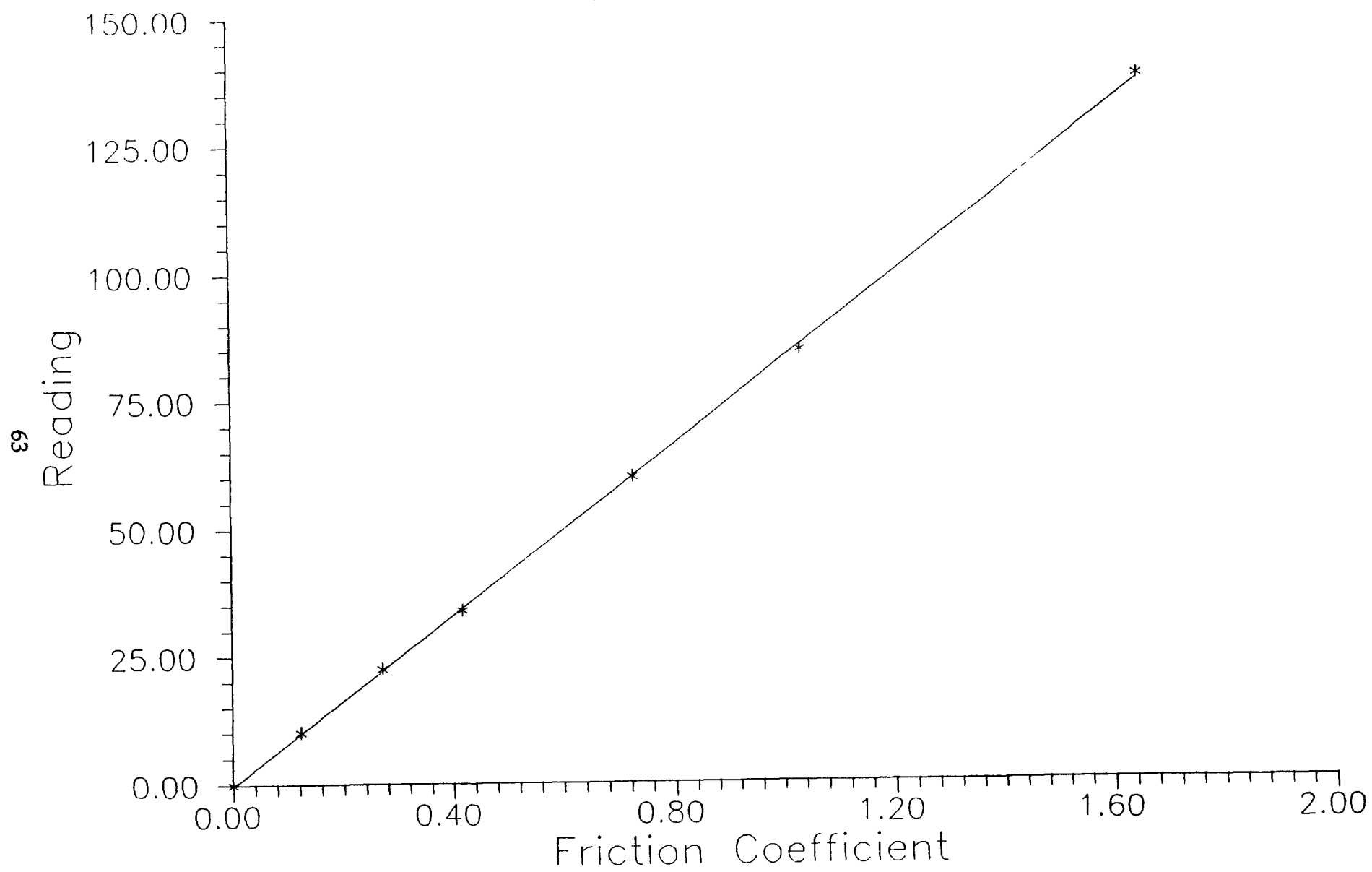


Fig. 4.4 Calibration Chart (Computer Reading vs. Friction Coefficient)

r = radius of roller = 1

$\frac{N}{N_r}$ = ratio of speed of motor to speed of roller = 6.3

η = efficiency of whole system = 0.8

W = applied load = 216

therefore

$$K' = 5.04$$

$$K = 0.0233$$

Since K' and K are constant, F_f and f can be calculate with the help of moment. Fig. 4.3 and 4.4 show the calibration charts obtained for these two parameter.

4.2 Testing Material

Four kinds of specimen are tested in this work. The size and design of specimens, which are shoes, are mentioned in section 3.3.3. Bulk material of all four specimen is same. Composition of which is shown in the following table.

Table 4.1 Chemical composition of specimen

Material	C	Si	Mn	Cr	V
AISI 420. W.-Nr. 1.2083	0.38 %	0.8%	0.5 %	13.6 %	0.3 %

First specimen 'A' has no coating on it and it is without any kind of treatment. While other three specimens have the same kind of Plasma Ion-Nitriding coating. After coating these three specimens are subjected to magnetic treatment with different number of cycles. Parameter used in Plasma machine while coating are optimized parameter which are shown in Table 4.2. While Table 4.3 shows different number of cycles for magnetic treatment.

Table 4.2 Ion-Nitriding Parameter

Material	Time	Temp.	Pressure	Vol% (H,N)
AISI 420 W.-Nr. 1.2083	6 hr	600 °C	4 torr	6,7

Table 4.3 Magnetic Treatment

Type	Number of Cycles
A1	20
A2	40
A3	60

Fig. 4.5 shows the microstructure view of Ion-Nitrided coating on the bulk material. Hardness of this material from surface to the inside of the bulk material is shown in Fig. 4.6.

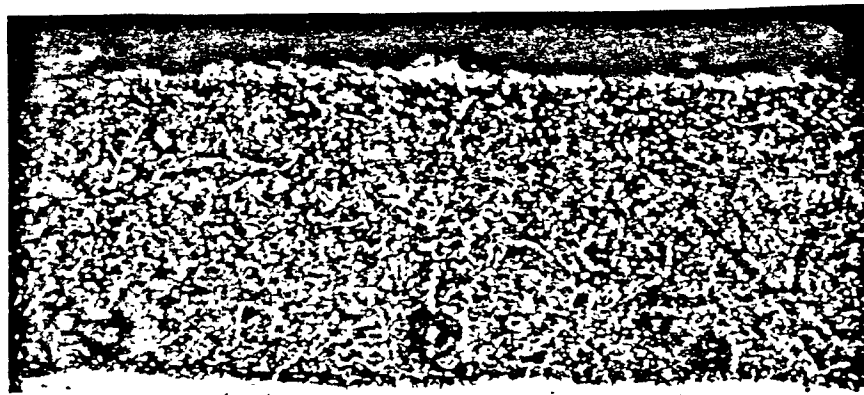


Fig. 4.5 Microstructure view showing Ion-Nitrided layer on bulk material

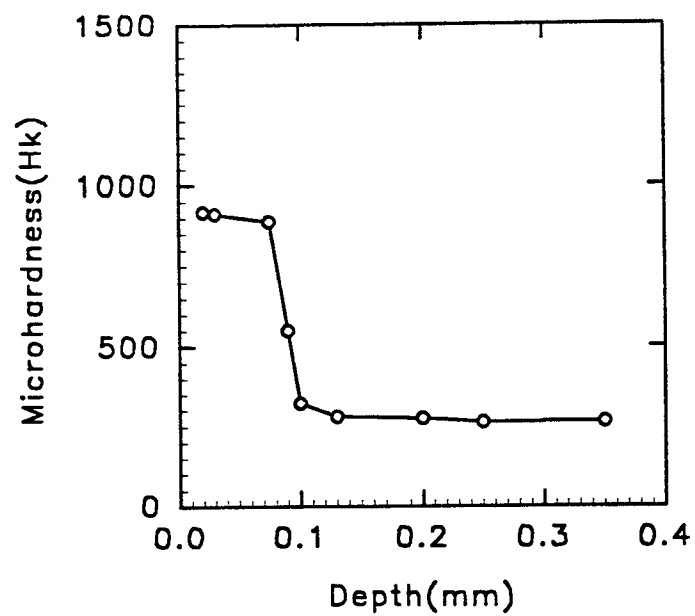


Fig. 4.6 Microhardness of Ion-Nitrided material

For the rollers, alloy steel is selected for all tests. Chemical composition of which is shown in Table 4.4.

Table 4.4 Chemical composition of roller

Material	C	Mn	P	S	Si	Ni	Cr	Mo
AISI 4340	0.4 %	0.7 %	0.03 %	0.03 %	0.2 %	1.7 %	0.7 %	0.2

4.3 Testing Parameter

Testing parameter used in this wear testing are shown in Table 4.5.

Table 4.5 Testing parameter

Shoe	Unnitrided and nitrided samples having different no. of cycles
Roller	Uncoated alloy steel AISI 4340
Speed	277.78 rpm
Load	216 lbs.
Test Environment	Lubricated at room temperature 70°F

4.4 Testing Procedure

The sequence of the procedure are listed as follow.

1. Clean the shoe and the roller in ultrasonic cleaner before the test as well as after the test.
2. Measure roughness and weights.
3. Fix the shoe and the roller in the testing machine. Make sure that shoe holder is horizontal.
4. Adjust the rod in loading mechanism so that when cam is rotated from 0° to 180°, shoe holder should move from no load to load position and vice versa.
5. Turn on D.C. motor to rotate cam to bring it at no load position.
6. Turn on controller and strain gauge recorder.
7. Start the machine.
8. Adjust the lubricant flow.
9. Load data acquisition program into PC and select the interval of data recording.
10. When PLC sounds three minute warming time up turn on D.C. motor to rotate cam to bring it at load position.
11. Test is stopped by PLC after some preset time.
12. Remove the shoe and roller from the machine.
13. Clean the pair in ultrasonic cleaner.
14. Measure surface roughness and weight.

4.5 Wear and Friction Analysis

Using the testing procedure and testing parameter described in the former sections, four specimens have been investigated. Fig. 4.7 to 4.10 show the friction coefficient against sliding distance. Wear rates of the shoes as well as rollers are shown in Fig. 4.11 to 4.14.

Fig. 4.7 which is related to the Type A (i.e. material without any treatment) has a very high friction coefficient at the beginning. It lost most of the weight in first few minutes and also the surface roughness is changed tremendously. The load for this type of material was high enough to cause catastrophic wear in first few minutes. Once the catastrophic condition reached it is beyond comparison with other materials. Fig. 4.15 shows the amount of weight lost in first 15 minutes. Difference is obvious that where teated material lost none of the weight, Type A lost 415.18 mg.

Fig. 4.8 to 4.10 are friction coefficient curves for the Ion-Nitrided materials with different magnetic treatment. The behavior of these curves are similar. At the beginning the friction coefficient is stable, which show the steady state region. Then as the sliding distance increases the friction coefficient tends to increase and at last the material reaches catastrophic region. In this region the friction coefficient is in very high range.

Fig. 4.12 to 4.14 are curves for wear rate related to these materials. In these figures the wear rate of shoes as well as rollers are shown. From figures steady state and catastrophic region can also be differentiated. Shoes which are coated

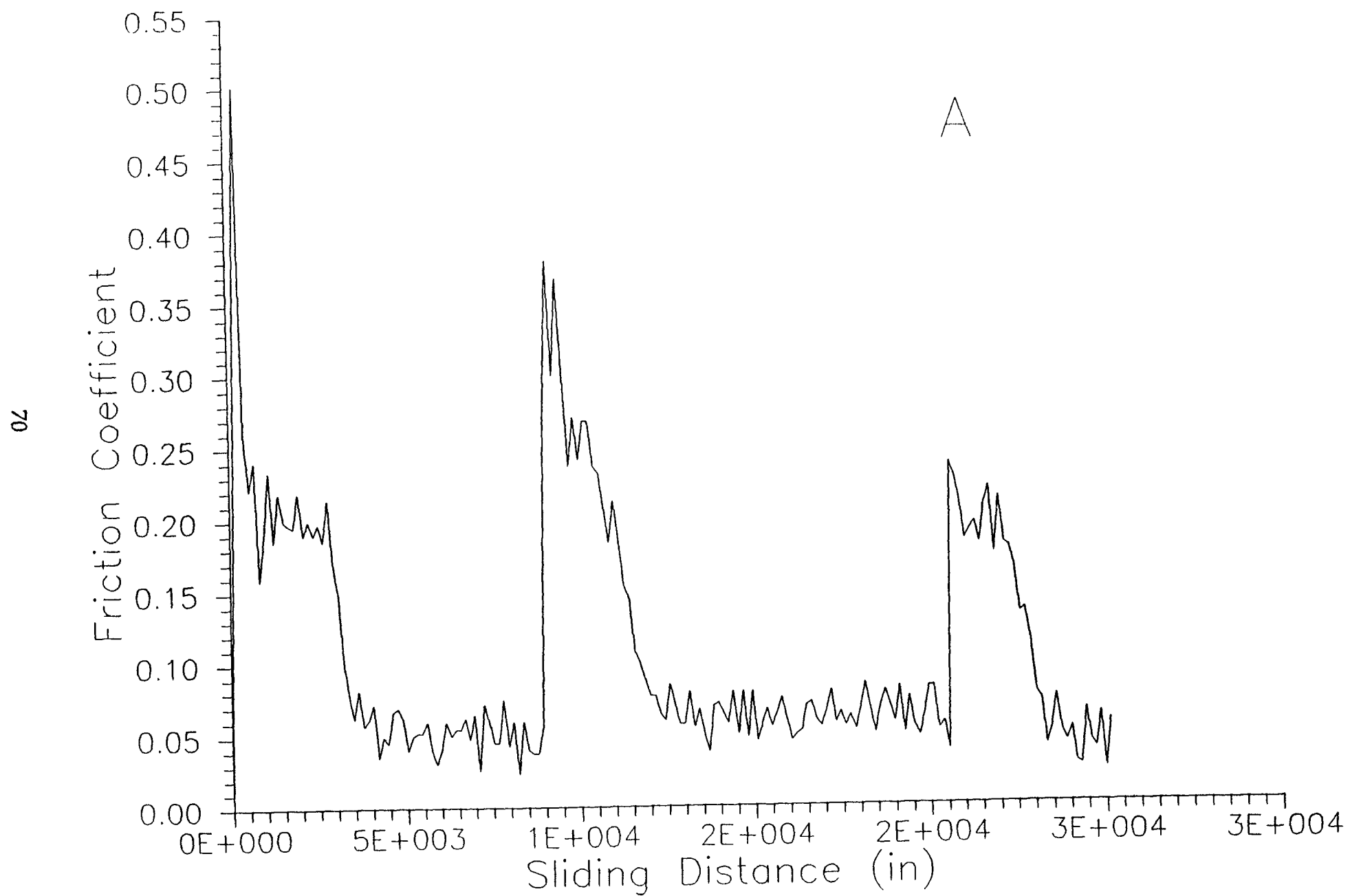


Fig. 4.7 Friction Coefficient vs. Sliding Distance (Type A)

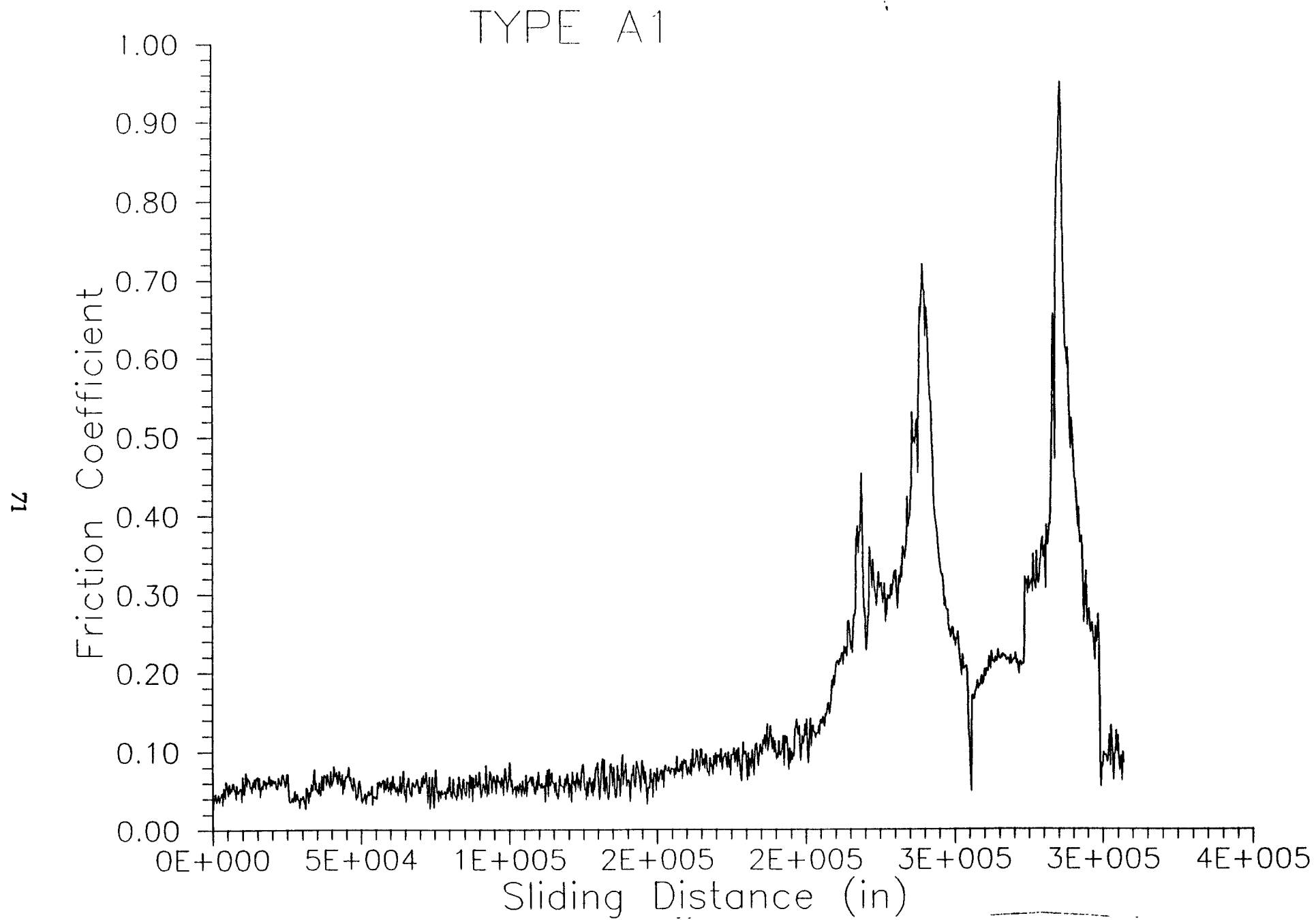


Fig. 4.8 Friction Coefficient vs. Sliding Distance (Type A1)

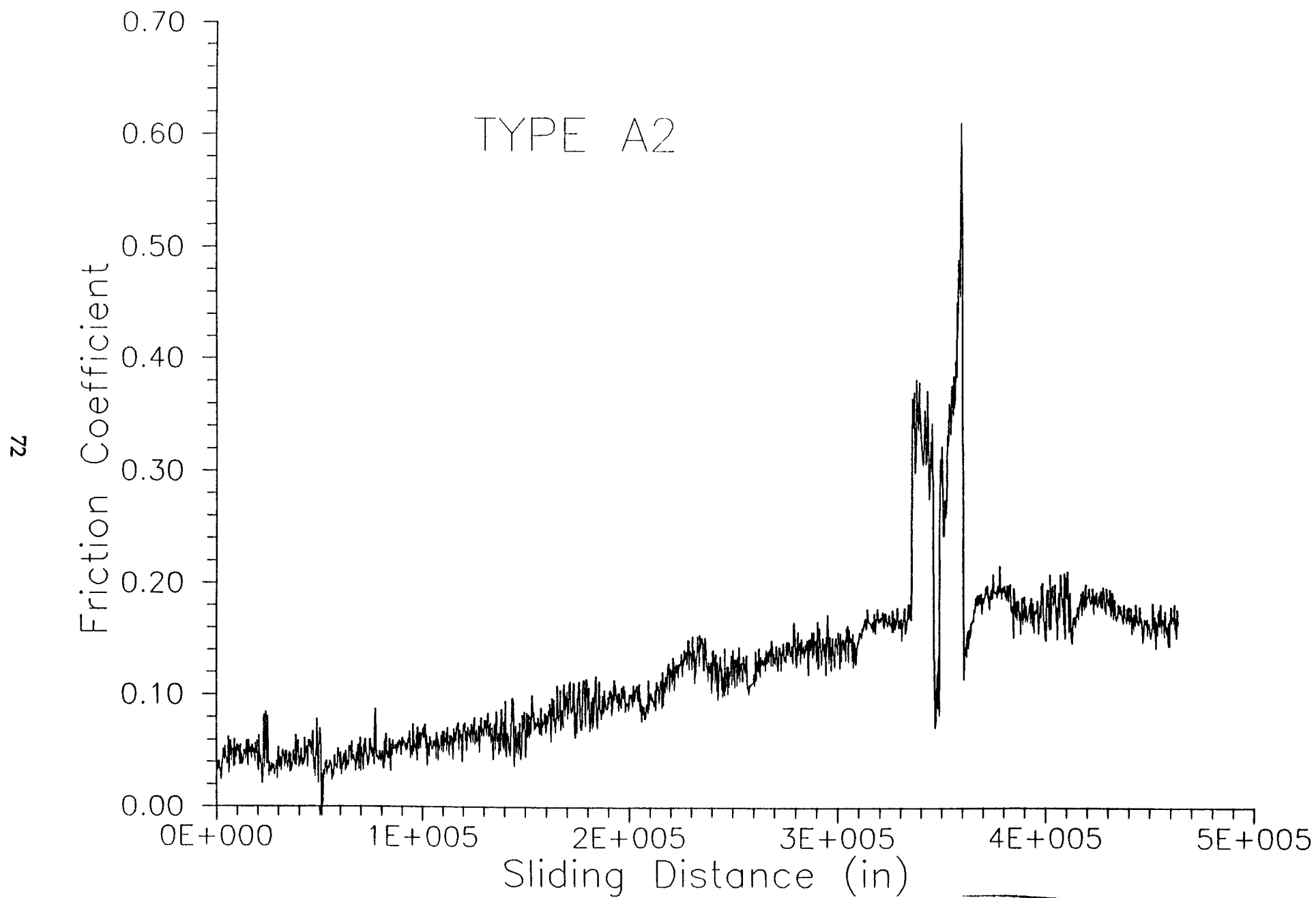


Fig. 4.9 Friction Coefficient vs. Sliding Distance (Type A2)

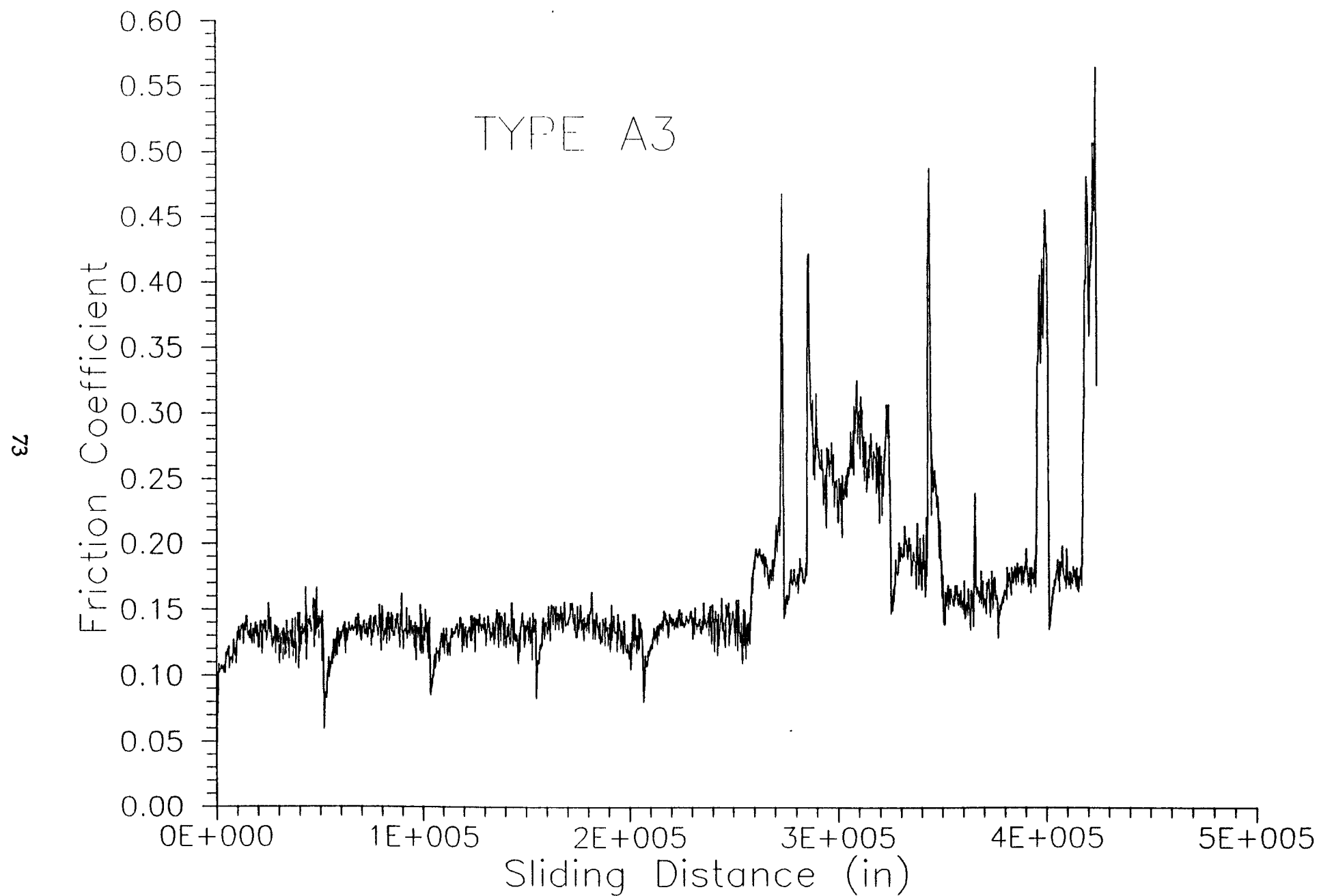


Fig. 4.10 Friction Coefficient vs. Sliding Distance (Type A3)

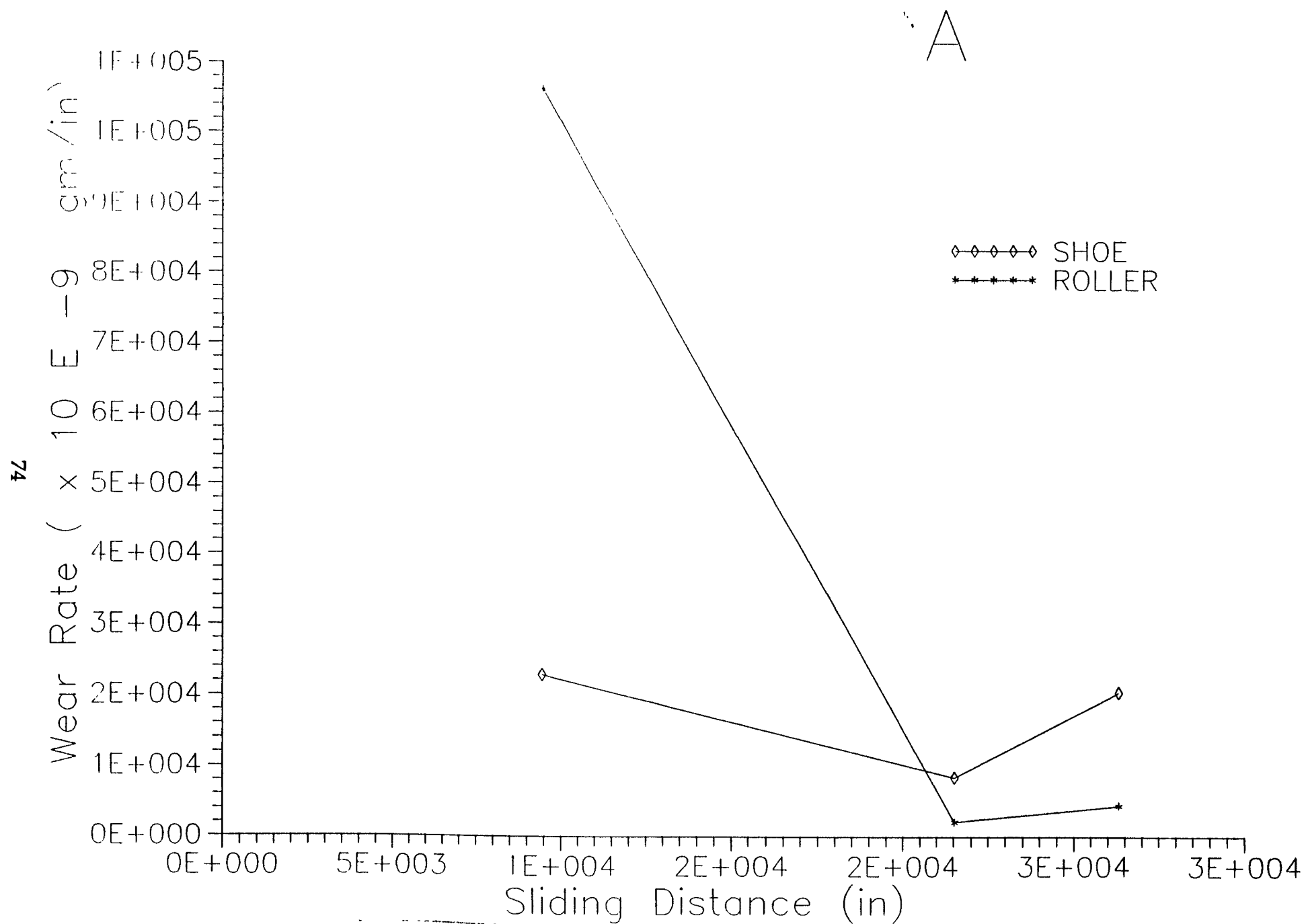


Fig. 4.11 Wear Rate vs. Sliding Distance (Type A)

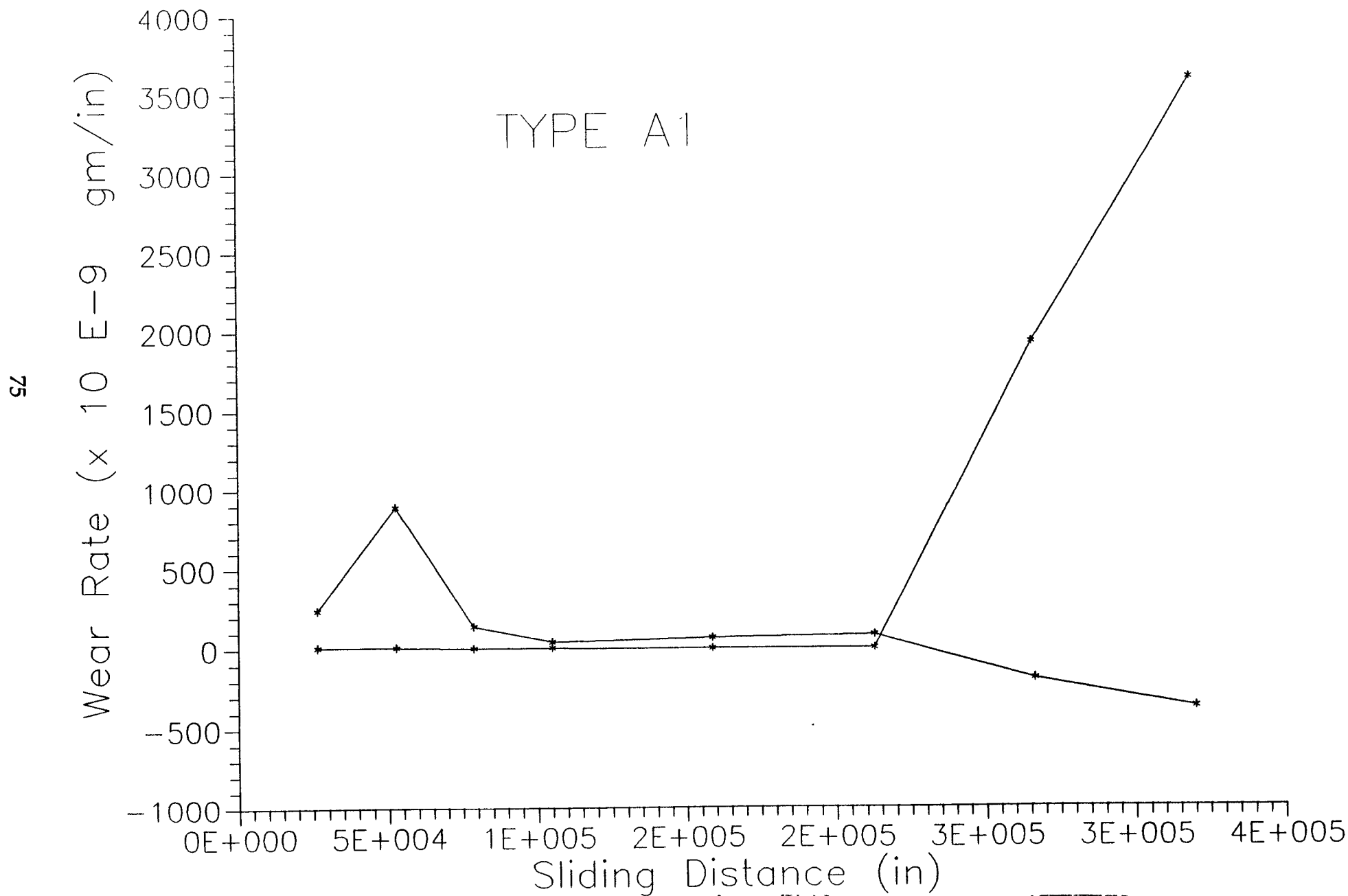


Fig. 4.12 Wear Rate vs. Sliding Distance (Type A1)

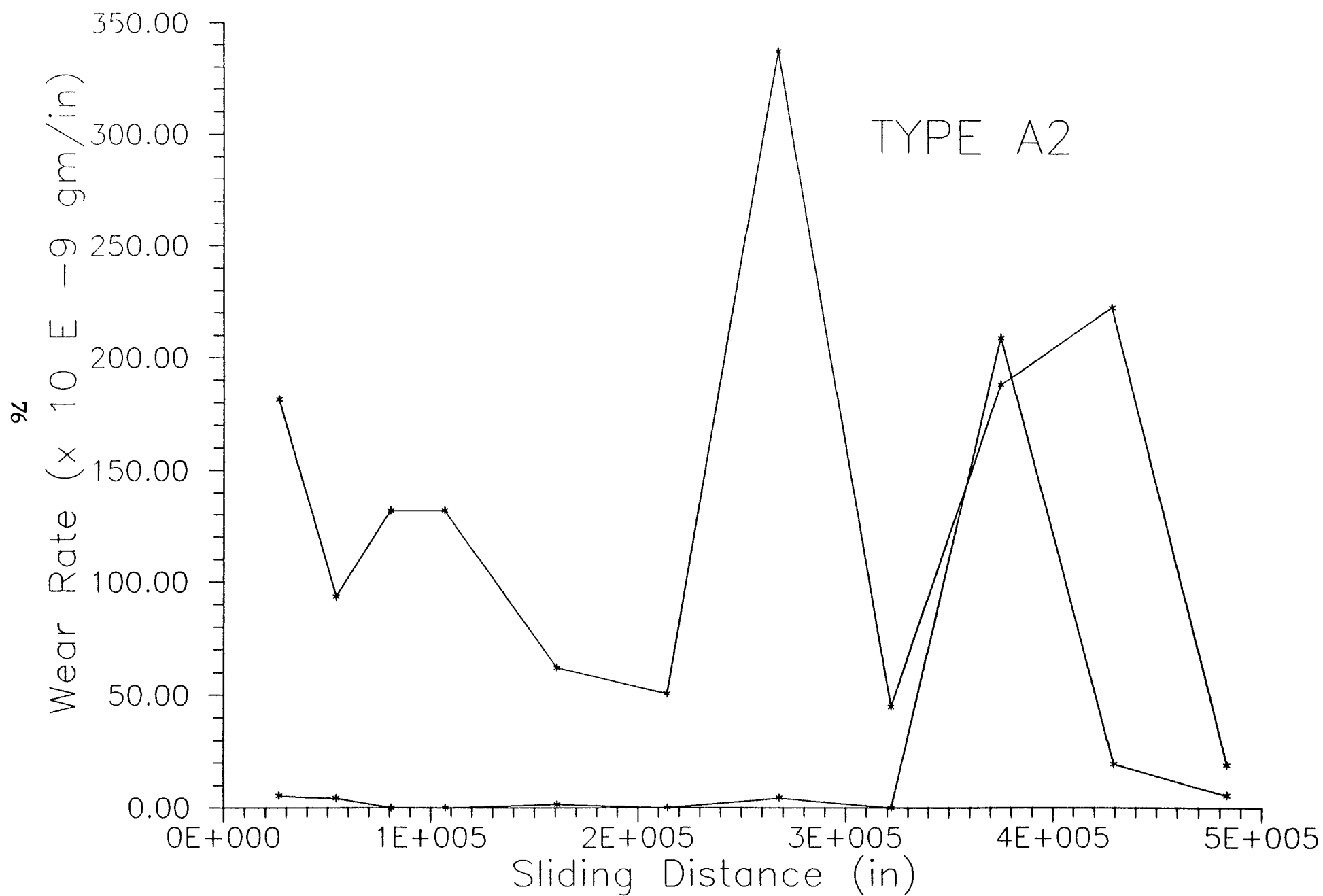


Fig. 4.13 Wear Rate vs. Sliding Distance (Type A2)

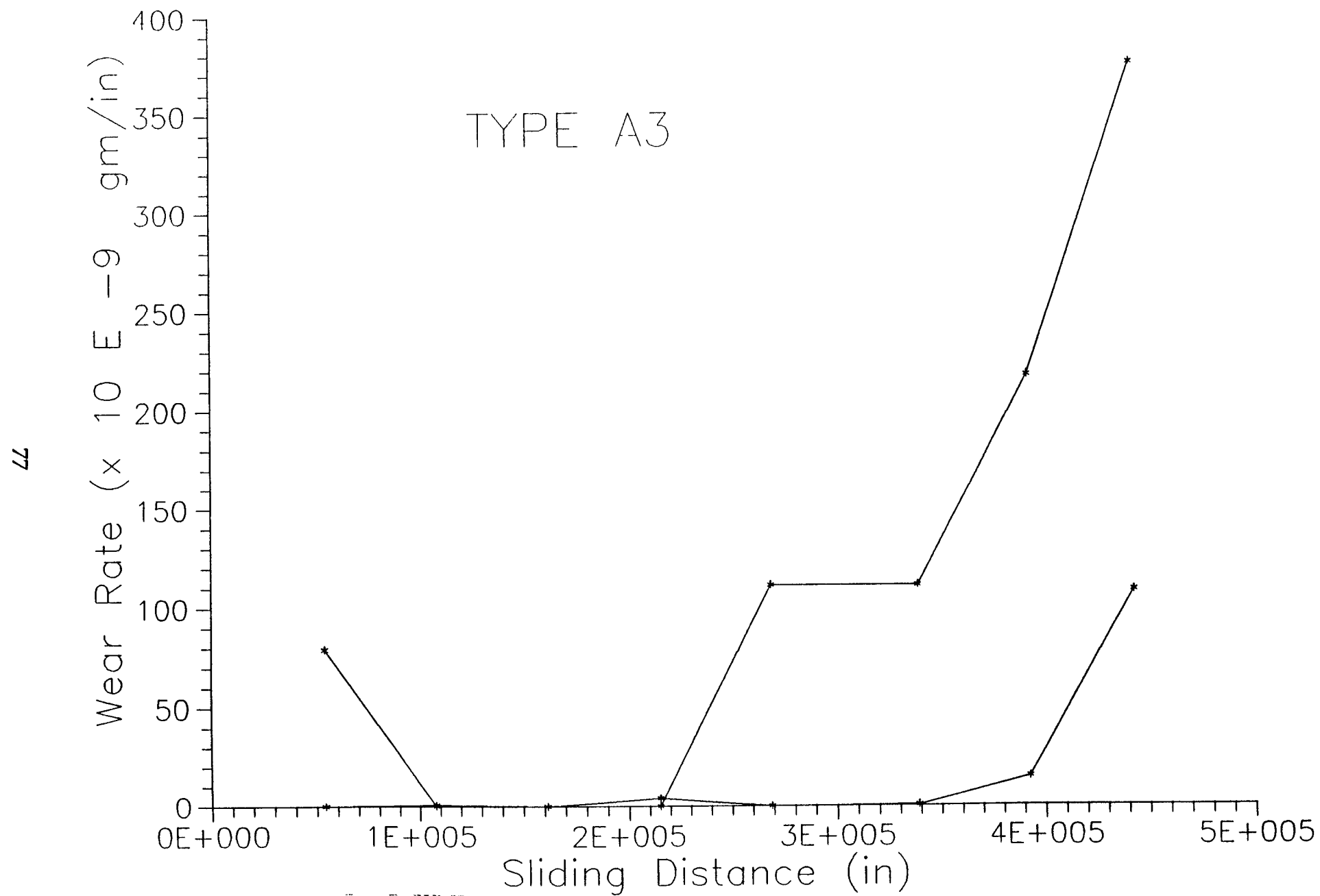


Fig. 4.14 Wear Rate vs. Sliding Distance (Type A3)

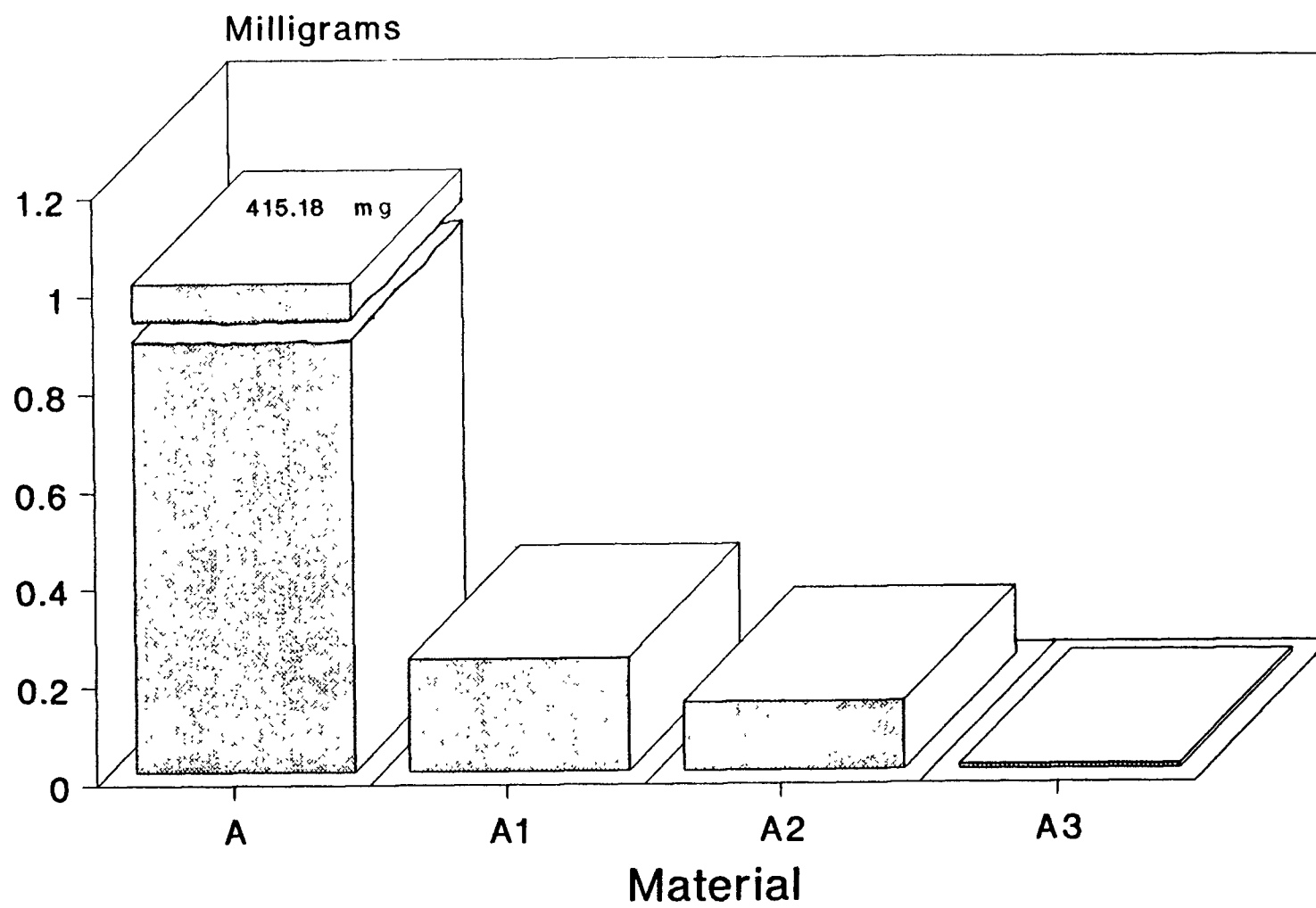


Fig. 4.15 Comparison of weight loss in 15 minutes

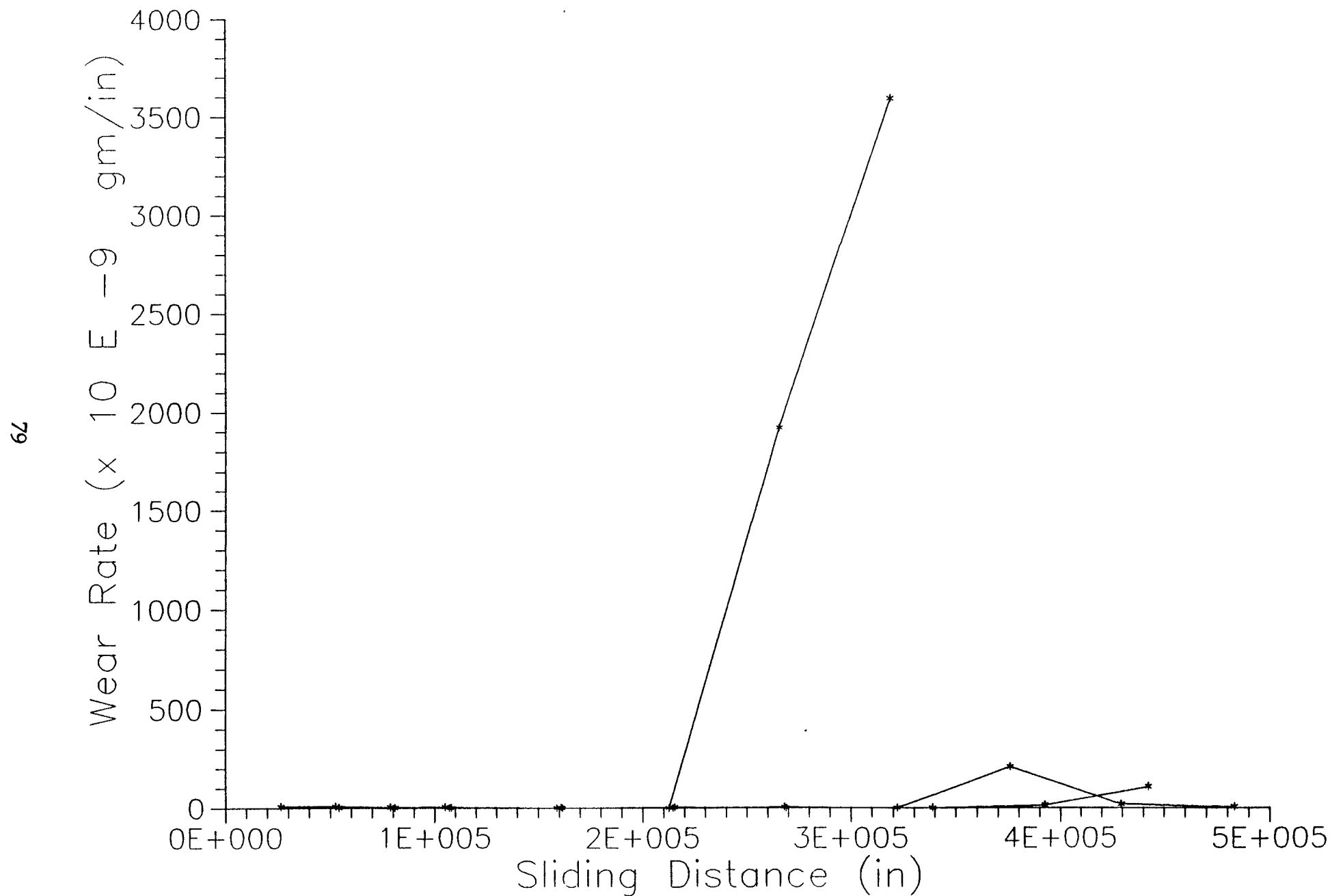


Fig. 4.19 Comparison of Wear Rate of Type A1, A2 and A3 Materials

have lower wear rate as compared to the rollers which are not treated. In the beginning the wear rate for these shoes are almost zero, but once the wear is in catastrophic region the wear rate increases rapidly. In Fig. 4.16 to 4.18 wear rate curves are combined with friction coefficient to see the effect of friction coefficient on wear rate. It is obvious that wear rate is high where friction coefficient is high.

In Fig. 4.12, which is for wear rate of Type A1 material, roller gained some weight where shoe lost most of its weight. Some of the material might be transferred from shoe to roller.

Fig. 4.19 shows the comparison of wear rate of Type A1, A2 and A3 materials. It is found that Type A1 which has been magnetic treated with only 20 cycles give increased wear rate after about 212,000 inches of sliding distance. While Type A2 has a higher wear rate after 320,000 inches of sliding distance. Finally Type A3 material which has been treated with 60 cycles has the best wear resistance. After 395,000 inches of sliding distance it gives some higher wear rate. Even in catastrophic region its wear rate does not increase rapidly. Fig 4.20 shows the amount of weight lost in these three types of material at different stages.

4.6 Surface Roughness Analysis

During testing the surface roughness of the pair of specimens have been investigated from time to time.

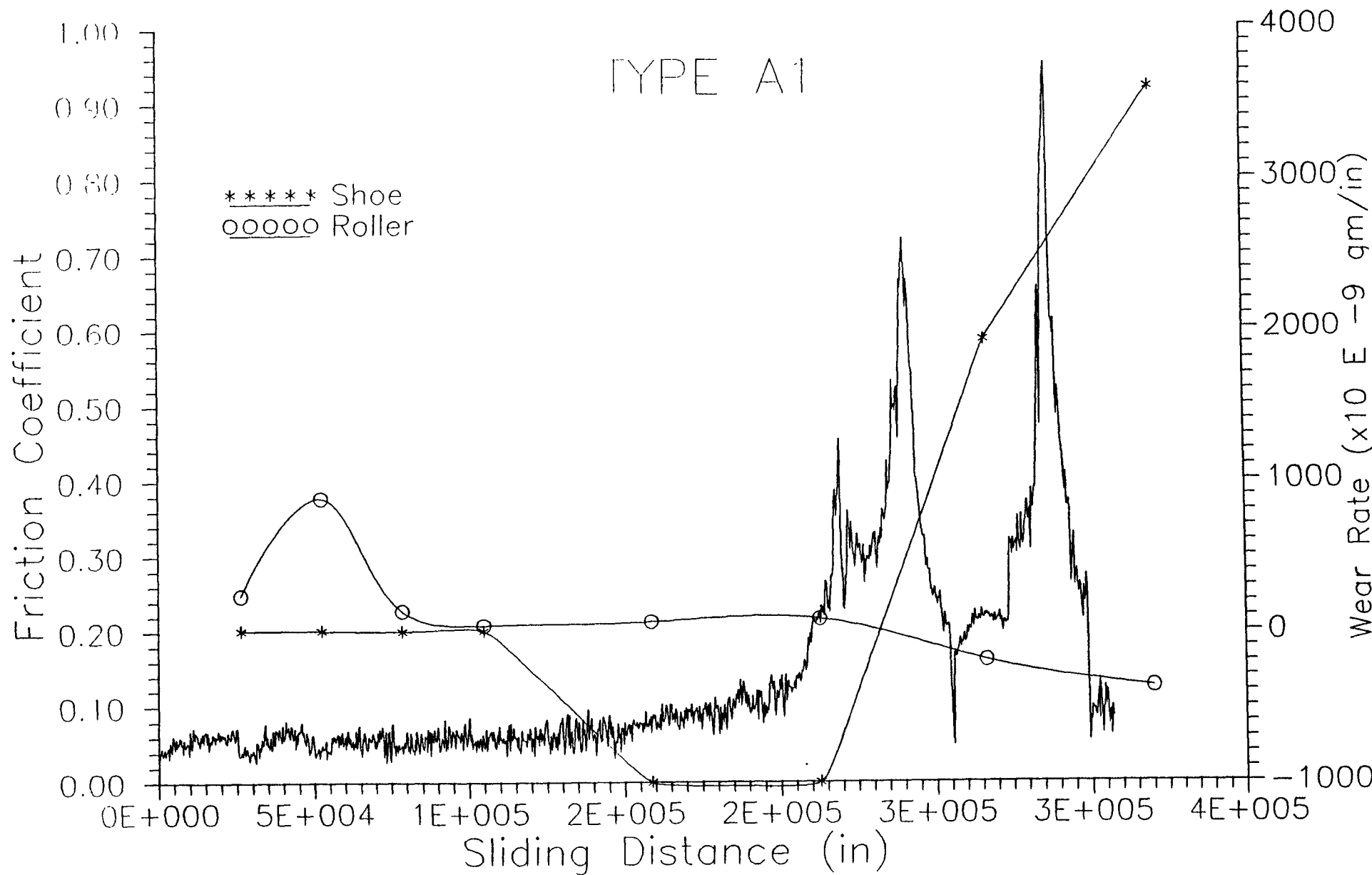


Fig. 4.16 Friction Coefficient and Wear Rate vs. Sliding Distance (Type A1)

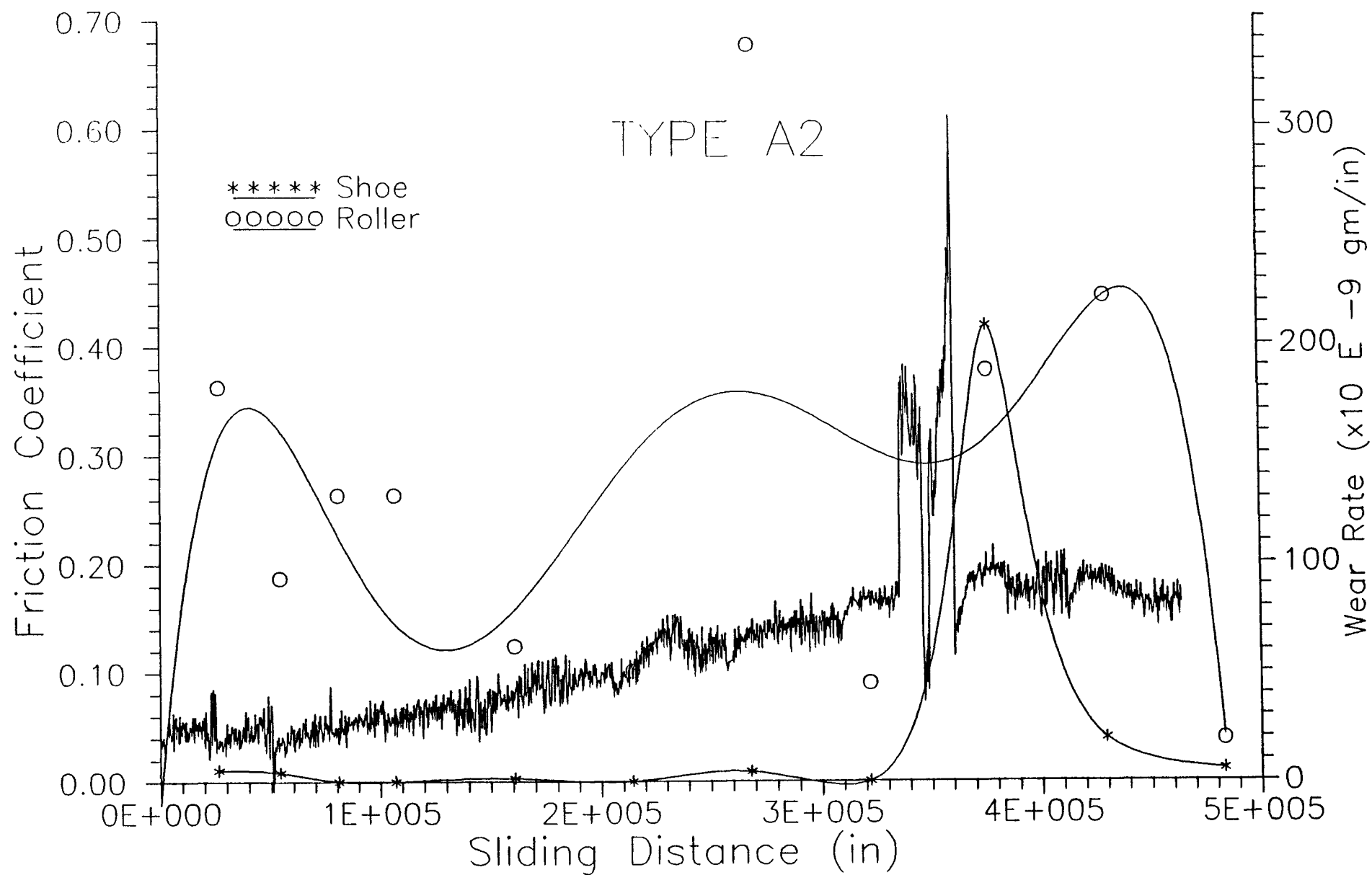


Fig. 4.17 Friction Coefficient and Wear Rate vs. Sliding Distance (Type A2)

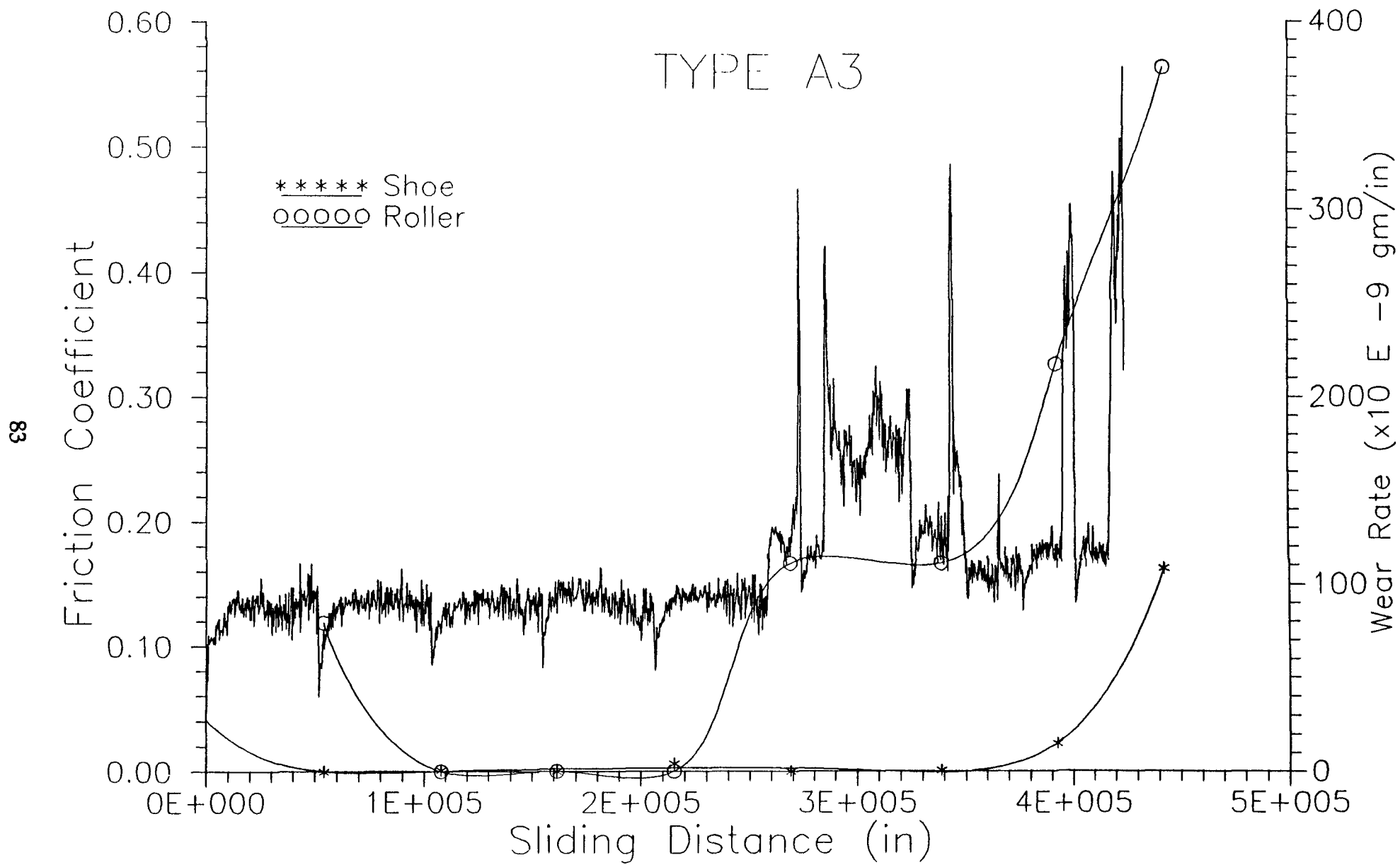


Fig. 18 Friction Coefficient and Wear Rate vs. Sliding Distance (Type A3)

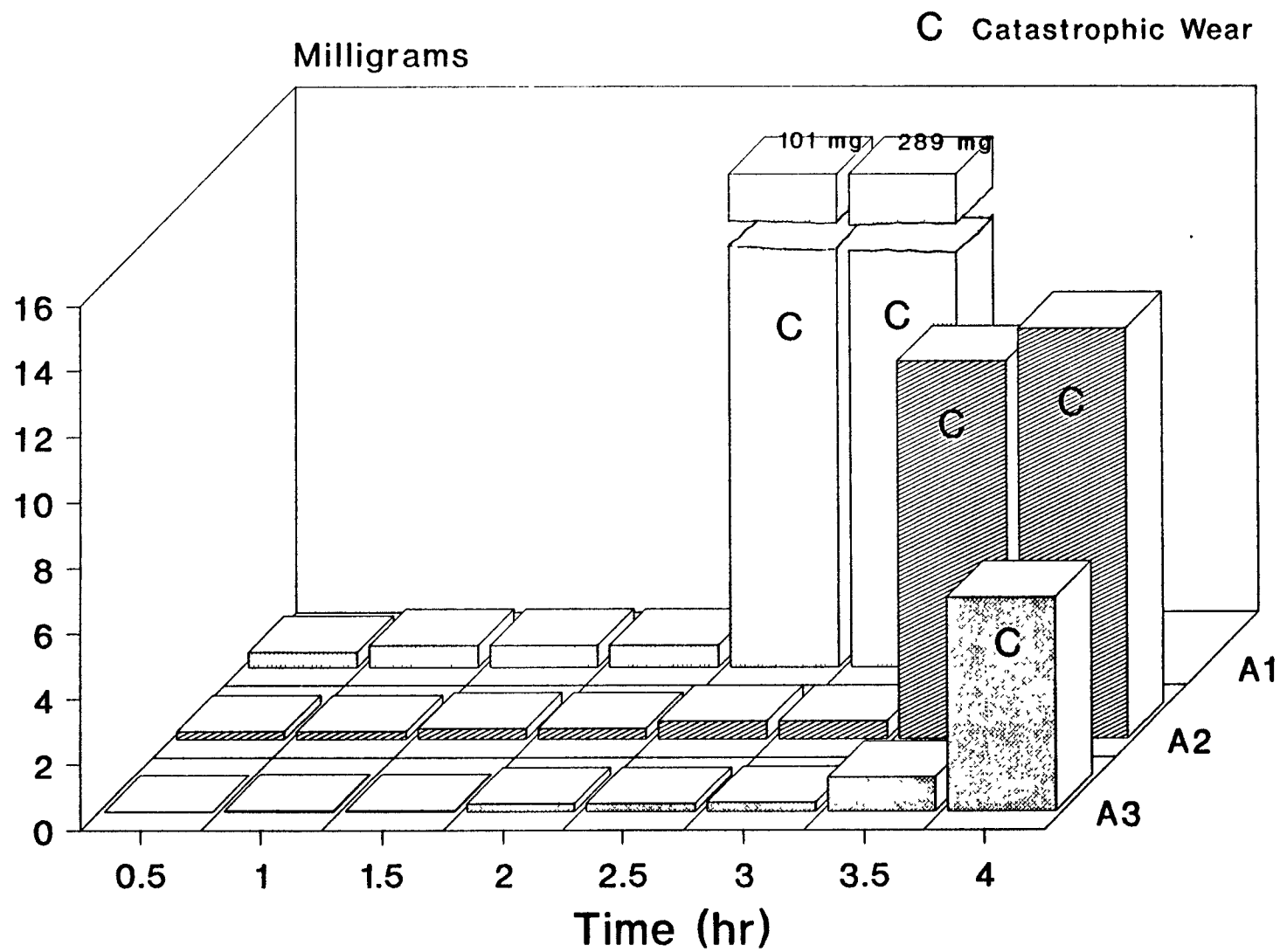


Fig. 4.20 Comparison of weight loss vs. time for Type A1, A2 and A3 materials

The roughness of worn surfaces depend on the sliding distance as well as on friction coefficient. These results are given in Fig. 4.21 to 4.24. Fig. 4.21 shows the Ra parameter for Type A material. In this case as the destruction of the material occurred the surface became worse.

Type A1, A2, A3 are tested for a longer time to reach the catastrophic region. Fig. 4.22 to 4.24 are the results of these coated materials. In all cases the surface roughness improved after some time which clearly indicated the steady state region. In the beginning the material has a lots of irregularities. At early stage these irregularities are deformed and broken as the material slides under load. After passing this stage surface roughness did not change so much until it reached catastrophic region. Once the wear rate changed the surface roughness also changed because of the destroyed surface. In all cases the difference between technological and operational surface roughness can be seen.

In Fig. 25 to 27, surface roughness parameter Ra curves are combined with friction coefficient curves. In all these three curves the trend of changing surface roughness with sliding distance is same. When the friction coefficient is stable Ra parameter is low but when friction coefficient is very high the Ra parameter is very high which shown the completely worn surfaces.

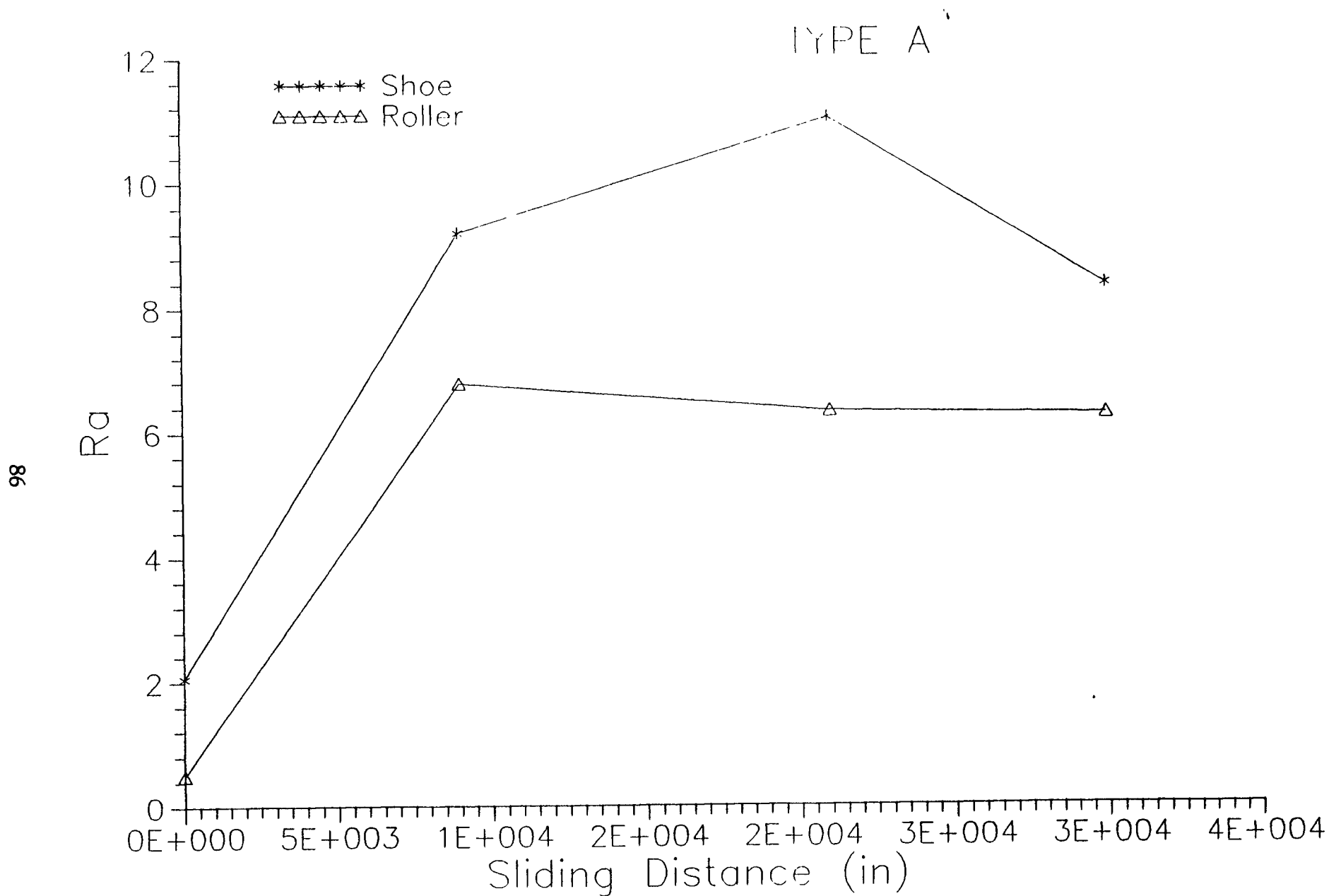


Fig. 4.21 Roughness Parameter Ra vs. Sliding Distance (Type A)

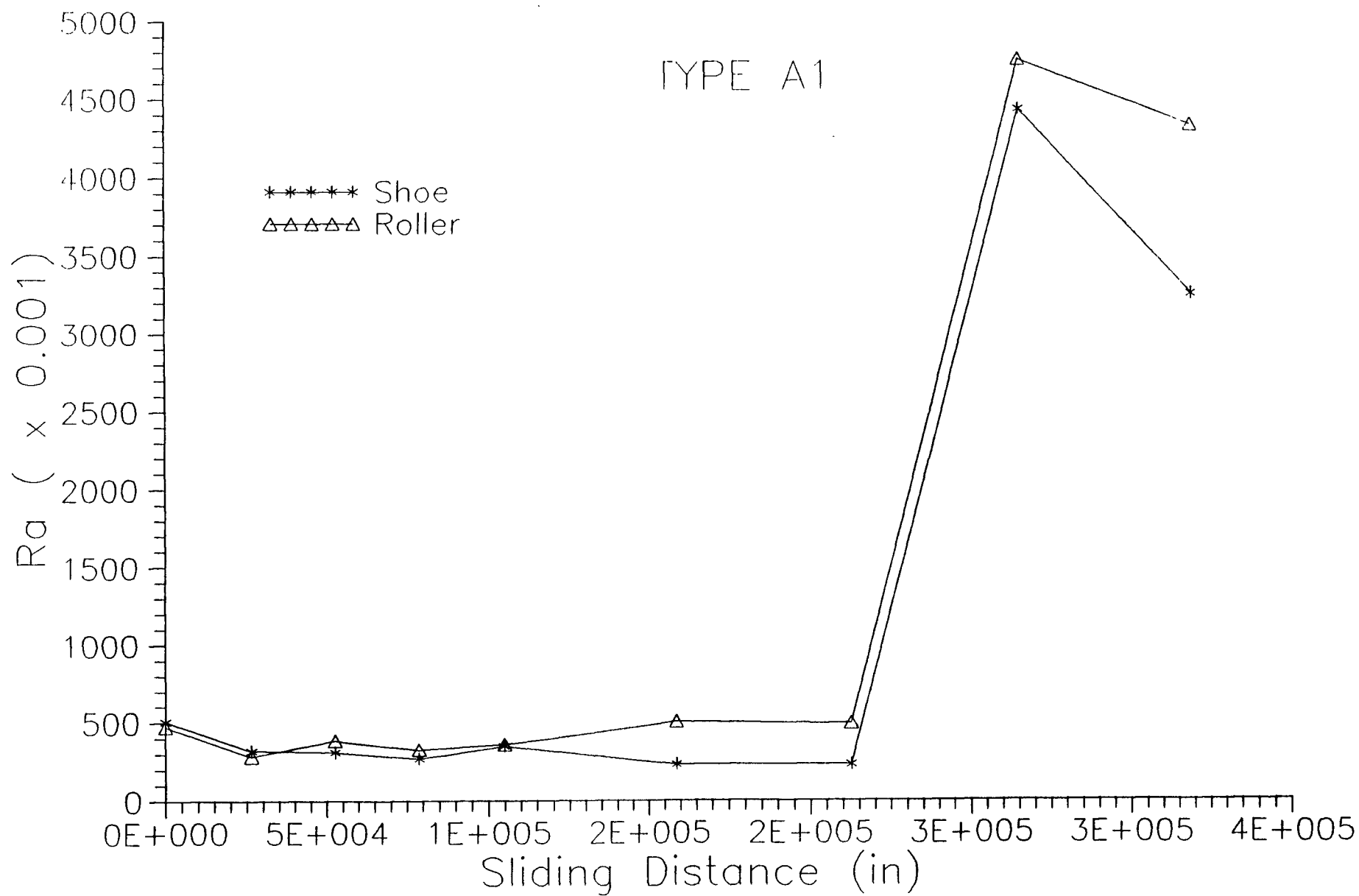


Fig. 4.22 Roughness Parameter Ra vs. Sliding Distance (Type A1)

TYPE A2

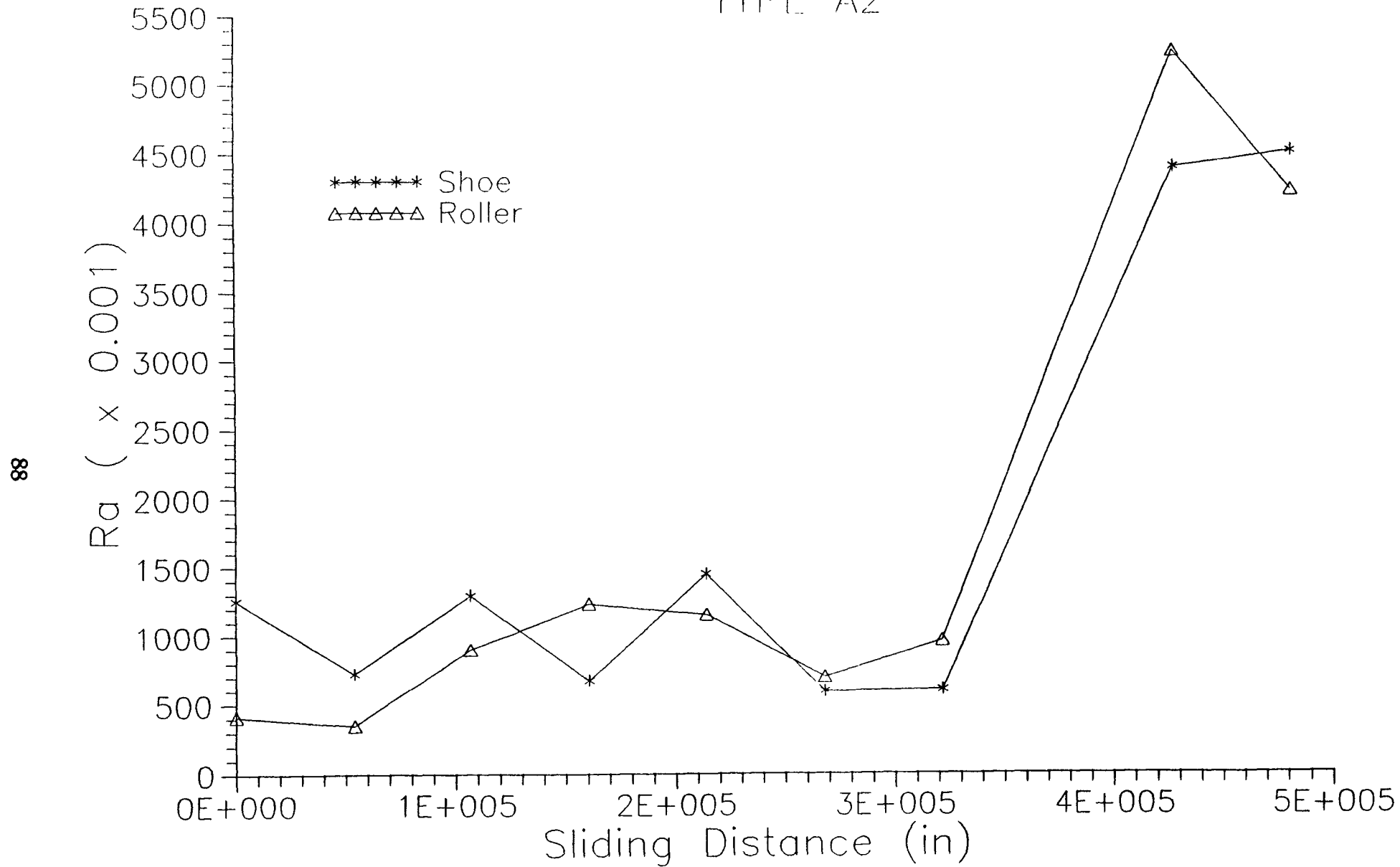


Fig. 4.23 Roughness Parameter Ra vs. Sliding Distance (Type A2)

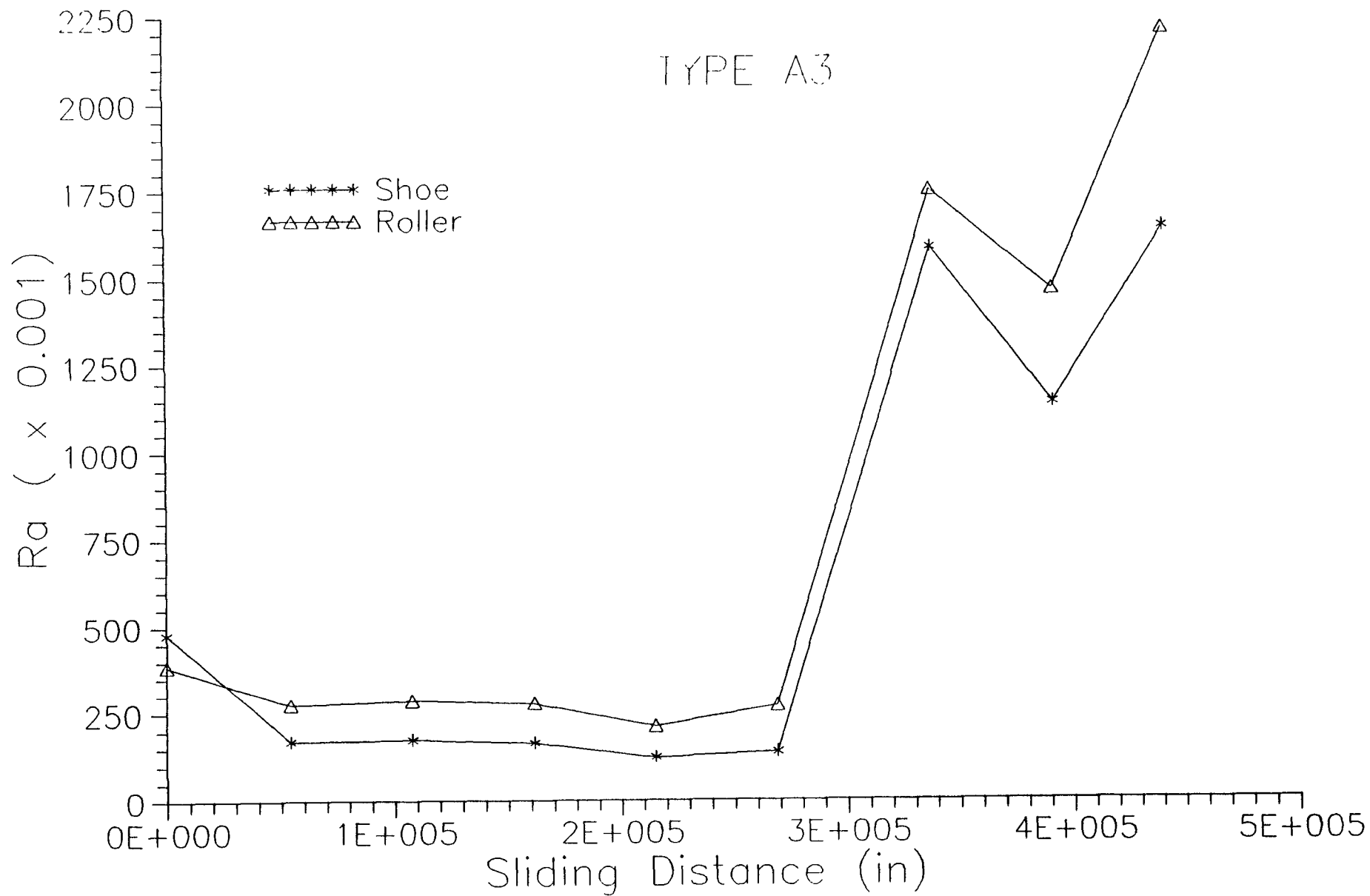


Fig. 4.24 Roughness Parameter Ra vs. Sliding Distance (Type A3)

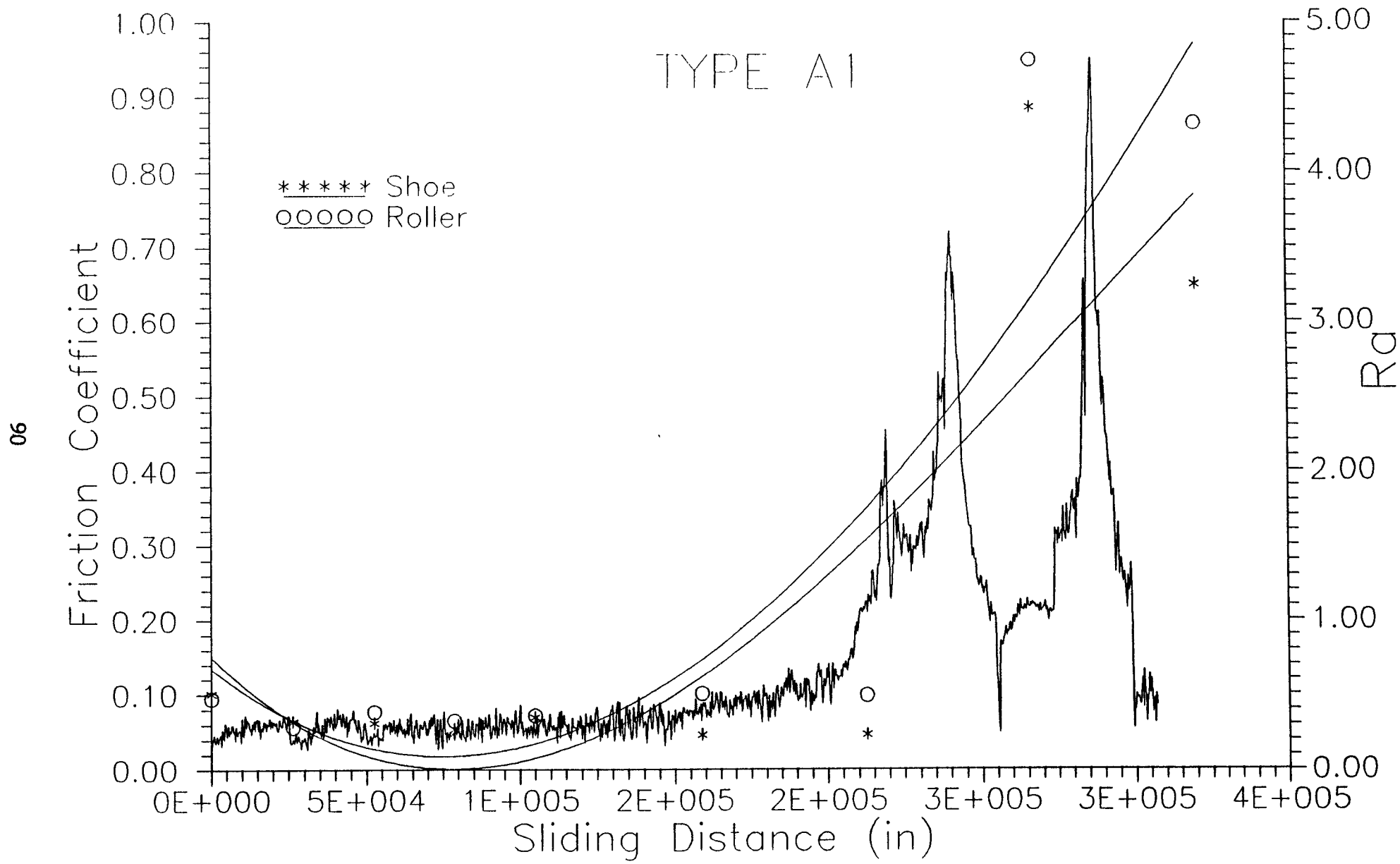


Fig. 4.25 Ra and Friction Coefficient vs. Sliding Distance (Type A1)

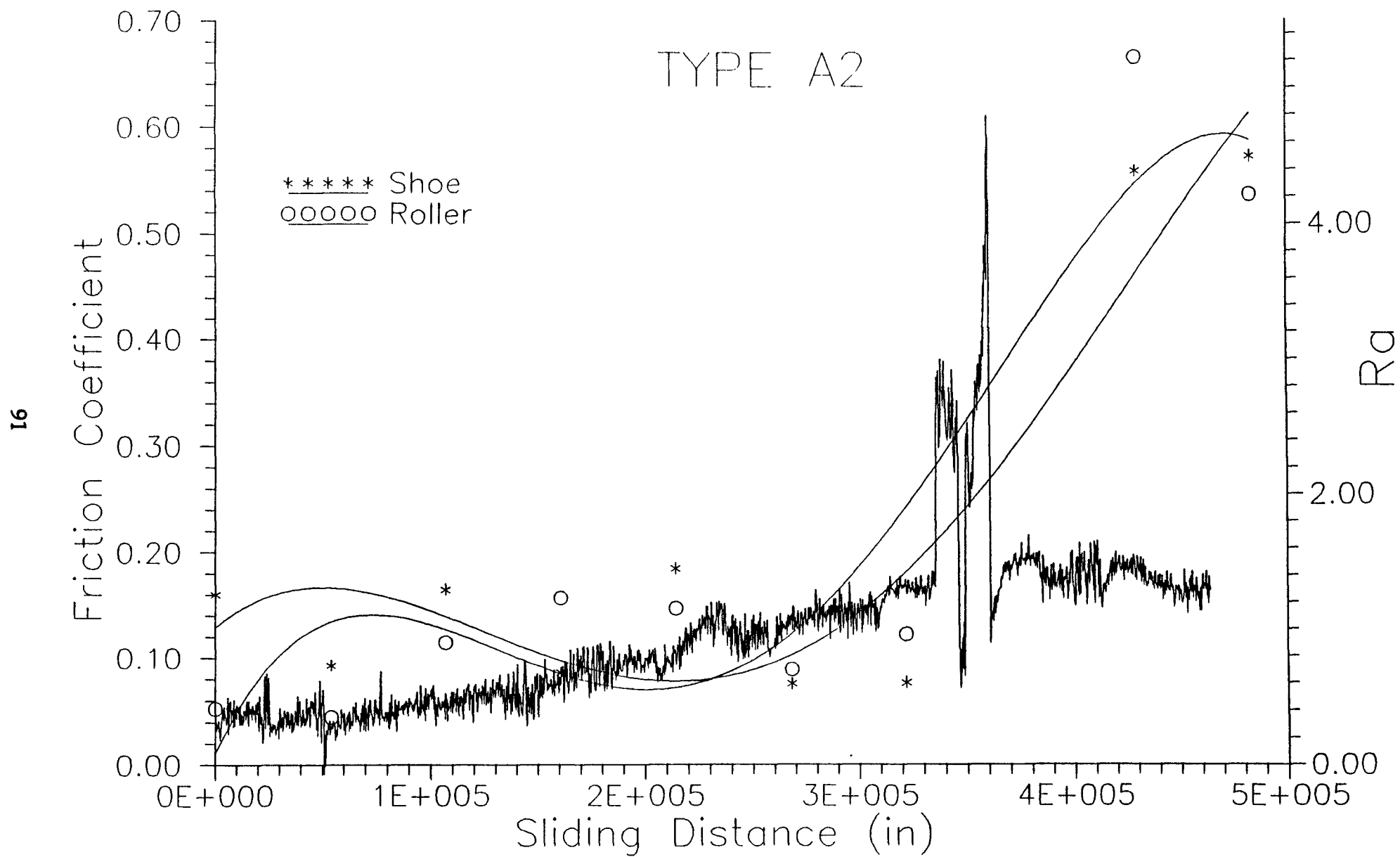


Fig. 4.26 Ra and Friction Coefficient vs. Sliding Distance (Type A2)

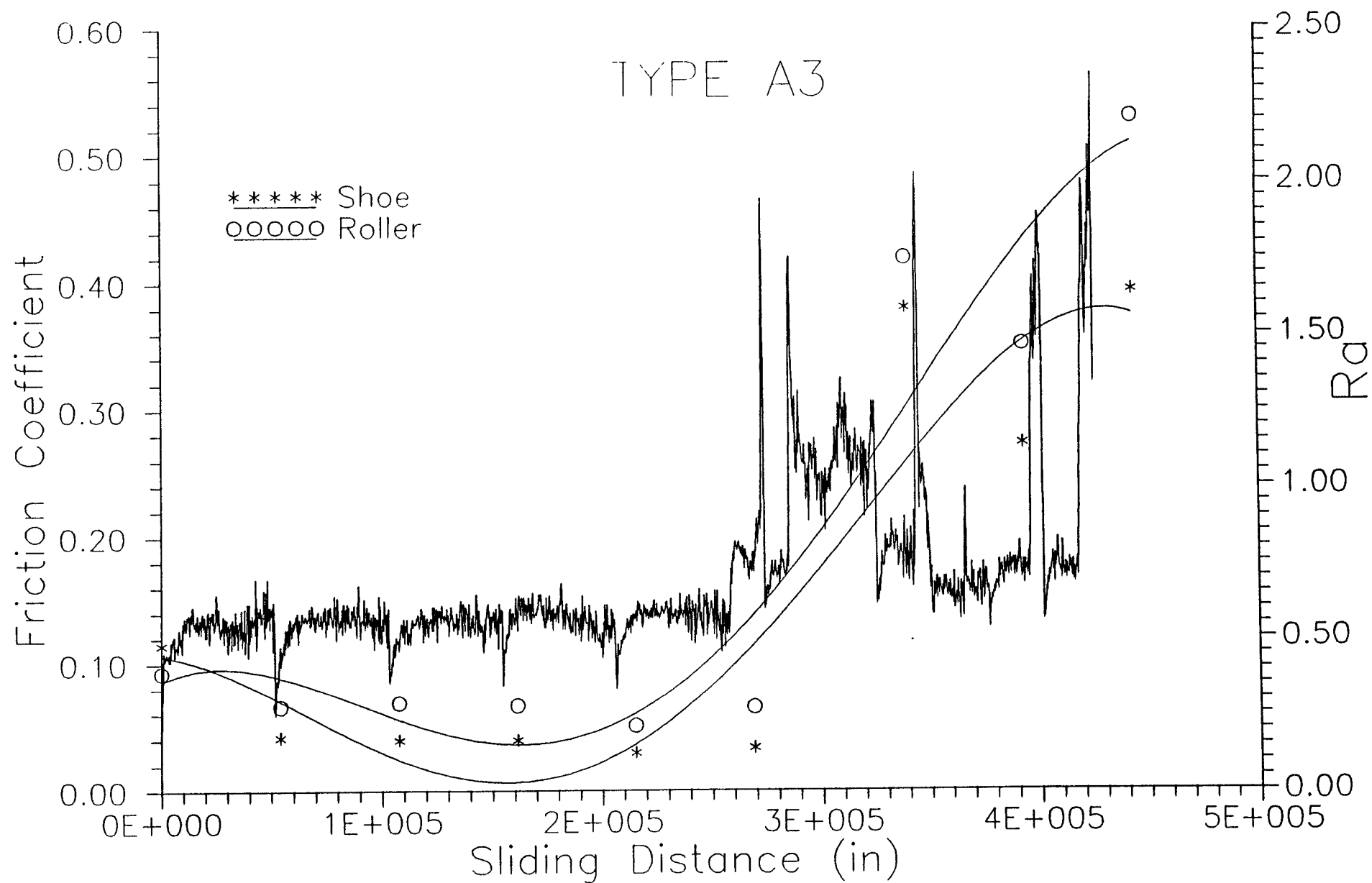


Fig. 4.27 Ra and Friction Coefficient vs. Sliding Distance (Type A3)

Chapter 5

CONCLUSION

Existing wear testing machine has been modified. A loading and unloading mechanism has been designed, manufactured and assembled in this work. The main part of this loading and unloading mechanism is a cam. To obtain the profile for this cam a seven degree polynomial curve has been selected and with the use of CAD softwares the profile has been generated. Later this cam has been manufactured on CNC milling machine. By this procedure, the cam produced has a higher degree of accuracy and good accelerating properties. By installing loading and unloading mechanism on wear testing machine, the loading time and duration of test can be controlled by a D.C. motor. This D.C. motor can be controlled by Programmable Logical Controller to make the testing completely automatic.

A new specimen and a specimen fixture have been designed and installed on existing machine. It is found that large numbers of shoes can be made from the given material by choosing new design. After using the new shoe holder, it is observed that fixing of shoe into the holder takes a shorter time. During the test shoe and shoe holder become very hot because of very high friction force is acting in the area of contact. By installing the new design, one can loose the fixture in minimum time and easily remove the shoe from the fixture, even when it is very hot.

On modified wear testing machine four kinds of specimen have been tested. One specimen which was untreated showed destructive wear in only 15 minutes. While other three specimens which were coated by Plasma Ion-Nitrided method have been tested for longer time without any large damage. The longest sliding distance covered by one of the treated specimen was nearly 500,000 inches. It is found that all treated specimen have lower wear rate as compared to the untreated roller . They gave very low wear rate even under a very high load.

All three coated shoes which were magnetically treated with different number of cycles, shows different wear rate. The specimen that was treated with less number of cycles give higher wear rate as compared to the specimen that was treated with high number of cycles. It can, therefore, inferred that magnetic treatment helps in removing surface stresses and thereby increases wear resistance property.

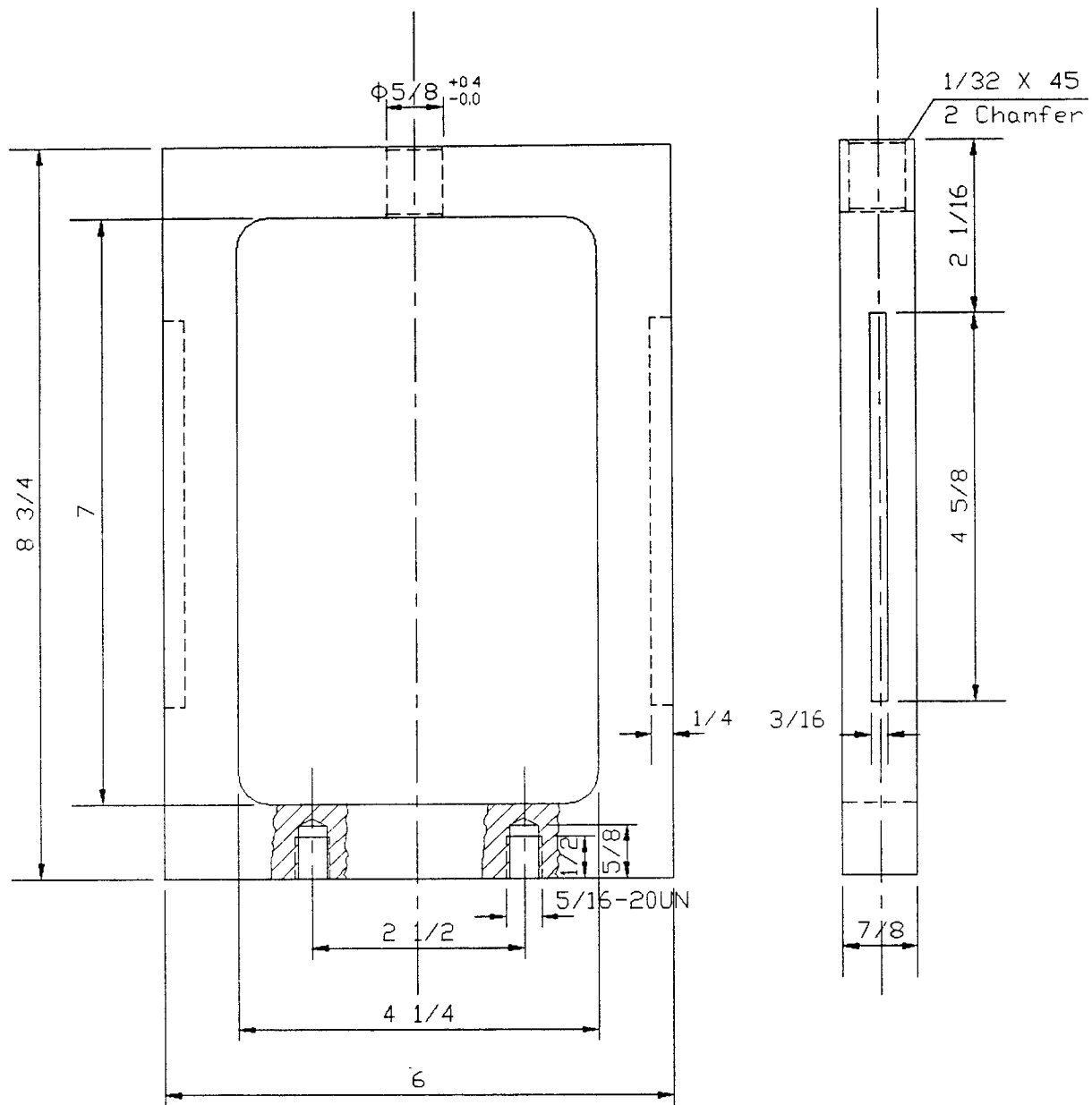
Friction coefficient have been obtained of all these materials using the methodology described in chapter 3. In all cases, friction coefficient rises with the sliding distance. Moreover, the catastrophic region can easily be distinguished from the steady state region.

At every step of the test surface roughness have been investigated. In all cases, the surface roughness have been improved after some time. At the beginning the surface has a lots of irregularities which is teared off due to tangential force during running in stage. Once the steady state has been reaches, the surface roughness does not change so rapidly. In catastrophic

region, where coefficient of friction, as well as wear rate, is very high the surface roughness has become worse.

By using the methodology of this wear testing device, a further improvement of machine is suggested. For this purpose a reducer has been modified in this work that will give another type of geometry for testing materials i.e. roller to roller. Other testing parameter like speed and temperature should be controlled in future.

APPENDIX



NEW JERSEY INSTITUTE OF TECHNOLOGY
MECHANICAL ENGINEERING DEPARTMENT

SCALE: 1 : 2

APPROVED BY:

DRAWN BY: M. FAROOQ

DATE: 16/2/89

DR. DUBROVSKY

REVISED BY:

FRAME

QTY

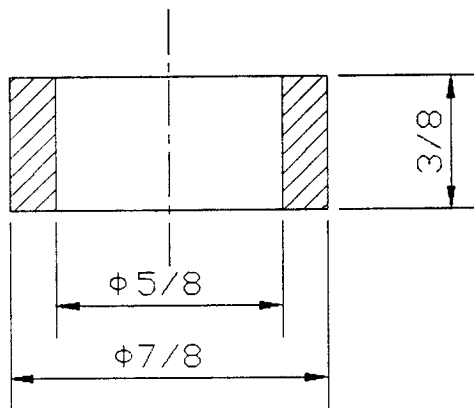
1

ALL DIMENSIONS ARE IN INCHES

DRAWING NO.

WTM 2-013-90-04

WTM 2-013-90-2



NEW JERSEY INSTITUTE OF TECHNOLOGY
MECHANICAL ENGINEERING DEPARTMENT

SCALE: 2 : 1

APPROVED BY:

DRAWN BY: M. FAPGOO

DATE: 11/2/89

DR. DUBROVSKY

REVISED BY:

TOP SPAER

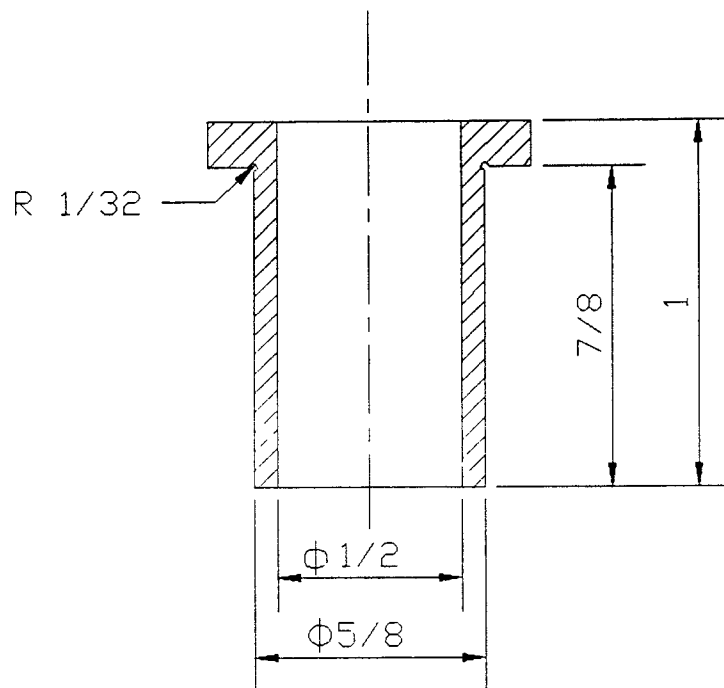
QTY

1

ALL DIMENSIONS ARE IN INCHES

DRAWING NO.

WTM 2-013-50-6



NEW JERSEY INSTITUTE OF TECHNOLOGY
MECHANICAL ENGINEERING DEPARTMENT

SCALE: 2 : 1

APPROVED BY:

DRAWN BY: M. FAROOQ

DATE: 15/2/89

DR. DUBROVSKY

REVISED BY

BUSH

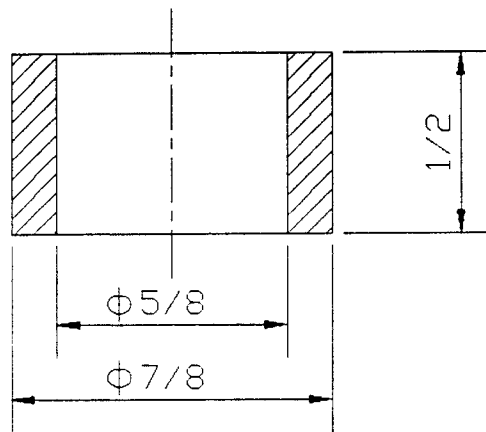
QTY

1

ALL DIMENSIONS ARE IN INCHES

DRAWING NO.

WTM 2-013-90-7



NEW JERSEY INSTITUTE OF TECHNOLOGY
MECHANICAL ENGINEERING DEPARTMENT

SCALE: 2 : 1

APPROVED BY:

DRAWN BY: M FAROOQ

DATE: 11/2/89

DR. DUBROVSKY

REVISED BY:

BOTTOM SPACER

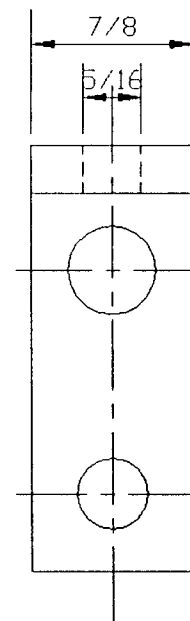
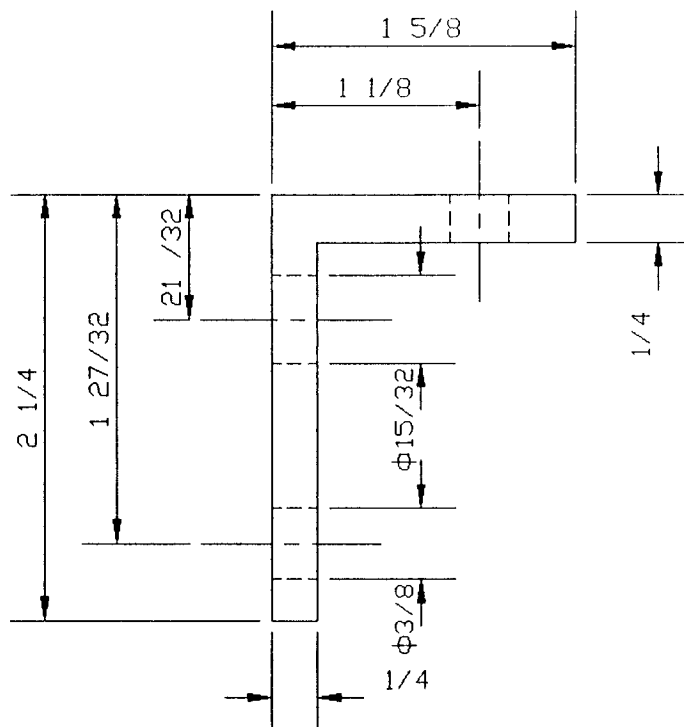
QTY

1

ALL DIMENSIONS ARE IN INCHES

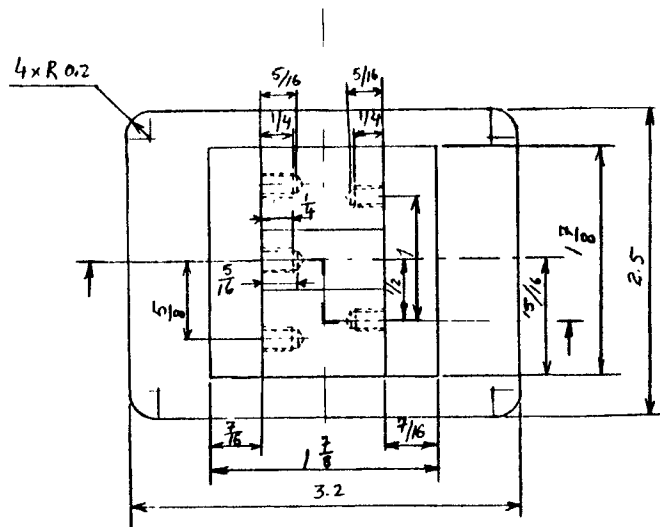
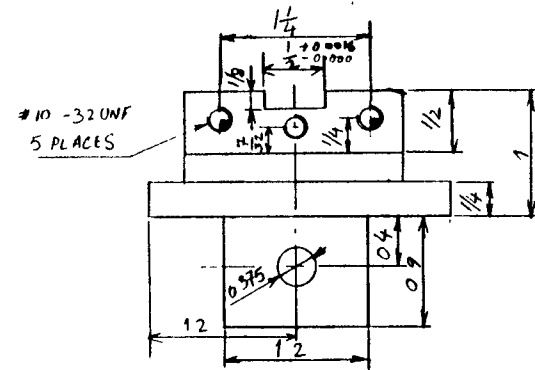
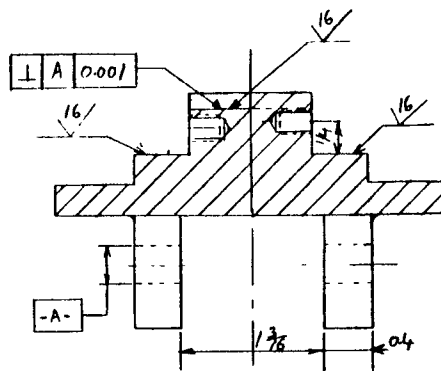
DRAWING NO.

WTM 2-013-90-8

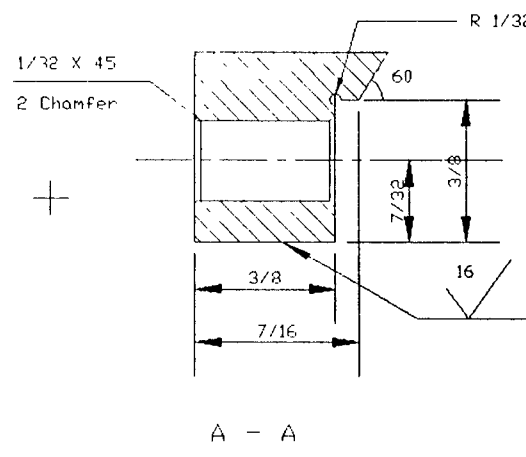
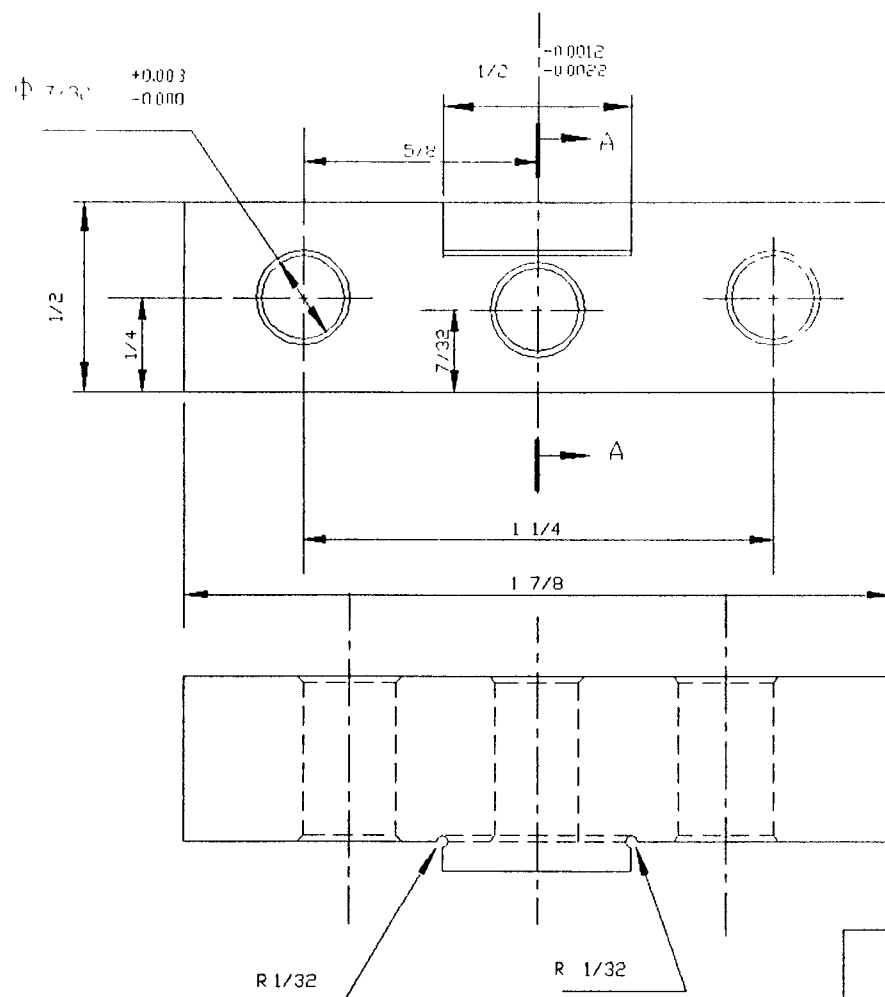


NEW JERSEY INSTITUTE OF TECHNOLOGY
MECHANICAL ENGINEERING DEPARTMENT

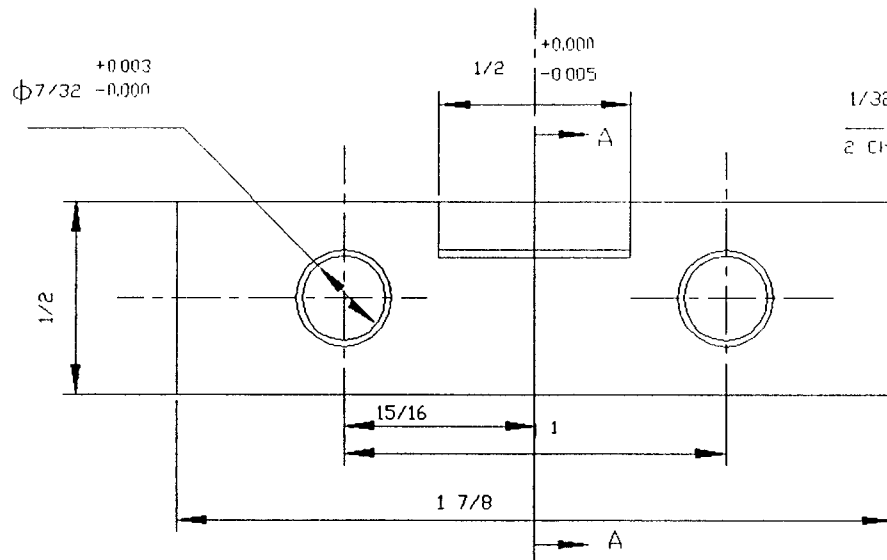
SCALE: 1 : 1	APPROVED BY:	DRAWN BY: M.FAROOQ
DATE: 11/25/89	DR. DUBROVSKY	REVISED BY:
ANGLE	QTY	2
ALL DIMENSIONS ARE IN INCHES		DRAWING NO:
		WTM 2-013-90-1



NEW JERSEY INSTITUTE OF TECHNOLOGY MECH ENG DEPARTMENT			
SCALE 1:1	APPROVED BY	DRAWN BY FAROOR	
DATE 6/1/90	<i>[Signature]</i>	REVISED BY	
BODY		QTY	1
ALL DIMENSIONS ARE IN INCHES			DRAWING NO WTM 00-09N-01N-06

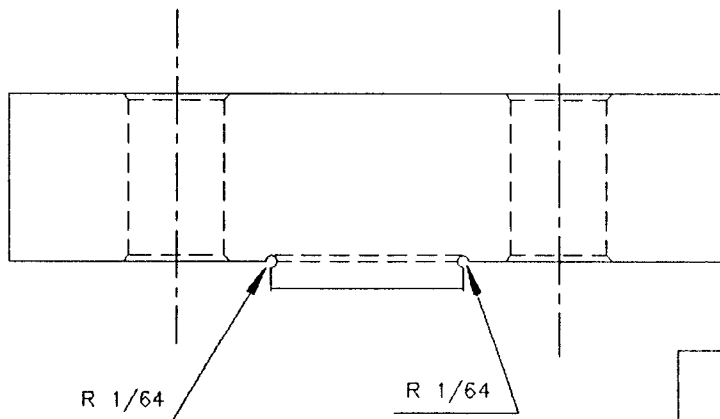
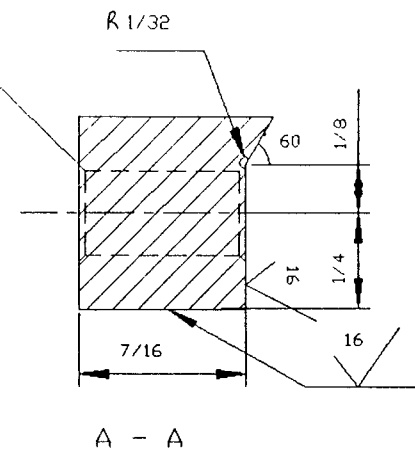


NEW JERSEY INSTITUTE OF TECHNOLOGY MECHANICAL ENGINEERING DEPT.			
SCALE 2:1	APPROVED BY: DR R. DUBROVSKY		DRAWN BY FARDOO
DATE 6/4/90			REVISED BY
LEFT SIDE SUPPORT		QTY	1
ALL DIMENSIONS ARE IN INCHES			DRAWING NO.
			WTM 00-09N-01N-04



$1/32 \times 45$

2 Chanfer



NEW JERSEY INSTITUTE OF TECHNOLOGY
MECHANICAL ENGINEERING DEPT.

SCALE 2:1

DATE 6/4/90

APPROVED BY:

DRAWN BY FAROOQ

REVISED BY

RIGHT SIDE SUPPORT

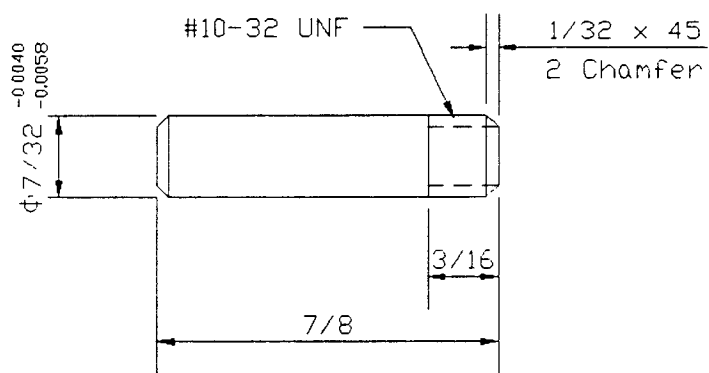
QTY

1

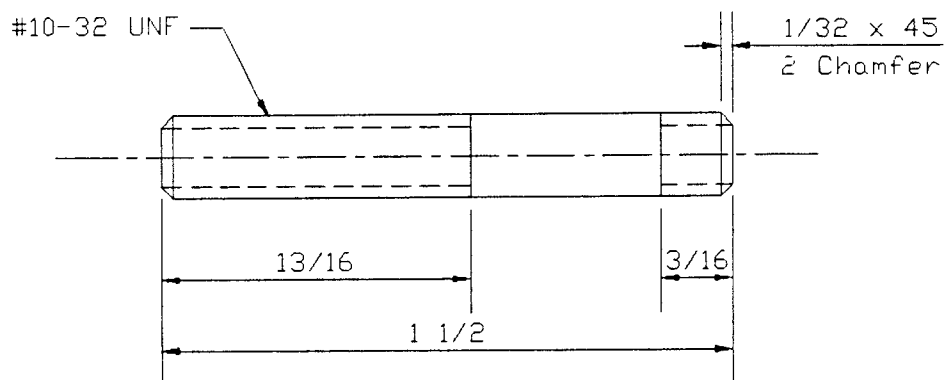
ALL DIMENSIONS ARE IN INCHES

DRAWING NO

WTM 00-09N-01N-02

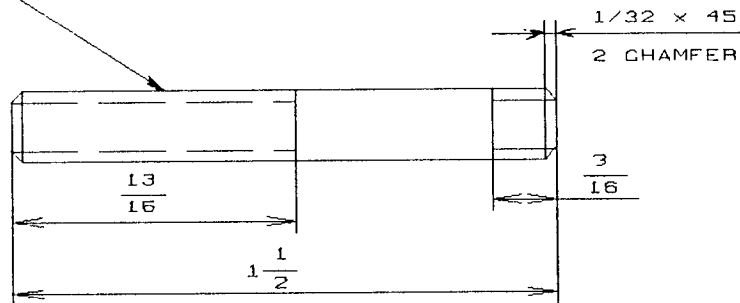


NEW JERSEY INSTITUTE OF TECHNOLOGY MECHANICAL ENGINEERING DEPARTMENT		
SCALE: 2 : 1	APPROVED BY:	DRAWN BY: M.FAROOQ
DATE: 6/5/90	DR. DUBROVSKY	REVISED BY:
GUIDE PIN	QTY	2
ALL DIMENSIONS ARE IN INCHES		DRAWING NO. WTM 00-0911-0111-09



NEW JERSEY INSTITUTE OF TECHNOLOGY MECHANICAL ENGINEERING DEPARTMENT		
SCALE: 2 : 1	APPROVED BY:	DRAWN BY: M. FAROOQ
DATE: 6/5/90	DR. DUBROVSKY	REVISED BY:
PIN	QTY	1
ALL DIMENSIONS ARE IN INCHES		DRAWING NO: WTM 00-0911-0111-07

#10-32 UNF



NEW JERSEY INSTITUTE OF TECHNOLOGY
MECHANICAL ENGINEERING DEPT.

SCALE 2.1	APPROVED BY	DRAWN BY FAROOQ	
DATE 6/5/90		REVISED BY	
PIN		QTY	1
ALL DIMENSIONS ARE IN INCHES		DRAWING NO	
		WTM-00-09N-01N-07	

```

/* CAM100.C */
#include <stdio.h>
#include <math.h>
main()
{
    int    i,a=60,b=100,c=40,d=100,e=60;
    float  n[361],r[361],x[361],y[361];
    float  t,ttl,tt2,rr;
    float  b1=100.,b2=100.,h=1.25,pi=3.1416;
    FILE   *out;
    out=fopen("a:cam100.dat","w");
    for (i=0;i<=a;i++)
    {
        n[i]=(float)i;
        r[i]=0.;
        rr=r[i]+0.75;
        x[i]=rr*sin(pi*n[i]/180.);
        y[i]=rr*cos(pi*n[i]/180.);
    }
    t=0.;
    for(i=a;i<=a+b;i++)
    {
        n[i]=(float)i;
        ttl=t/b1;
        r[i]=h*(35.*pow(ttl,4.)-84.*pow(ttl,5.)
                +70.*pow(ttl,6.)-20.*pow(ttl,7.));
        rr=r[i]+0.75;
        x[i]=rr*sin(pi*n[i]/180.);
        y[i]=rr*cos(pi*n[i]/180.);
        t+=1.;
    }
    for(i=a+b;i<=a+b+c;i++)
    {
        n[i]=(float)i;
        r[i]=1.25;
        rr=r[i]+0.75;
        x[i]=rr*sin(pi*n[i]/180.);
        y[i]=rr*cos(pi*n[i]/180.);
    }
    t=0.;
    for(i=a+b+c;i<=a+b+c+d;i++)
    {
        n[i]=(float)i;
        ttl=t/b2;
        r[i]=h*(1.-(35.*pow(ttl,4.)-84.*pow(ttl,5.)
                +70.*pow(ttl,6.)-20.*pow(ttl,7.)));
        rr=r[i]+0.75;
        x[i]=rr*sin(pi*n[i]/180.);
        y[i]=rr*cos(pi*n[i]/180.);
        t+=1.;
    }
    for(i=a+b+c+d;i<=a+b+c+d+e;i++)
    {
        n[i]=(float)i;
        r[i]=0.;
        rr=r[i]+0.75;
        x[i]=rr*sin(pi*n[i]/180.);
        y[i]=rr*cos(pi*n[i]/180.);
    }
    for(i=0;i<=360;i++)
    {

```

```
        printf("working!    i=%3d\n",i);
        fprintf(out,"          %5.1f  %6.3f  %6.3f  %6.3f\n",n[i],
                r[i],x[i],y[i]);
    }
    fclose(out);
}
```

0.0	0.000	0.000	0.750
1.0	0.000	0.013	0.750
2.0	0.000	0.026	0.750
3.0	0.000	0.039	0.749
4.0	0.000	0.052	0.748
5.0	0.000	0.065	0.747
6.0	0.000	0.078	0.746
7.0	0.000	0.091	0.744
8.0	0.000	0.104	0.743
9.0	0.000	0.117	0.741
10.0	0.000	0.130	0.739
11.0	0.000	0.143	0.736
12.0	0.000	0.156	0.734
13.0	0.000	0.169	0.731
14.0	0.000	0.181	0.728
15.0	0.000	0.194	0.724
16.0	0.000	0.207	0.721
17.0	0.000	0.219	0.717
18.0	0.000	0.232	0.713
19.0	0.000	0.244	0.709
20.0	0.000	0.257	0.705
21.0	0.000	0.269	0.700
22.0	0.000	0.281	0.695
23.0	0.000	0.293	0.690
24.0	0.000	0.305	0.685
25.0	0.000	0.317	0.680
26.0	0.000	0.329	0.674
27.0	0.000	0.340	0.668
28.0	0.000	0.352	0.662
29.0	0.000	0.364	0.656
30.0	0.000	0.375	0.650
31.0	0.000	0.386	0.643
32.0	0.000	0.397	0.636
33.0	0.000	0.408	0.629
34.0	0.000	0.419	0.622
35.0	0.000	0.430	0.614
36.0	0.000	0.441	0.607
37.0	0.000	0.451	0.599
38.0	0.000	0.462	0.591
39.0	0.000	0.472	0.583
40.0	0.000	0.482	0.575
41.0	0.000	0.492	0.566
42.0	0.000	0.502	0.557
43.0	0.000	0.511	0.549
44.0	0.000	0.521	0.540
45.0	0.000	0.530	0.530
46.0	0.000	0.540	0.521
47.0	0.000	0.549	0.511
48.0	0.000	0.557	0.502
49.0	0.000	0.566	0.492
50.0	0.000	0.575	0.482
51.0	0.000	0.583	0.472
52.0	0.000	0.591	0.462
53.0	0.000	0.599	0.451
54.0	0.000	0.607	0.441
55.0	0.000	0.614	0.430
56.0	0.000	0.622	0.419
57.0	0.000	0.629	0.408
58.0	0.000	0.636	0.397
59.0	0.000	0.643	0.386

60.0	0.000	0.650	0.375
61.0	0.000	0.656	0.364
62.0	0.000	0.662	0.352
63.0	0.000	0.668	0.341
64.0	0.000	0.674	0.329
65.0	0.000	0.680	0.317
66.0	0.000	0.686	0.305
67.0	0.001	0.691	0.293
68.0	0.001	0.697	0.282
69.0	0.002	0.702	0.270
70.0	0.003	0.708	0.258
71.0	0.005	0.714	0.246
72.0	0.007	0.720	0.234
73.0	0.009	0.726	0.222
74.0	0.012	0.732	0.210
75.0	0.015	0.739	0.198
76.0	0.019	0.746	0.186
77.0	0.024	0.754	0.174
78.0	0.029	0.762	0.162
79.0	0.035	0.770	0.150
80.0	0.042	0.780	0.137
81.0	0.049	0.789	0.125
82.0	0.058	0.800	0.112
83.0	0.067	0.811	0.100
84.0	0.077	0.823	0.086
85.0	0.088	0.835	0.073
86.0	0.100	0.848	0.059
87.0	0.113	0.862	0.045
88.0	0.127	0.876	0.031
89.0	0.142	0.892	0.016
90.0	0.158	0.908	-0.000
91.0	0.174	0.924	-0.016
92.0	0.192	0.941	-0.033
93.0	0.210	0.959	-0.050
94.0	0.230	0.977	-0.068
95.0	0.250	0.996	-0.087
96.0	0.271	1.015	-0.107
97.0	0.293	1.035	-0.127
98.0	0.315	1.055	-0.148
99.0	0.338	1.075	-0.170
100.0	0.362	1.095	-0.193
101.0	0.387	1.116	-0.217
102.0	0.412	1.136	-0.242
103.0	0.437	1.157	-0.267
104.0	0.463	1.177	-0.294
105.0	0.490	1.197	-0.321
106.0	0.516	1.217	-0.349
107.0	0.543	1.237	-0.378
108.0	0.570	1.256	-0.408
109.0	0.598	1.274	-0.439
110.0	0.625	1.292	-0.470
111.0	0.652	1.309	-0.503
112.0	0.680	1.325	-0.536
113.0	0.707	1.341	-0.569
114.0	0.734	1.355	-0.603
115.0	0.760	1.369	-0.638
116.0	0.787	1.381	-0.674
117.0	0.813	1.392	-0.709
118.0	0.838	1.402	-0.746
119.0	0.863	1.411	-0.782

120.0	0.888	1.418	-0.819
121.0	0.912	1.424	-0.856
122.0	0.935	1.429	-0.893
123.0	0.957	1.432	-0.930
124.0	0.979	1.434	-0.967
125.0	1.000	1.434	-1.004
126.0	1.020	1.432	-1.041
127.0	1.040	1.429	-1.077
128.0	1.058	1.425	-1.113
129.0	1.076	1.419	-1.149
130.0	1.092	1.411	-1.184
131.0	1.108	1.402	-1.219
132.0	1.123	1.392	-1.253
133.0	1.137	1.380	-1.287
134.0	1.150	1.367	-1.320
135.0	1.162	1.352	-1.352
136.0	1.173	1.336	-1.383
137.0	1.183	1.318	-1.414
138.0	1.192	1.300	-1.443
139.0	1.201	1.280	-1.472
140.0	1.208	1.259	-1.500
141.0	1.215	1.237	-1.527
142.0	1.221	1.214	-1.553
143.0	1.226	1.189	-1.578
144.0	1.231	1.164	-1.603
145.0	1.235	1.138	-1.626
146.0	1.238	1.112	-1.648
147.0	1.241	1.084	-1.670
148.0	1.243	1.056	-1.690
149.0	1.245	1.028	-1.710
150.0	1.247	0.998	-1.729
151.0	1.248	0.968	-1.747
152.0	1.249	0.938	-1.765
153.0	1.249	0.908	-1.781
154.0	1.250	0.877	-1.797
155.0	1.250	0.845	-1.812
156.0	1.250	0.813	-1.827
157.0	1.250	0.781	-1.841
158.0	1.250	0.749	-1.854
159.0	1.250	0.717	-1.867
160.0	1.250	0.684	-1.879
161.0	1.250	0.651	-1.891
162.0	1.250	0.618	-1.902
163.0	1.250	0.585	-1.913
164.0	1.250	0.551	-1.923
165.0	1.250	0.518	-1.932
166.0	1.250	0.484	-1.941
167.0	1.250	0.450	-1.949
168.0	1.250	0.416	-1.956
169.0	1.250	0.382	-1.963
170.0	1.250	0.347	-1.970
171.0	1.250	0.313	-1.975
172.0	1.250	0.278	-1.981
173.0	1.250	0.244	-1.985
174.0	1.250	0.209	-1.989
175.0	1.250	0.174	-1.992
176.0	1.250	0.139	-1.995
177.0	1.250	0.105	-1.997
178.0	1.250	0.070	-1.999
179.0	1.250	0.035	-2.000

180.0	1.250	-0.000	-2.000
181.0	1.250	-0.035	-2.000
182.0	1.250	-0.070	-1.999
183.0	1.250	-0.105	-1.997
184.0	1.250	-0.140	-1.995
185.0	1.250	-0.174	-1.992
186.0	1.250	-0.209	-1.989
187.0	1.250	-0.244	-1.985
188.0	1.250	-0.278	-1.981
189.0	1.250	-0.313	-1.975
190.0	1.250	-0.347	-1.970
191.0	1.250	-0.382	-1.963
192.0	1.250	-0.416	-1.956
193.0	1.250	-0.450	-1.949
194.0	1.250	-0.484	-1.941
195.0	1.250	-0.518	-1.932
196.0	1.250	-0.551	-1.923
197.0	1.250	-0.585	-1.913
198.0	1.250	-0.618	-1.902
199.0	1.250	-0.651	-1.891
200.0	1.250	-0.684	-1.879
201.0	1.250	-0.717	-1.867
202.0	1.250	-0.749	-1.854
203.0	1.250	-0.781	-1.841
204.0	1.250	-0.813	-1.827
205.0	1.250	-0.845	-1.812
206.0	1.250	-0.877	-1.797
207.0	1.249	-0.908	-1.781
208.0	1.249	-0.938	-1.765
209.0	1.248	-0.969	-1.747
210.0	1.247	-0.998	-1.729
211.0	1.245	-1.028	-1.710
212.0	1.243	-1.056	-1.690
213.0	1.241	-1.084	-1.670
214.0	1.238	-1.112	-1.648
215.0	1.235	-1.138	-1.626
216.0	1.231	-1.164	-1.603
217.0	1.226	-1.189	-1.578
218.0	1.221	-1.214	-1.553
219.0	1.215	-1.237	-1.527
220.0	1.208	-1.259	-1.500
221.0	1.201	-1.280	-1.472
222.0	1.192	-1.300	-1.443
223.0	1.183	-1.318	-1.414
224.0	1.173	-1.336	-1.383
225.0	1.162	-1.352	-1.352
226.0	1.150	-1.367	-1.320
227.0	1.137	-1.380	-1.287
228.0	1.123	-1.392	-1.253
229.0	1.108	-1.402	-1.219
230.0	1.092	-1.411	-1.184
231.0	1.076	-1.419	-1.149
232.0	1.058	-1.425	-1.113
233.0	1.040	-1.429	-1.077
234.0	1.020	-1.432	-1.041
235.0	1.000	-1.434	-1.004
236.0	0.979	-1.434	-0.967
237.0	0.957	-1.432	-0.930
238.0	0.935	-1.429	-0.893
239.0	0.912	-1.424	-0.856

240.0	0.888	-1.418	-0.819
241.0	0.863	-1.411	-0.782
242.0	0.838	-1.402	-0.746
243.0	0.813	-1.392	-0.709
244.0	0.787	-1.381	-0.674
245.0	0.760	-1.369	-0.638
246.0	0.734	-1.355	-0.603
247.0	0.707	-1.341	-0.569
248.0	0.680	-1.326	-0.536
249.0	0.652	-1.309	-0.503
250.0	0.625	-1.292	-0.470
251.0	0.598	-1.274	-0.439
252.0	0.570	-1.256	-0.408
253.0	0.543	-1.237	-0.378
254.0	0.516	-1.217	-0.349
255.0	0.490	-1.197	-0.321
256.0	0.463	-1.177	-0.294
257.0	0.437	-1.157	-0.267
258.0	0.412	-1.136	-0.242
259.0	0.387	-1.116	-0.217
260.0	0.362	-1.095	-0.193
261.0	0.338	-1.075	-0.170
262.0	0.315	-1.055	-0.148
263.0	0.293	-1.035	-0.127
264.0	0.271	-1.015	-0.107
265.0	0.250	-0.996	-0.087
266.0	0.230	-0.977	-0.068
267.0	0.210	-0.959	-0.050
268.0	0.192	-0.941	-0.033
269.0	0.174	-0.924	-0.016
270.0	0.158	-0.908	0.000
271.0	0.142	-0.892	0.016
272.0	0.127	-0.876	0.031
273.0	0.113	-0.862	0.045
274.0	0.100	-0.848	0.059
275.0	0.088	-0.835	0.073
276.0	0.077	-0.823	0.086
277.0	0.067	-0.811	0.100
278.0	0.058	-0.800	0.112
279.0	0.049	-0.789	0.125
280.0	0.042	-0.780	0.137
281.0	0.035	-0.770	0.150
282.0	0.029	-0.762	0.162
283.0	0.024	-0.754	0.174
284.0	0.019	-0.746	0.186
285.0	0.015	-0.739	0.198
286.0	0.012	-0.732	0.210
287.0	0.009	-0.726	0.222
288.0	0.007	-0.720	0.234
289.0	0.005	-0.714	0.246
290.0	0.003	-0.708	0.258
291.0	0.002	-0.702	0.270
292.0	0.001	-0.697	0.282
293.0	0.001	-0.691	0.293
294.0	0.000	-0.686	0.305
295.0	0.000	-0.680	0.317
296.0	0.000	-0.674	0.329
297.0	0.000	-0.668	0.341
298.0	0.000	-0.662	0.352
299.0	0.000	-0.656	0.364

300.0	0.000	-0.650	0.375
301.0	0.000	-0.643	0.386
302.0	0.000	-0.636	0.397
303.0	0.000	-0.629	0.408
304.0	0.000	-0.622	0.419
305.0	0.000	-0.614	0.430
306.0	0.000	-0.607	0.441
307.0	0.000	-0.599	0.451
308.0	0.000	-0.591	0.462
309.0	0.000	-0.583	0.472
310.0	0.000	-0.575	0.482
311.0	0.000	-0.566	0.492
312.0	0.000	-0.557	0.502
313.0	0.000	-0.549	0.512
314.0	0.000	-0.539	0.521
315.0	0.000	-0.530	0.530
316.0	0.000	-0.521	0.540
317.0	0.000	-0.511	0.549
318.0	0.000	-0.502	0.557
319.0	0.000	-0.492	0.566
320.0	0.000	-0.482	0.575
321.0	0.000	-0.472	0.583
322.0	0.000	-0.462	0.591
323.0	0.000	-0.451	0.599
324.0	0.000	-0.441	0.607
325.0	0.000	-0.430	0.614
326.0	0.000	-0.419	0.622
327.0	0.000	-0.408	0.629
328.0	0.000	-0.397	0.636
329.0	0.000	-0.386	0.643
330.0	0.000	-0.375	0.650
331.0	0.000	-0.364	0.656
332.0	0.000	-0.352	0.662
333.0	0.000	-0.340	0.668
334.0	0.000	-0.329	0.674
335.0	0.000	-0.317	0.680
336.0	0.000	-0.305	0.685
337.0	0.000	-0.293	0.690
338.0	0.000	-0.281	0.695
339.0	0.000	-0.269	0.700
340.0	0.000	-0.257	0.705
341.0	0.000	-0.244	0.709
342.0	0.000	-0.232	0.713
343.0	0.000	-0.219	0.717
344.0	0.000	-0.207	0.721
345.0	0.000	-0.194	0.724
346.0	0.000	-0.181	0.728
347.0	0.000	-0.169	0.731
348.0	0.000	-0.156	0.734
349.0	0.000	-0.143	0.736
350.0	0.000	-0.130	0.739
351.0	0.000	-0.117	0.741
352.0	0.000	-0.104	0.743
353.0	0.000	-0.091	0.744
354.0	0.000	-0.078	0.746
355.0	0.000	-0.065	0.747
356.0	0.000	-0.052	0.748
357.0	0.000	-0.039	0.749
358.0	0.000	-0.026	0.750
359.0	0.000	-0.013	0.750

360.0 0.000 0.000 0.750

References

- [1] Eyre, T. S., "Wear Characteristics of Metals", Source Book on Wear Control Technology, ed. Rigney, D. A. and Glaeser, W. A., American Society for Metals, 1988 p 1-9.
- [2] Peterson, M.B., "Wear Testing Objectives and Approaches", Source Book on Wear Control Technology, ed. Rigney, D. A. and Glaeser, W. A., American Society for Metals, 1988
- [3] Benzing, R., Goldblatt, I., Hopkins, V., Jamison, W., Mecklenburg, K. and Peterson, M., "Friction and Wear Devices", ASLE 1976
- [4] Lipson, C., "Wear Consideration in Design", Prentice-Hall, Inc., 1976
- [5] Moore, D. F., "Principles and Application of Tribology", Pergamon Press, 1975
- [6] Lansdown, A. R., and Price, A. L., "Material to Resist Wear", Pergamon Press 1986
- [7] Barwell, F. T., "Wear of Machine Element", Fundamentals of Tribology", ed., Suh, N. P. and Saka, N., The MIT Press, 1978 p 401-442
- [8] Kislik, V. A., "The Wear of Railway Engine Components, "Transzheldouzoat, 1948.
- [9] Kragelskii, I. V., "Friction and Wear", Butterworths, Washington D. C., 1965
- [10] Archard, J. F., "A review of Wear Studies", Proceedings, Interdisciplinary Approach to Friction and Wear, National Aeronautics and Space Administration, Washington, D. C.

- [11] Archard, J. F. and Hirst, W., Proceedings of the Royal Society of London, Vol. A 236, 1956, p 397.
- [12] Peterson, M. B. " Mechanism of Wear", Boundary Lubrication, An Appraisal of World Literature, F. F. Ling, E. E. Klaus, and R. S. Fein, Eds., American Society of Mechanical Engineers, 1969.
- [13] Ozbaysal, K. and Inal, O.T., " Structure and Properties of Ion-Nitrided Stainless Steel", Journal of Material Science 21, 1986, p 4318-4326.
- [14] Kurny, A.S.W., Ras, M.M. and Mallya, R.M. "Design and Construction of a Laboratory Model Ion-Nitriding Unit", Indian Journal of Technology, v 24, Oct 1986, p 671-675.
- [15] Spalvin, T., "Advances and Directions of Ion-Nitriding/Carburizing", Ion-Nitriding and Ion-Carburizing, ed Spalvins, T. and Kovacs, W.L, ASM International 1989, p 1-4.
- [16] Zlatanovic, M., "(Ti,Al)N Coating on Plasma Nitrided Surfaces", Ion-Nitriding and Ion-Carburizing, ed Spalvins, T. and Kovacs, K.L., ASM International 1989, p 99-104.
- [17] Dubrovsky, R., Kin, Y. and Shih, I-Tsung, "Development of the Computer Controlled Wear Testing Methodology", 1988.
- [18] Shih, I-Tsung, "Seizure and Wear Testing Methodology", 1988.
- [19] Smith, A. F., Radford, T. J., Mawson, D. and Kaye, P., "A New Reciprocating Sliding Wear Testing Apparatus for High Temperature Gaseous environment", Journal of Physics, v 21, 1988, p 826-831.
- [20] Kuno, M., Dinsdale, K., Pearson, B. R., Ottewell, B. and Waterhouse, R. B., "A New Fretting Wear Test Apparatus", Journal of Physics", v 21 1988, p 929-931.

- [21] Blickensderfer, R. and Laird, G., " A Pin-on-Drum Abrasive Wear Test and Comparison with Other Pin Tests", Journal of Testing and Evaluation, JTEVA, Vol. 16, No. 6, Nov. 1988, p 516-526.
- [22] Sridharan, G., "Improvised Sliding-Wear Testing Device", Experimental Techniques, June 1986, p 26-27.
- [23] Peter, J. B., "Wear Testing and Standardization", ASTM Standardization News, Oct. 1985, p 34-36.
- [24] Jost, H. P., "Tribology - Origin and Future", Wear, 136 (1990), p 1-17.
- [25] Rabinowicz, E., "Investigating A Tribological Failure", Wear, 136 (1990), p 199-206.